VILNIUS GEDIMINAS TECHNICAL UNIVERSITY

Vytautas ABROMAVIČIUS

EXTRACTION AND INVESTIGATION OF BIOSIGNAL FEATURES FOR VISUAL DISCOMFORT EVALUATION

DOCTORAL DISSERTATION

TECHNOLOGICAL SCIENCES,
ELECTRICAL AND ELECTRONIC ENGINEERING (T 001)

VGTU
LEIDYKLA
TECHNIKA
Vilnius 2019

Doctoral dissertation was prepared at Vilnius Gediminas Technical University in 2015–2019.

Scientific supervisor

Prof. Dr Artūras SERACKIS (Vilnius Gediminas Technical University, Electrical and Electronic Engineering – T 001).

The Dissertation Defense Council of Scientific Field of Electrical and Electronic Engineering of Vilnius Gediminas Technical University:

Chairman

Prof. Dr Habil. Romanas MARTAVIČIUS (Vilnius Gediminas Technical University, Electrical and Electronic Engineering – T 001).

Members:

Prof. Dr Adriano DE OLIVEIRA ANDRADE (Federal University of Uberlandia, Brasil, Electrical and Electronic Engineering – T 001),

Dr Rytis MASKELIŪNAS (Kaunas University of Technology, Informatics Engineering – T 007),

Assoc. Prof. Dr Vitalij NOVICKIJ (Vilnius Gediminas Technical University, Electrical and Electronic Engineering – T 001),

Prof. Dr Nerija ŽURAUSKIENĖ (State Research Institute Center for Physical Sciences and Technology, Electrical and Electronic Engineering – T 001).

The dissertation will be defended at the public meeting of the Dissertation Defense Council of Electrical and Electronic Engineering in the Senate Hall of Vilnius Gediminas Technical University at **2 p. m. on 16 September 2019**.

Address: Saulėtekio al. 11, LT-10223 Vilnius, Lithuania.
Tel. +370 5 274 4956; fax +370 5 270 0112; e-mail: doktor@vgtu.lt

A notification on the intend defending of the dissertation was send on 14 August 2019.

A copy of the doctoral dissertation is available for review at VGTU repository http://dspace.vgtu.lt and at the Library of Vilnius Gediminas Technical University (Saulėtekio al. 14, LT-10223 Vilnius, Lithuania) and at the Wroblewski Library of the Lithuanian Academy of Sciences (Žygimantų st. 1, LT-01102 Vilnius, Lithuania).

VGTU leidyklos TECHNIKA 2019-033-M mokslo literatūros knyga

Parengta LaTeX2$_\varepsilon$ sistema

ISBN 978-609-476-190-4

vytautas.abromavicius@vgtu.lt

VILNIAUS GEDIMINO TECHNIKOS UNIVERSITETAS

Vytautas ABROMAVIČIUS

BIOSIGNALŲ POŽYMIŲ REGOS DISKOMFORTUI VERTINTI IŠSKYRIMAS IR TYRIMAS

DAKTARO DISERTACIJA

TECHNOLOGIJOS MOKSLAI,
ELEKTROS IR ELEKTRONIKOS INŽINERIJA (T 001)

VGTU
LEIDYKLA
Vilnius TECHNIKA 2019

Disertacija rengta 2015–2019 metais Vilniaus Gedimino technikos universitete.

Vadovas

prof. dr. Artūras SERACKIS (Vilniaus Gedimino technikos universitetas, elektros ir elektronikos inžinerija – T 001).

Vilniaus Gedimino technikos universiteto Elektros ir elektronikos inžinerijos mokslo krypties disertacijos gynimo taryba:

Pirmininkas

prof. habil. dr. Romanas MARTAVIČIUS (Vilniaus Gedimino technikos universitetas, elektros ir elektronikos inžinerija – T 001).

Nariai:

prof. dr. Adriano DE OLIVEIRA ANDRADE (Federalinis Uberlandijos universitetas, Brazilija, elektros ir elektronikos inžinerija – T 001),

dr. Rytis MASKELIŪNAS (Kauno technologijos universitetas, informatikos inžinerija – T 007),

doc. dr. Vitalij NOVICKIJ (Vilniaus Gedimino technikos universitetas, elektros ir elektronikos inžinerija – T 001),

prof. dr. Nerija ŽURAUSKIENĖ (Valstybinis mokslinių tyrimų institutas Fizinių ir technologijos mokslų centras, elektros ir elektronikos inžinerija – T 001).

Disertacija bus ginama viešame Elektros ir elektronikos inžinerijos mokslo krypties disertacijos gynimo tarybos posėdyje **2019 m. rugsėjo 16 d. 14 val.** Vilniaus Gedimino technikos universiteto senato posėdžių salėje.

Adresas: Saulėtekio al. 11, LT-10223 Vilnius, Lietuva.
Tel.: (8 5) 274 4956; faksas (8 5) 270 0112; el. paštas: doktor@vgtu.lt

Pranešimai apie numatomą ginti disertaciją išsiųsti 2019 m. rugpjūčio 14 d.

Disertaciją galima peržiūrėti VGTU talpykloje http://dspace.vgtu.lt, Vilniaus Gedimino technikos universiteto bibliotekoje (Saulėtekio al. 14, LT-10223 Vilnius, Lietuva), Lietuvos mokslų akademijos Vrublevskių bibliotekoje (Žygimantų g. 1, LT-01102 Vilnius, Lietuva).

Abstract

Comfortable stereoscopic perception continues to be an essential area of research. The growing interest in virtual reality content and increasing market for head-mounted displays (HMDs) still cause issues of balancing depth perception and comfortable viewing. Stereoscopic views are stimulating binocular cues – one type of several available human visual depth cues which becomes conflicting cues when stereoscopic displays are used. Depth perception by binocular cues is based on matching of image features from one retina with corresponding features from the second retina. It is known that our eyes can tolerate small amounts of retinal defocus, which is also known as Depth of Focus. When magnitudes are larger, a problem of visual discomfort arises.

The research object of the doctoral dissertation is a visual discomfort level. This work aimed at the objective evaluation of visual discomfort, based on physiological signals. Different levels of disparity and the number of details in stereoscopic views in some cases make it difficult to find the focus point for comfortable depth perception quickly. During this investigation, a tendency for differences in single sensor-based electroencephalographic EEG signal activity at specific frequencies was found. Additionally, changes in eye tracker collected gaze signals were also found. A dataset of EEG and gaze signal records from 28 control subjects was collected and used for further evaluation.

The dissertation consists of an introduction, three chapters and general conclusions. The first chapter reveals the fundamental knowledge ways of measuring visual discomfort based on objective and subjective methods. In the second chapter theoretical research results are presented. This research was aimed to investigate methods which use physiological signals to detect changes on the level of sense of presence. Results of the experimental research are presented in the third chapter. This research aimed to find differences in collected physiological signals when a level of visual discomfort changes. An experiment with 28 control subjects was conducted to collect these signals.

The results of the thesis were published in six scientific publications – three in peer-reviewed scientific papers, three in conference proceedings. Additionally, the results of the research were presented in 8 conferences.

Reziumė

Virtualios realybės turiniui peržiūrėti skirti atvaizdavimo įrenginiai praktikoje naudojami mažai ne dėl aukštos jų kainos ar nepakankamos vaizdo kokybės, o neretai dėl dažnai sukeliamo regos diskomforto. Regos diskomforto lygis yra individualus kiekvienam naudotojui, todėl reikalingos techninės priemonės, leidžiančios aptikti pirmuosius regos diskomforto požymius naudojant virtualiosios realybės akinius. Rinkoje jau pasirodė virtualiosios realybės akiniai su integruota akių sekimo įranga, taip pat akinių gamintojai bendradarbiauja su elektroencefalogramų nuskaitymo įrenginius gaminančiomis įmonėmis. Tačiau nėra sukurti būdai regos diskomfortui aptikti naudojant akių aktyvumo ar elektroencefalogramų registravimo įrenginius. Siekiant aptikti akių diskomfortą sąlygojančias situacijas vaizdo peržiūros metu, disertacijoje sprendžiama vaizdo pojūčių kiekybinio įvertinimo problema.

Šios disertacijos tyrimo objektas yra paieška išmatuojamų kiekybinių parametrų, kurie leistų atpažinti, kada žmogus stebi vaizdus neįtempdamas akių judesius valdančius raumenis, atskirti, kada vaizdo gylio suvokimui akys yra tinkamoje padėtyje, o kada gylio suvokimui tinkamos akių padėties ilgai nepavyksta rasti. Darbas skirtas prisidėti vystant objektyvaus regos diskomforto įvertinimo metodus, remiantis fiziologiniais matavimais. Skirtingas matomų objektų gylis ir detalių skaičius stereovaizduose neleidžia aiškiai suvokti matomo objekto atstumo erdvėje, arba atstumo suvokimui reikia ilgesnio laiko nei įprastai. Tyrimo metu buvo nustatyti požymiai, išskirti iš elektroencefalogramos, naudojant vienu elektrodu matuotą signalą, kurie leidžia atpažinti vartotojo regos diskomfortą. Taip pat buvo pasiūlyti požymiai leidžiantys taikyti akių sekimo įrenginius stereoskopinių vaizdų sukeltam regos diskomfortui įvertinti. Duomenims surinkti buvo atliktas eksperimentas matuojant 28 savanorių fiziologinius signalus, gautus stereoskopinio turinio stebėjimo metu.

Disertaciją sudaro įvadas, trys skyriai ir bendrosios išvados. Pirmajame skyriuje apibrėžiama regos diskomforto problema, nagrinėjami metodai skirti regos diskomforto matavimui, remiantis objektyviais ir subjektyviais matavimais. Antrajame skyriuje pateikiami teorinių tyrimų rezultatai. Šiais tyrimais buvo analizuojami metodai, kurie naudoja fiziologinius matavimų rezultatus, norint aptikti patirtos kokybės pokytį vizualaus turinio stebėjimo metu. Trečiajame skyriuje yra pateikti eksperimentinio tyrimo rezultatai. Buvo tikimasi, kad surinktuose signaluose galima išskirti požymius, kurie leis atskirti skirtingą regos diskomfortą sukeliančius vaizdus.

Pagrindiniai disertacijos rezultatai paskelbti 6 mokslinėse publikacijose – trys iš jų atspausdintos recenzuojamuose mokslo žurnaluose, trys konferencijų medžiagoje. Rezultatai viešinti 8 mokslininkų konferencijose.

Notations

Abbreviations

ANOVA	Analysis of variance
bpm	Beats per minute
Co	Comfortable
DPM	Depth Perception Moment
ECG	Electrocardiogram
EEG	Electroencephalogram
ERP	Event-related potential
ICA	Independent Component Analysis
MdUn	Mildly uncomfortable
SoP	Sense of presence
SSVEP	Steady-state visually evoked potential
Un	Uncomfortable
VCo	Very comfortable
VUn	Very uncomfortable
wICA	Wavelet Independent Component Analysis

Contents

[1]The annexes are supplied in the enclosed compact disc.

Introduction

Problem Formulation

This thesis is focusing on the problem of quantitative evaluation of individual visual discomfort levels. During a natural view our perception of depth is achieved by acquiring visual information through binocular vision. Distance between our eyes lets us to perceive a depth of the 3D objects. The problem arises during sustained visual perception of unnatural stereoscopic content.

When a person is watching stereoscopic content a bipolar gaze is necessary to perceive a depth of the content. However, to produce stereoscopic view natural laws are violated, e.g., the disparity between two views gives a possibility to support better depth perception. The disparity between image objects helps to distinguish similar objects situated at different distances from the viewer. However, high disparities are related to the higher visual discomfort levels and may cause the eye fatigue during extended stereoscopic perception time.

In order to solve this problem an experiment were conducted to collect physiological data during the consumption of the stereoscopic content. It was expected that the measured physiological signals would be affected by different visual comfort levels since natural mechanisms of binocular vision are violated with the usage of artificial stereoscopic cues.

Relevance of the Thesis

A field of visualization in 1987 was declared as a strategic direction by the National Science Foundation (NSF) of the USA (Johnson *et al.* 2005). During the last 30 years, a successful developments were made. However, according to NSF challenges in the field of visualization remains, such as: 1) view-dependent problems for the user, 2) image-based rendering, 3) multiresolution, 4) importance-based, 5) adaptive resource-aware algorithms. These problems should be solved based on specific requirements for the content.

When analyzing future perspectives of the systems of 3D visualization there are several studies for the perspectives and development of the field. According to the Grand View Research, global visualization and 3D rendering software market size was valued USD 952.4 million in 2016 and is projected to reach USD 5.63 Bn by 2025 (Grand View Research, 2018). A study published by PnS Market Research reported that visualization market is projected to reach USD 3.84 Bn by 2023 (PnS Market Research, 2017).

The importance of this problem is supported by the increased attention to the head-mounted displays, such as VR glasses and immersive visual content (e.g., 360-degree video records). A stereoscopy effect is achieved by presenting an individual view for each eye. The disparity between two views gives a possibility to support better depth perception. The disparity between image objects helps to distinguish similar objects situated at different distances from the viewer. However, high disparities are related to the higher visual discomfort levels and may cause the eye fatigue during extended stereoscopic perception time (Read, Bohr 2014; Solimini 2013).

The Object of the Research

The research object of the doctoral dissertation is quantitative parameters, obtained using electroencephalogram, electrocardiogram and eye-tracking data.

Obtained parameters were analyzed to find a difference in visual comfort level during stereoscopic perception. The level of visual comfort, acquired using mean opinion scores was used as a reference.

The Aim of the Thesis

The aim of the thesis is to develop means of objectively measuring visual comfort by investigating effects of brain activity and gaze signals on different levels of stereoscopic stimuli.

The Objectives of the Thesis

In order to solve the stated problem and reach the aim of the thesis the following objectives were formulated:

1. To investigate the audiovisual content's influence on the measured physiological signals at a different sense of presence levels.
2. To investigate electroencephalogram signals when stereoscopic stimuli with different visual discomfort levels is presented and propose features to detect visual discomfort level.
3. To investigate gaze signals when stereoscopic stimuli with different visual discomfort levels is presented and propose features to detect visual discomfort level.

Research Methodology

Investigation in this dissertation is divided into two parts. In the first part, using physiological signals, features were extracted and compared with subjective evaluations of the sense of presence level (SoP). Physiological signals used in this research were acquired by Perrin *et al.* (2016). During this experiment a group of 20 volunteers consumed three different levels of audiovisual stimuli, while their physiological signals were measured.

In the second part of the investigation features extracted from physiological signals were statistically compared to find significant differences, which would indicate a level of visual discomfort. Physiological signals were collected from the subjects consuming stereoscopic stimuli with five different levels of visual discomfort. In the experiment a total of 120 stereoscopic images were shown to 28 volunteers. Brain activity and gaze signals were measured during the experiment. For the reference of visual discomfort level, subjective measurements, such as visual discomfort level, using five grade scale and stable depth perception time, were collected.

Scientific Novelty of the Thesis

1. Changes in high beta power spectrum density, extracted from the temporal and parietal lobes of the electroencephalogram signal and estimated heart rhythm using electrocardiogram are proposed as features to detect different sense of presence level.

2. Pupil size, focus point, binocular disparity, crossed disparity features extracted from gaze signals are proposed as features to detect different visual discomfort level.
3. Ratio of α and β_{h} spectrum density extracted from the frontal lobe of the electroencephalogram signal is proposed as a feature, which can indicate different level of visual discomfort.

Practical Value of the Research Findings

Results of the research are to be used to replace mean opinion scores when evaluating a level of visual discomfort for the user. Features extracted from the users physiological signals are individual, and can represent personal experience when consuming stereoscopic content, and eventually feeling the visual discomfort.

New consumer friendly eye tracking and brain activity measuring devices are entering the market annually. Recently released virtual reality headset (VIVE PRO 2019) includes an integrated eye-tracker. Therefore, eye-tracker obtained features, proposed in this thesis, can be applied to this device to detect visual discomfort level in virtual reality environment. Additionally, frontal lobe is a probable location for the virtual reality headset with embedded electroencephalogram sensor, and in this work features were proposed, which can indicate a level of visual discomfort from the frontal lobe brain activity signals.

The Defended Statements

1. β_{h} and β_{l} frequency band is a feature to evaluate Sense of Presence from electroencephalogram signals, measured near Parietal (left or right) and Occipital (left or right) regions.
2. 8–13 Hz and 21–30 Hz spectral power ratio of electroencephalogram signal, measured at the frontal lobe is a feature to detect a level of visual discomfort if using an analysis frame from 2 to 7 s before the moment of depth perception.
3. The number of focus points is a feature to detect a level of visual discomfort if using an analysis frame of 2 s before the moment of depth perception.
4. The pupil size can be used as a feature to detect a level of visual discomfort, when analysing a time frame from stimulus shown to the moment of depth perception. However, when using 5 s analysing a time frame binocular disparity must be used.

Approval of the Research Findings

The results of the research were published in six scientific publications – three in peer-reviewed scientific papers, three in conference proceedings. Additionally, the results of the research were presented in following conferences:

- International Conference *Computing in Cardiology*, 2015, Nice, France;
- Three Young Scientist Conferences *Science – Future of Lithuania*, 2016–2018, Vilnius, Lithuania;
- International Conference *Electrical, Electronic and Information Sciences (eStream)*, 2017, Vilnius, Lithuania;
- International Conference *Advances in Information, Electronic and Electrical Engineering AIEEE*, 2017, Riga, Latvia;
- Two International Conferences *Data Analysis Methods for Software Systems*, 2017–2018, Druskininkai, Lithuania;

Structure of the Dissertation

The dissertation consists of an introduction, three chapters and general conclusions. The volume of the dissertation is 106 pages, in which are given: 28 figures and 21 tables. Additionally, 158 items are cited in the dissertation.

Acknowledgements

I would like to thank Prof. Dr Artūras Serackis for supervising me in this journey. Without his guidance and support I wouldn't be here. Thank you for showing me the way. I want to thank everyone and all of the Department of Electronic Systems for providing positive environment, motivation and encouragement. Also, I am grateful for Prof. Dr Sridhar Krishnan for inviting me to the SAR lab in the Ryerson University, and introducing me the „SARians“ and fellow interns: Mariana, Guru, Giordano, Alice, Jeevan, Saeed, Yash and others. Time in Toronto was stimulating and too short. Finally, I would like to thank my parents, my sister and my nephew, Gary for the support and the patience.

1

Literature Survey of Visual Discomfort Detection

In this chapter, the overview of the current research on the topic of the dissertation and field of visual discomfort are presented. The rendering of stereoscopic images may have different set-ups which have a direct influence on the comfort of visual perception and ability to focus on the object of interest in the image. If there would be possible to estimate the comfort level during individual stereoscopic perception, various virtual camera separation parameters may be adjusted (Shao *et al.* 2016) to avoid visually uncomfortable scenes in the rendered video stream. Virtual camera separation, used during the rendering of stereoscopic views, depending on the scene, causes different image disparities followed by too much or too little-perceived depth on a target display.

Depending on the field of the studies (medical, technological, etc.), terminologies for visual fatigue and discomfort differ; presented definitions can be ambiguous. For example, terms such as fatigue, strain, and asthenopia are coexisting in the literature, but their differences are unclear. In their works Lambooij *et al.* (2009, 2007) did excellent work in providing cross-fields definitions for fatigue and discomfort. They define fatigue as a decrease in the performance of the human visual system as an outcome of physiological tension or stress occurring from excessive exertion (Lambooij *et al.* 2007).

The research results, presented in this chapter are presented at international "AIEEE" (Riga, 2017), "DAMSS" (Druskininkai, 2018) and national "Science – Future of Lithuania" (Vilnius, 2016) scientific conferences.

1.1. Visual Fatigue and Visual Discomfort

The assessment of visual discomfort can be performed in two ways: using subjective means or objective means. During the subjective assessment, visual stimuli are presented to a group of viewers, and during the experiment (or after it) subjects are asked to fill the questionnaire about their impression on different stereo images or long-lasting video. The objective measurements require observing the body response during stereoscopic perception of differently rendered stereoscopic images. The most widely used tools to follow the body response in the research field are eye-tracking devices (Bernhard *et al.* 2014; Iatsun *et al.* 2015; Lin, Kao 2018) and brain scanning devices (Fischmeister, Bauer 2006; Frey *et al.* 2016; Moon, Lee 2017). However, other means to measure visual discomfort are also investigated, e.g., Lee et al. 2016 showed it is possible to measure visual discomfort using facial expressions.

Barkowsky *et al.* (2011); Zhou *et al.* (2017) in their research showed that adaptation mechanisms from the visual system are sometimes known to improve its performances, yet the adaptation itself may as well induce fatigue: both decreases and increases in performances of the visual system may be related to visual fatigue. As for visual discomfort, it is perceived instantaneously, while fatigue is induced after a given duration of effort. Finally, how fatigue relates to discomfort is still an open question (Lambooij *et al.* 2009). These observations show the need for further efforts in defining visual fatigue and discomfort, to notably account for both worsening and improving effects, as well as temporal aspects Urvoy *et al.* (2013).

Typically, questionnaires are used to assess the presence of symptoms for fatigue and discomfort. In Kennedy *et al.* (1993), Kennedy proposed a questionnaire assessing simulator sickness. As visual fatigue, discomfort and simulator sickness share common symptoms; this questionnaire was soon adapted by Howarth and Costello for more general purposes (Howarth, Costello 1997). Now these questionnaires are also used in VR field (Fernandes, Feiner 2016). Discomfort, in particular, is often evaluated with subjective scales (Song *et al.* 2016; Yano *et al.* 2002).

Objective tests can also be conducted in order to assess the presence of fatigue. In their work Lambooij *et al.* (2007), for instance, measure the tear film breakup time to determine the dryness of the eye. Experimental designs assessing visual fatigue usually follow one of two approaches: (1) following a visual task, the presence of symptoms is assessed along with the perceived degree of fatigue (Dettmann, Bullinger 2018; Gupta *et al.* 2013; Yano *et al.* 2002); (2) fatigue is voluntarily induced through demanding and repeated visual tasks which allows for symptoms identification Wann *et al.* (2014).

1.1.1. Objective Signs of Visual Discomfort

There is a large number of objective and subjective signs for visual fatigue (Urvoy *et al.* 2013), such as dried mucus of the eyes, tears around the eyelid, changes in blinking rate (Jaschinski *et al.* 1996), and reduction of the speed of eye movements (Saito 1992). Researchers particularly focused their efforts on the near vision triad (accommodation, vergence, and pupillary response): even in 2D displays, numerous studies reviewed by Klamm, Tarnow (2015) showed that visual fatigues transiently induces accommodation and vergence disorders.

The pupil size and its changes are affected by visual fatigue as well. In Wang *et al.* (2015), showed that pupillary disorders were more frequent among a group of patients suffering from asthenopia than in a group of unaffected patients. In Murata *et al.* (2001); Uetake *et al.* (2000), the perceived fatigue reported by the observers, after visualization of 60 min of 2D video sequences, correlated with a reduction of the pupil diameter. In their work, Ukai, Howarth (2008) showed that in 30% of cases, patients experiencing visual fatigue show an abnormal exaggeration of the rhythmic contraction (myosis) and dilation (mydriasis) of the pupil, independent of changes in illumination or in fixation of the eyes, called hippus (Bouma, Baghuis 1971). Finally, a study by Ando *et al.* (2002) showed that the pupillary light reflex is less controlled in a group of patients suffering from mild autonomous dysfunctions.

While visual fatigue manifests itself through ocular disorders, it also induces cerebral and psychological disorders such as headaches (Ando *et al.* 2002). Furthermore, studies notably showed that the visualization of 3D stereoscopic sequences may further delay event-related potentials (ERPs) such as P100 (at 100 ms) (Ando *et al.* 2002) and P700 (at 700 ms) (Frey *et al.* 2016). These observations tend to demonstrate that visual fatigue also affects cognitive processes from the human visual system. More specifically, cognitive fatigue with 3D stereoscopic stimuli may affect stereopsis, the process by which left and right views are fused into a single percept featuring depth information. The performance of the binocular fusion is usually assessed by the fusion range: the interval of retinal disparities for which it is possible to fuse left and right retinal images.

In Lambooij *et al.* (2007), authors correlated short-term visual fatigue, induced by the reading of a 3D stereoscopic text (Wilkins test) to an increase of the fusion range. Inversely, several studies correlated long-term fatigue, induced by the visualization of 60 min of 3D stereoscopic stimuli to a reduction of the fusion range Emoto *et al.* (2005, 2004); Hua (2017); baseline fusion range was restored after 5 to 10-min rest. Similarly to ocular deficiencies, the fusion range may be used to identify persons susceptible to visual fatigue Lambooij *et al.* (2009): persons with small fusion range reported more visual fatigue symptoms.

It is believed that physiology not only contributes to the success of individual experiments, but that it can be instrumental in furthering the field of multimedia research. In the existing literature, internal cognitive processes and experiences are widely hypothesised towards definitions of terms such as quality and SoP. Physiological methods can help to improve understanding and validating these internal processes in the media consumer. Toward this end, one strength of physiological measurements that should be exploited is the detection of target stimuli that would stay undetected in self-reporting experiments, for instance, through early pre-conscious brain activity components. Capturing such effects can be expected to have a profound impact in the context of extensive media consumption, where distortion may not be actively perceived but may have a long-term effect on overall SoP including, for instance, visual fatigue. Careful experimental design is needed to identify physiological thresholds for the objective evaluation of the SoP and visual discomfort.

1.1.2. Psychophysical Methods

To build sufficient psychophysiological evidence in support of identifying the various factors impacting SoP and to enable effective algorithm development it is essential to have adequate psychophysiological data. It is argued that such evidence needs to be created collectively and made openly accessible to the research community. An overview of some already available databases is presented in Perrin *et al.* (2016) published two extensive databases from their study on multimodal Quality of Experience assessment of immersive media. Koelstra *et al.* (2012) present DEAP, a multimodal data set for the analysis of human affective states when watching a video and Zheng, Lu (2015) provide the SJTU Emotion EEG Dataset (SEED) from their study on emotion recognition when viewing a video. Probably the most extensive range of databases exists for gaze tracking recordings. Winkler, Subramanian (2013) surveyed 28 gaze tracking databases for image and video applications and provided an excellent overview of their characteristics. While these data sets are highly relevant for the research community, they give only small pieces of the overall puzzle. Significantly, more data sets need to be made publicly available to fully understand all the factors influencing SoP Engelke *et al.* (2017). In that regard, systematic methodologies are also required to make compatible and integrate physiological data of different databases to allow for effective analytics and hypothesis testing.

1.1.3. Saliency Maps for Visual Discomfort Detection

Following a somewhat different approach, Iatsun *et al.* (2015) developed a model for predicting discomfort based on eye tracking data: fixations, blinks and fo-

cus. They found that discomfort strongly correlated with spatial saliency, motion intensity and disparity range. Cho, Kang (2014) used object salience derived from region-based algorithms. Then they extracted features including disparity, motion, contrast, spatial complexity of salient objects and brightness and binocular asymmetries degree between left and right image to construct their model. The features were fed into an support vector regression model to predict discomfort. Several models have used saliency maps to improve discomfort prediction, but it is also true that discomfort drives attention. Jiang *et al.* (2016) proposed a 3D saliency model which explicitly accounts for visual discomfort. They combined color saliency, texture saliency and spatial compactness with global disparity contrast to train a comfort prediction function which classifies scenes into High-Comfortable and Low-Comfortable Visual Scenes and used this information to generate a saliency map based on viewing comfort. Kim *et al.* (2014) add a predicted discomfort score to other saliency attributes such as motion, disparity and texture, in order to create a refined 3D saliency map.

1.2. Eye Measurement Based Visual Discomfort Detection

Psychological and physiological processes: At any instance in time, the human eye is exposed to an abundant amount of visual information. Attentional mechanisms in the human visual system are fundamental to reducing the complexity of scene analysis. There are distinguished between bottom-up and top-down attention. Bottom-up attention is reflexive, signal driven, and independent of a particular task. Top-down attention is driven by higher level cognitive factors and external influences such as contextual effects, viewing task, and personal experience. Both attentional mechanisms guide eye movements to the most relevant information in a given context. Gaze tracking is deployed to capture these eye movements and the underlying attentional mechanisms. It is noted that gaze tracking records only overt visual attention (shifting of the eyes to a stimulus) but not covert visual attention (mental shift of attention), which can be measured using EEG (Engelke *et al.* 2017).

1.2.1. Gaze Tracking

Eye trackers are integrated into experiments to capture overt visual attention during visual stimulus observation. Modern eye trackers are non-invasive video based systems with an infra-red camera, typically installed under a stimulus screen, that measure corneal reflections to determine the direction of gaze. Some eye trackers

come with a head rest and are installed at the location of the observer. In real-world experiments, head mounted eye trackers are used to record gaze behaviour in 3-dimensional space. In any case, the eye tracker has to be carefully time-synchronised with the stimulus presentation to accurately capture eye movements. This is particularly important if accuracy at the speed of saccadic eye movements is needed (Harezlak *et al.* 2014). To assure spatial accuracy, eye trackers have to be carefully calibrated to each individual observer using pre-defined calibration patterns. For long experiments, the calibration often needs to be repeated to maintain high spatial accuracy. Spatial accuracy usually diminishes towards the periphery of the visual field for which reason it is important to carefully take into account the visual angle of the presented stimulus.

Eye movements are recorded at frequencies starting typically from 50 Hz and going beyond 1000 Hz for high-end devices. The resulting raw gaze patterns are usually rather inconclusive and therefore need post-processing into more meaningful fixation density maps (Engelke *et al.* 2009). Typical analysis of eye tracking data includes determining fixation location, duration, and order. In the context of SoP it is critical to also compare two fixation density maps, for instance, between distorted and reference stimuli. Some of the most commonly used comparison metrics include the Kullback-Leibler divergence, area under the ROC curve, normalised scanpath saliency, and Pearson linear correlation coefficient. These metrics capture different aspects of the eye tracking data and are often used conjointly (Engelke *et al.* 2017).

Gaze tracking has been extensively investigated in the context of visual SoP assessment, the rationale being that eye gaze is directed not only by the natural content but also by potential induced distortions. The relative interplay of these and the resulting gaze behavior is conjectured to have a major impact on the overall SoP. While the potential benefit of recording gaze behavior has been widely recognized by the research community, the conclusions drawn from individual studies vary considerably. Covering the entire spectrum of the prior art exceeds the scope of this article and the interested reader is referred to recent survey articles Engelke *et al.* (2011); Le Callet, Niebur (2013).

Several studies have investigated the relationship between overt visual attention in distorted and undistorted visual stimuli and the related impact on overall quality perception. In Engelke *et al.* (2010b), the impact of content saliency relative to distortion location was investigated for H.264 coded video with localized packet loss distortions. It was shown that distortions located in salient regions have a significantly higher impact on quality perception as compared to distortions in non-salient regions. This is partly attributed to a shift of attention needed in case of non-salient region distortions whereas distortions in salient regions are perceived more severely.

Global compression distortions were found by Le Meur *et al.* (2010a) to not alter viewing patterns considerably. Liu *et al.* (2013) showed that differences in observers' viewing behavior depends strongly on the image content. The more distinct a salient region, the higher the agreement between observers, and the larger the performance gain when including eye tracking data into objective quality metrics. Importantly, Lee *et al.* (2009) reported that audio is a strong attractor of visual attention, and should therefore not be disregarded, but its interplay with the visual stimulus should be accounted for.

Eye tracking data is often integrated into image and video quality metrics to further improve their quality prediction performance. Ninassi *et al.* (2007) integrated fixation density maps into several quality metrics to predict JPEG and JPEG2000 distortions, but no improvements were found for the considered metrics. Based on the fixation density maps and positive outcomes in Engelke *et al.* (2010b), Engelke *et al.* (2010a) integrated spatial saliency weighting into a video quality metric, TetraVQM (Barkowsky *et al.* 2009), successfully improving the metric's prediction accuracy. The task given to the observer is also known to influence gaze behavior and it is generally agreed that the integration of task-free eye tracking data into quality prediction models is more successful than when using eye tracking data obtained during quality assessment task (Le Meur *et al.* 2010b; Liu, Heynderickx 2011). While the value of task-free eye tracking data is widely accepted and several databases have been made publicly available, Engelke *et al.* (2013) compared three databases and found that differences amongst their fixation density maps were small with low impact on the integration into quality metrics.

In summary, the value of eye tracking data for studying visual SoP is widely agreed upon and integration into computational models was generally found to be more successful for video rather than image applications, local rather than global distortions, and task-free rather than task-driven eye tracking data. Despite this field being well explored, further research is needed to fully understand the interaction between overt visual attention to audiovisual content and induced distortions.

1.2.2. Pupillometry

Tasks involving cognitive processing cause short-onset latency (100-200 ms) transient pupil dilation that peaks after a few hundred milliseconds and then rapidly reverts following task completion. Pupil responses have been shown for cognitive load and reasoning, memory, visual attention, and language processing (Trani, Verhaeghen 2018).

In constant low-light conditions, pupil dilation has long been known to involve the activation of the locus coeruleus and its neuromodulatory influence through norepinephrine signaling pathways. More recently it was shown using extracellular recordings and stimulation in locus coeruleus with simultaneous monitoring of

pupil diameter fluctuations that there is a causal functional relationship (Aston-Jones, Cohen 2005; Joshi *et al.* 2016; Varazzani *et al.* 2015).

The locus coeruleus makes widespread projections and functional inter actions with many brain regions from cortex and cerebellum to other brainstem structures and spinal cord. It contributes ascending pathways responsible for arousal and engagement with novel environmental stimuli, e.g., optimizing the levels of exploration versus exploitation in adaptive behavior, and is implicated in cognition, emotional processing, perceptual rivalry and memory retrieval. This is not the exclusive site of activity coupled to the pupil. For instance, the pupillary light-reflex via the iris sphincter muscle is served via distinct parasympathetic pathways, and connections between the eye and other modulating brain structures are not completely understood. However, it is known that both sympathetic and parasympathetic nervous system activation affects the radial dilator muscles of the pupil and muscles in the iris, leading to pupil dilation as sympathetic activation increases and constriction with activation decrease and an opposing response for parasympathetic activity Thompson, Kardon (2006); Yoshitomi *et al.* (1985).

Key parameters for collecting pupillometry data are speed, resolution and accuracy of eye tracking. Sufficient temporal resolution and precision are required to track the time course of change on the order of milliseconds and synchronise with external task-related stimuli. Eye tracking systems vary from tens of hertz to several kilohertz for high-speed systems used to acquire other events like microsaccades, small involuntary eye movements that occur during fixation. Increased image resolution and repeated trials averaging enables sensitive tracking of pupillary size changes up to hundredths of a millimeter (Engelke *et al.* 2017).

Image processing algorithms can be used to reliably track pupil location and diameter as eye movements occur. Although pupil dilations have a higher signal to noise ratio relative to other measurements like EEG, noise and artifacts can contaminate the signal. These artifacts, such as eye blinks, can be removed in post-hoc analysis using techniques such as independent component analysis (ICA) identification. Other sources of noise can arise during large head movements, so in some experimental contexts head stabilization techniques such as chin rests, or head tracking algorithms, are employed (Partala, Surakka 2003).

Once pupil responses during repeated task-related trials are imaged, the diameter metric can be processed in a variety of ways. Artifact removal and filtering to smoothen traces or reduce noise can improve signal fidelity depending on the application. Based on the type of task being conducted, measurements of tonic (windowed) overall average pupil diameter or phasic (time-varying) responses can be extracted. Phasic responses can be useful because the time series contains the peak minimum or maximum pupillary change, the time at which these events occur relative to the task, and consequently the acceleration or rate of change leading to the maximum effect observed (Partala, Surakka 2003).

Pupillometry has not been used extensively in primary SoP studies, but shows promise as a non-invasive physiological measurement due to pupil diameter correlations with processing load, memory, emotion, and arousal (Beatty 1982). Early studies demonstrated that simple memory recall of increasing numbers of digits in a sequence corresponds to increasing pupil size (Kahneman, Beatty 1966). Pupil dilation has also been shown to vary with the strength of memories during retrieval in a paired-association task [67], a further indication of processing load. Retrieval of emotional memories triggers LC activation and corresponding pupillary responses (Van Rijn *et al.* 2012), something that may bear relevance to emotional versus neutral states elicited by enhanced QoE. Pupillometry shows that graded LC-NE responses follow evolving strategies for a gambling task with an evolving payoff structure (Jepma, Nieuwenhuis 2011). Effects have also been observed in the context of visual processing. For instance, visual search tasks using distractors that increase difficulty of target recognition lead to increases in pupil diameter (Porter *et al.* 2007). Further, pupillometry has been used to probe linguistic processing, and increased syntactic complexity or effortful listening leads to pupil dilation (Zekveld *et al.* 2010). Given the importance of intelligibility in SoP quantification, this suggests a meaningful way to assess heightened cognitive load that may accompany difficulty in understanding language in various types of content consumption.

1.3. Neurophysiology Based Visual Discomfort Detection

Electroencephalography (EEG) is a minimally invasive physiological measurement of voltage changes at the scalp arising from electrical activity of neuronal ensembles that underlie cognitive states and experience (Urigüen, Garcia-Zapirain 2015). Physiological measurements have been studied for many decades with Hans Berger credited as the first to record EEG in humans (Berger 1929) in 1924. While the precise links between EEG and psychological phenomena are incompletely understood, several relations are widely accepted.

1.3.1. Event-Related Potential Based Detection

Event-related potentials (ERP), large scale electrical events related to high and low-level sensory and cognitive processing, have been thoroughly characterised. Event related potentials consist of stereotypic changes in electrical activity usually evoked by time-locked sensory stimuli and related cognitive events. They are characterized by their time-dependent amplitude according to a common nomen-

clature, with the first letter referring to the polarity of a particular component and subsequent number(s) indicating latency (in ms) or relative position in the order of components. For example, the well-known P300 component exhibits a positive peak around 300ms after stimulus onset. The amplitude of its subcomponent P3b is known to increase with decreased expectation of a stimulus, thus indicating the novelty of a stimulus. Other event-related potentials have been shown to be involved with object representation and memory operations in a variety of task behaviors.

1.3.2. Spectral Based Detection

Chen et al. Cho, Kang (2014) investigated visual fatigue for 2DTV and 3DTV viewing using 16-channel EEG measurements. Significant decreases in gravity frequency and power spectral entropy, related to alertness level decline, were observed in several brain regions after extended 3DTV viewing. Based on these findings and psychophysical responses, an accurate evaluation model for 3DTV fatigue was established. A related study Chen *et al.* (2013) compared the 2D/3D changes of energy values in four spectral bands (α, β, θ, δ) with four fatigue-related parameters. All bands except the θ rhythm changed significantly when subjects viewed 3DTV. In particular, the energy decreased in α and β frequency bands while δ activity increased significantly. All four fatigue related parameters showed a significant increase, with the highest increase More comprehensive reviews on using EEG in QoE research can be found in Arndt *et al.* (2016); Bosse *et al.* (2016) papers.

1.4. Multimodal and Other Methods

There is a trend of physiological measurements being integrated into modern computing devices, such as heart rate monitors in smart watches and gaze trackers in tablet computers. The wide adoption in mass consumer markets indicates that this trend will continue for the years to come and even move on to more advanced technologies like smart glasses and other wearables. This may provide an opportunity for continuous SoP monitoring in minimally invasive ways and in the natural environment of the users.

With the advent of advanced media technologies and related immersive and interactive experiences it is expected that overall visual discomfort cannot be measured with any one physiological modality alone. It is more likely that combining measurements from multiple, complementary physiological modalities will improve inference across a wider range of cognitive processes and thus lead to a deeper insight into the experience of the user. In this section some multimodal

approaches that aim to capture high-level visual discomfort concepts such as engagement, immersion, and sense of presence are presented.

1.4.1. Steady-State Visually Evoked Potentials

Another neurophysiological response to temporally isolated stimuli is the steady-state visually evoked potential (SSVEP) (Norcia *et al.* 2015). While event-related potentials are typically observed in response to surprising or novel stimuli, SSVEP are observed in response to sustained, periodic stimuli. The response to this kind of stimulation is usually stable in amplitude and phase as suggested by its name. Sensory drive elicited by such periodic stimuli results in increased narrowband EEG spectral power at the tagged stimulus frequency in corresponding sensory areas of the brain. SSVEP are typically described by their amplitude, phase and spatial channel distribution (for the tagged frequency and its associated harmonic components) (Norcia *et al.* 2015). Neural oscillations due to synchronization of neuronal ensembles are measurable as peaks in the power spectrum of the EEG. Such rhythmic activity has been linked to a large number of psychological processes.

1.4.2. Electrocardiography

Electrocardiography (ECG) is a time-varying measure reflecting the ionic current flow produced by the cardiac fibres contracting and relaxing with each heartbeat cycle. A single normal period of the ECG can be approximately associated with the peaks and troughs of the canonical ECG waveform. A wide range of variables are often extracted from ECG measurements with heart rate and heart rate variability being among the most common. In the context of multimedia, these are thought to relate to excitement, fatigue and discomfort (Castellar *et al.* 2014; Drachen *et al.* 2010; Kroupi *et al.* 2014).

ECG measurements have recently been investigated in the context of multimedia assessment, often in conjunction with neurophysiological measures like EEG. Kroupi *et al.* (2014) investigated perceived SoP for 2D and 3D multimedia stimuli, and specifically a “Sensation of Reality”, based on ECG, EEG, and respiration rate. ECG and EEG were found to be predictive of this high level visual discomfort phenomenon, with EEG being more accurate. Barreda-Ángeles *et al.* (2014); Bryant, Oliver (2009) studied visual discomfort for stereoscopic 3D on viewers’ emotions. While self-reporting did not reveal any effects of visual discomfort, physiological measures in terms of heart rate measured through ECG, dermal activity and facial electromyography were found to strongly correlate with visual discomfort.

1.5. First Chapter Conclusions and Formulation of the Thesis Objectives

1. A trend of wearable devices with integrated physiological measurements provides an opportunity for continuous SoP monitoring in minimally invasive ways and in the natural environment of the users.
2. Studies to date mainly focus on experimental paradigms where participants still perform self-reporting in addition to physiological measurements. Research focused on the estimation of conscious responses and measurement of the consumer state may lead to more truthful results as the media experience is less disturbed. Therefore, physiological measurement devices need to be as non-intrusive as possible.
3. Previous studies have demonstrated that physiological measurements provide valuable insight into SoP of advanced media technologies. Some measures, such as EEG and gaze tracking, are well established in the existing body of research, while the other measures have been comparatively less thoroughly explored in the context of SoP.
4. Neurophysiological measures as well as eye measurements are typically deployed as primary sources of information. In general, there is a consensus that multimodal approaches are needed to fully understand this field of advanced media technologies. It is argued that physiology should be used to learn more about the internal cognitive processes to mitigate our assumptions about the quality formation process in humans. The increased body of research as well as recent efforts towards standardization will lead closer to this goal.
5. In practice, the 3D value chain brings numerous artifacts and constraints that impair the results. Shooting, compression and transmission artifacts, for instance, introduces impairments that are known to generate discomfort. However, there are a few guidelines that, if respected, can limit the occurrence of discomfort or fatigue. While there is a small number of comparative studies between 3D displaying technologies, it appears that active and passive, LCD-based and projection-based technologies perform similarly.

Two hypotheses were formulated as a result of the performed literature survey:

1. Different sense of presence levels can be detected from measured physiological signals after the audiovisual content is presented to the user.
2. By using features obtained from the electroencephalogram, measured with consumer oriented device or a gaze tracker it is possible to detect visual discomfort when stereoscopic content is presented to the user.

In order to test proposed hypotheses the following objectives were formulated:

1. To investigate the audiovisual content's influence on the measured physiological signals at a different sense of presence levels.s
2. To investigate electroencephalogram signals when stereoscopic stimuli with different visual discomfort levels is presented and propose features to detect visual discomfort level.
3. To investigate gaze signals when stereoscopic stimuli with different visual discomfort levels is presented and propose features to detect visual discomfort level.

2

Theoretical Research of Sense of Presence Detection

In this chapter results of the theoretical research are presented. This research aimed to find how different levels of SoP affect brainwave activity and heart rhythm. For this purpose, a dataset published by Perrin *et al.* (2016) was used. This dataset is composed of physiological signals, particularly: EEG, ECG and respiratory signals, which were measured during three sessions, during which subjects were consuming audiovisual content with a different level of SoP. Authors of the paper, through subjective measurements, showed that each device configuration induces a distinct level of SoP.

In the first section materials and methods used in the research will be discussed, such as physiological signals database, how signals were collected, what was subjective measurements were conducted. In the subsections of this chapter, methods for processing these signals will be discussed. In the second section, the results of the research will be given. This section is divided into two subsections as well, the first subsection contains results of the investigation with ECG signals, and the second subsection contains results of the investigation using EEG signals. The third section contains a discussion of the results. Conclusions are presented in the final section.

The research results, presented in this chapter are published in three papers (Abromavičius 2017; Abromavičius *et al.* 2017; Serackis *et al.* 2015) and announced at international "CINC" (Nice, 2015), "eSTREAM" (Vilnius, 2017) and national "Science – Future of Lithuania" (Vilnius, 2017) scientific conferences.

2.1. Materials and Methods of Sense of Presence Detection

In this section, the dataset which was used in our study will be discussed. Additionally, methods for the statistical feature analysis are proposed in this section. The investigated dataset was collected and made publicly available by Perrin *et al.* (2016). Detailed information about methods which were applied for the signal preprocessing and feature extraction of ECG and EEG signals will be described in the following subsections.

A contribution of this section is a systematic approach for the feature extraction from the ECG and EEG signals. Physiological signals were acquired while conducting an experiment, which investigated correlations between SoP as experienced and explicitly assessed by the subjects. General structure of the experiment is illustrated in Fig. 2.1. Different levels of sense of presence are induced using three devices. 20 Subjects subjectively evaluated the stimuli, while their physiological signals were measured. In order to find the most beneficial approach for the feature extraction, it is important to have sufficient information about the chosen dataset. Main details of the methodology of the experiment, description of the stimuli, equipment used for the acquisition of the physiological signals, information about the participants and subjective assessment procedure are described in this section. However, detailed information about the dataset can be found in the original paper by Perrin *et al.* (2016).

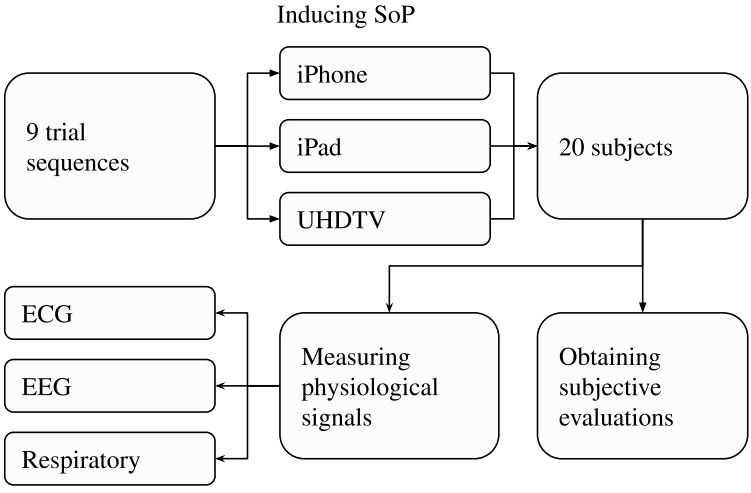

Fig. 2.1. Structure of the experiment. More detailed illustration of a trial is given in Fig. 2.2

A total of 20 subjects participated in the study; their age was varying from 18 to 25 years (21 in average with a 2.2 standard deviation). Ten were males, ten – females. All subjects passed visual acuity and color vision tests, which are described in Birch (1997); ITU-R BT.500-13. Subjects were given oral and written instructions and signed a consent form before the experiment. Additionally, subjects had a training session to get familiar with the assessment procedure.

Ten video sequences were used for producing the dataset. Nine sequences were used as stimuli and one for training the subjects. Sequences were selected using spatial and temporal perceptual information, described in ITU-T Rec. P.910. Therefore, three sequences contain a high level of motion and a low level of detail, five sequences contains a low level of detail and a little motion, and two test sequences contain a little motion and a high level of detail.

In the experiment, different levels of SoP were induced using three different devices. The low level of SoP was induced using the iPhone5 (iPhone 5 specification). The iPad4 (iPad 4th specification) was used to induce the middle level of SoP. The high level of SoP was induced using the 56-inch 4K quality monitor (SRM-L560 specification). Stereo audio signals were used for the iPad and iPhone, and 5.1 surround audio signals were used for the monitor. Viewing distances for each device was set according to ITU-R BT.2022 guidelines. In order to reduce noise in the recorded EEG signals, all devices were in a fixed position in front of the subjects.

The experiment consisted of three sessions, for each level of SoP. Nine stimuli were presented using the same device during each session. The training phase, the set up of physiological signals acquisition devices and a session lasted approximately one hour. In order to avoid any statistical bias between levels of SoP and fatigue of the subjects, sessions were organized on separate days. In total, each subject participated in 27 trials and evaluated 27 stimuli. The order of the trials was randomized for each subject. An example of a trial is illustrated in Fig. 2.2. A trial consists of a baseline phase, a stimulus period and a voting phase. During the baseline phase, which lasts 10 seconds, subjects were asked to focus on a white cross on the screen. Afterward, a stimulus was shown. Physiological signals were recorded during the baseline phase and stimulus period. After the stimulus period, subjects were asked to evaluate the stimulus on a 9-point scale. Subjective assessment procedure was based on the ITU-T Rec. P.910 methodology.

The analysis of the subjective ratings, conducted by Perrin *et al.* (2016), showed that each device induces a different level of SoP. In average, the sense of presence brought to subjects by the UHDTV is higher when compared to the iPad and iPhone. However, confidence intervals of the subjective ratings overlapped. Additionally, physiological signals (EEG, ECG, and respiration) were recorded for each test condition, i.e., a combination of device and content. The recorded physiological signals and subjective ratings were made publicly available.

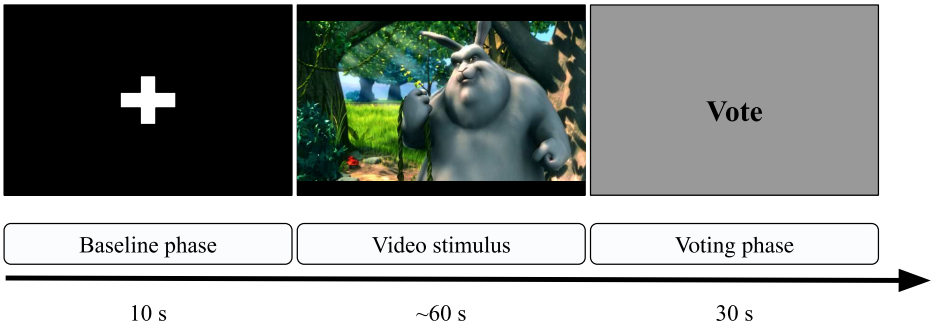

Fig. 2.2. Example of a trial (Perrin *et al.* 2016)

Collected physiological signals (ECG and EEG) were analyzed in this investigation. This section contains description of the analysis and feature extraction methods. The results of the analysis are given in the next section. The goal of this investigation was to find features, extracted from the physiological signals, which are statistically different for each level of SoP. Using the ECG signals heartbeat annotations for each trial were obtained and analyzed. Thus, a heart rate of the subjects consuming different level of SoP was compared. Methods used for the preprocessing and feature extraction from the ECG signals are described in the 2.1.1 subsection. Using EEG signals power density spectrum of the brain activity was obtained and analyzed. Methods employed for the preprocessing and feature extraction from the EEG signals are described in the 2.1.2 subsection.

Obtained features were analyzed using one-way analysis of variance (ANOVA). One-way ANOVA test is used to assess the statistical group differences of the obtained features. ANOVA uses F-tests to statistically test the equality of means, by measuring a ratio of group variances. A result of ANOVA analysis – a sum of squares, degrees of freedom, mean squares, F-value and p-value. The F-value which is the ratio of mean squares between groups to mean squares within groups indicates the degree of group difference. A probability (p-value) is in inverse proportion to the F-value, and it means the error probability when the group difference is not significant, i.e., indicating a risk in a percentage of concluding that a difference exists when there is no actual difference. A threshold for significance is denoted as alpha significance level; generally, when the p-value is below 0.05, it is considered as the significance level in statistics. Moreover, a sum of squares, degrees of freedom and mean squares are interim parameters used to calculate values of F and p, and they could not reflect the group difference intuitively (Freund, Littell 1981; Guyon, Elisseeff 2003; Mertler, Reinhart 2016). Based on the guidelines by Cohen (2011), the alpha significance level in our experiment was set to 0.05.

2.1.1. Electrocardiogram Signals Preprocessing and Peak Detection

A goal of this research was to investigate an effect on a heart rate with three different levels of SoP. Heart rate was extracted from an ECG signal using Pan-Tompkins algorithm, then the statistical parameters for three different levels of SoP were calculated. Results were investigated using statistical analysis tools. In this subsection methods used for the feature extraction and preprocessing of the ECG signal are presented.

ECG signals investigated in this experiment were recorded by Perrin *et al.* (2016) using two standard ECG electrodes placed on the lower right rib cage and the upper left clavicle. A sample of a collected ECG signal is shown in Fig. 2.3. A heart rate from the ECG signal can be calculated using RR intervals, which can be easily detected in the signals without significant abnormalities. RR interval is a duration between two consecutive heartbeats measured at their R wave peaks. Thus a heart rate is an inverse of RR interval, which, in our research, was averaged for the episodes of 60 seconds. An ECG signal frame with nine R wave peaks is shown in the bottom graph of Fig. 2.3. A test sequence includes a baseline period and stimulus. Stimulus begins at the 0 s mark.

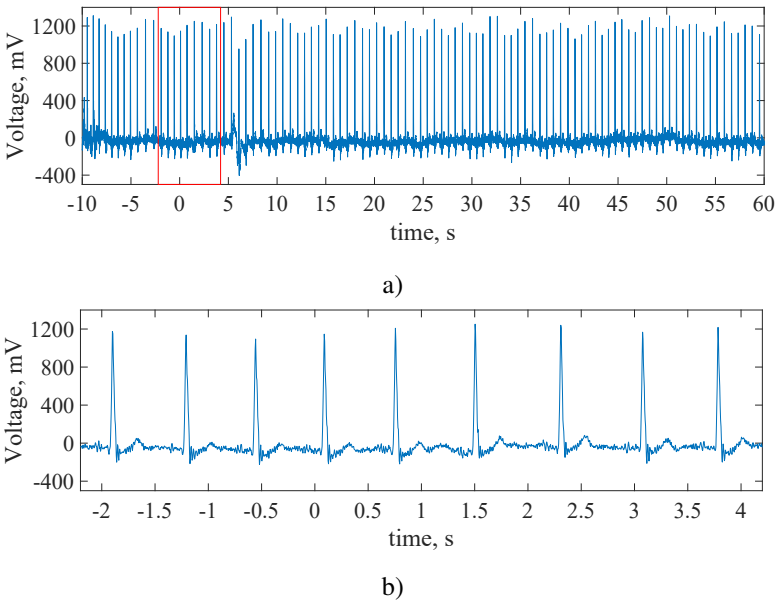

Fig. 2.3. Electrocardiogram signal of a test sequence: a) raw electrocardiogram signal; b) its frame of 6 seconds

ECG signals were filtered using Savitzky-Golay filter (Savitzky, Golay 1964). Savitzky-Golay filtering can be thought of as a generalized moving average. Filter coefficients are derived by performing an unweighted linear least squares fit using a polynomial of a given degree. For this reason, a Savitzky-Golay filter is also called a digital smoothing polynomial filter or a least squares smoothing filter. A higher degree polynomial makes it possible to achieve a high level of smoothing without attenuation of data features. The Savitzky-Golay filtering method is often used with frequency data or with peak data (Bronzino 1999; Oppenheim, Schafer 2014; Semmlow, Griffel 2014).

For frequency data, the method is effective at preserving the high-frequency components of the signal. For peak data, the method is effective at preserving higher moments of the peak such as the line width. By comparison, the moving average filter tends to filter out a significant portion of the signal's high-frequency content, and it can only preserve the lower moments of a peak such as a centroid. However, Savitzky-Golay filtering can be less successful than a moving average filter at rejecting noise (Lascu, Lascu 2008).

According to the guidelines provided by Krishnan, Seelamantula (2013) and experimental results of our data Savitzky-Golay filter was designed with the polynomial order of 8 and frame size of 31. A power supply noise was filtered using second-order notch filter with Q-factor set to 30. A sampling rate of the ECG signal was 250 Hz. Signals were divided to intervals of 70 seconds: 10 s of baseline period and 60 s of stimulus period. A filtered ECG signal is shown in Fig. 2.4. A test sequence includes a b aseline period and stimulus. Stimulus begins at the 0 s mark.

The slope of the R wave is a common signal feature used to locate the QRS complex in many QRS detectors. The Pan-Tompkins algorithm (Pan, Tompkins 1985) was used on the denoised ECG signal for the detection of the QRS complex. It analyzes the slope, amplitude, and width. Fig. 2.5 shows an ECG signal with heartbeat annotations, which are marked using a circle. A test sequence includes a baseline period and stimulus. Stimulus begins at the 0 s mark.

The algorithm consists of four steps. In the first step, the low pass and high pass filters form a bandpass filter, which reduces noise in the ECG signal. In the second step, to distinguish QRS complexes from low-frequency ECG components such as the P and T waves, the signal is passed through a differentiator to highlight the high slopes. The third step is the squaring operation, which places stress on the higher values that are mainly present because of QRS complexes. Then, the squared signal passes through a Moving-Window Integrator of the desired length, which is typically around 150 ms. Using adaptive detection thresholds, refractory period and a search back for missed beats a smooth peak ECG cycle is obtained (Luz *et al.* 2016).

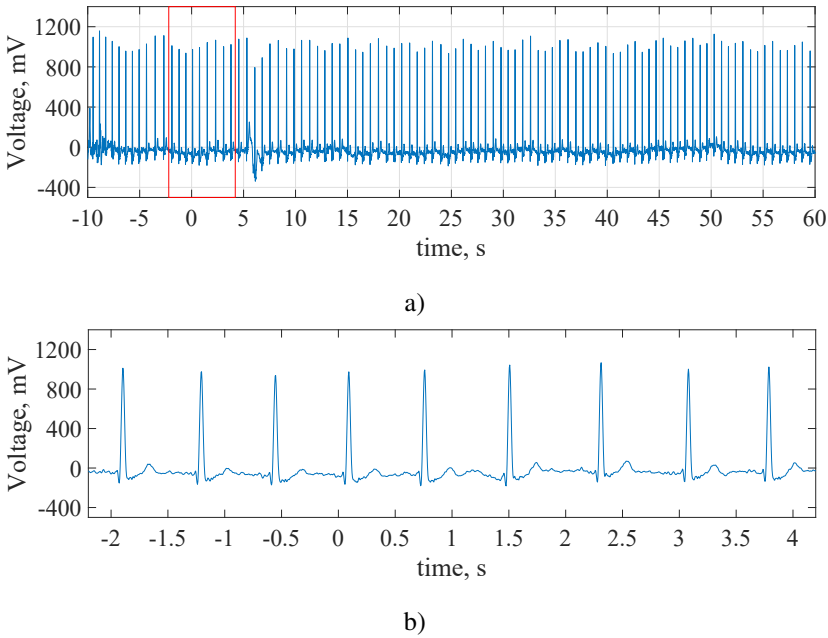

Fig. 2.4. Electrocardiogram signal of a test sequence: a) filtered electrocardiogram signal; b) its frame of 6 seconds

The refractory period and energy threshold parameters were adjusted manually according to the obtained data. The refractory period for the algorithm was set to 250 ms, it was not modified from the default value. However, the energy threshold for the detector was reduced to 0.35 (arbitrary units). 10% of randomly selected ECG signals were inspected visually, the algorithm successfully detected all of the heartbeats in the visually inspected data. The algorithm detected 83 heartbeats after the baseline period. Thus, a heart rate of a subject during the trial was 83 bpm.

2.1.2. Electroencephalogram Signal Preprocessing and Analysis

The goal of this research was to investigate an effect on a brainwave activity with three different levels of SoP. Brainwave activity was extracted from an EEG signal, the statistical parameters for three different levels of SoP were calculated. Results were investigated using statistical analysis tools. In this section methods used for the feature extraction and preprocessing of the EEG signal are presented.

An EEG signal has a frequency content ranging from 0.01 to around 100 Hz and varies from a few microvolts to approximately 100 μV, but the amplitude may

be well above this, especially when corrupted by non-cerebral activity. The slow components around 0.01 Hz correspond to slow cortical potentials that in clinical routine are usually filtered out (Urigüen, Garcia-Zapirain 2015). When investigating the effects of SoP, Gamma waves (30–100 Hz) usually are not investigated for various reasons, such as the high possibility of mismeasurement (Whitham *et al.* 2008, 2007; Yuval-Greenberg *et al.* 2008). Additionally, the energy of background EEG is more concentrated in the lower range of the spectrum (Daly *et al.* 2012). In fact, its frequency content is known to present a decay inversely proportional to the frequency ($1/f^{\alpha}$, with α approximately 1) (Goncharova *et al.* 2003; Urigüen, Garcia-Zapirain 2015; Vos *et al.* 2010).

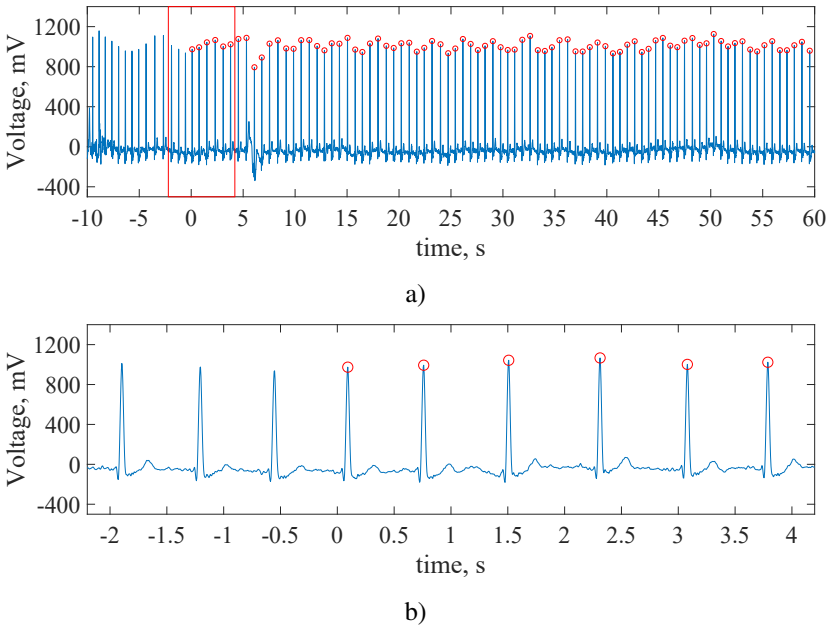

Fig. 2.5. Electrocardiogram signal of a test sequence: a) filtered electrocardiogram signal with heartbeat annotations; b) its frame of 6 seconds

Artifacts are undesired signals that may introduce changes in the measurements and affect the signal of interest. While the ideal way of working with an EEG signal is to avoid the occurrence of artifacts when recording (Minguillon *et al.* 2017) the EEG signal is unfortunately often contaminated with various physiological factors other than cerebral activity, which are typically not of interest. For instance, cardiac activity, ocular movements, eye blinks and muscular activity are among the most common kinds of artifacts (Daly *et al.* 2013, 2012; Muthukumaraswamy 2013; Sood *et al.* 2013; Urigüen, Garcia-Zapirain 2015).

An EGIs Geodesic EEG System 300 was used to record, amplify, and digitize the EEG signals. The EEG data were obtained from 256 electrodes placed at the standard positions on the scalp. The duration of each episode was 1 min. EEG signals were sampled at 250 Hz. This dataset was acquired by Perrin *et al.* (2016). Electrodes with impedances higher than $50\ \Omega$ were removed from further processing. Afterward, the episodes were filtered using 4^{th}–order digital Butterworth bandpass filter with cutoff frequencies between 0.01 Hz and 40 Hz. The EEG Signals were referenced the Cz electrode and re-referenced to the common average. Each episode had a baseline period of 10 s recorded. This period was used to perform a baseline correction and later it was removed from the further processing and analysis. To eliminate the presence of artifacts wavelet ICA (wICA) method (Castellanos, Makarov 2006) was used, two default parameters were modified: a threshold multiplier was reduced to 0.5 and fastICA algorithm (Hyvarinen 1999; Hyvärinen, Oja 2000) was used for the extraction of ICA components.

Spectral analysis of the EEG signal was carried out using multi-taper Fourier transform (Thomson 1982). The method uses orthogonal windowing functions, known as Slepian tapers, and then computes a weighted average of the obtained spectra (Gramfort *et al.* 2014). Using a set of tapers rather than a spectral window, or a unique data taper, allows us to reduce the variance of a spectral estimate (Haykin *et al.* 2005). Spectral analysis was performed on the entire episode of video stimuli (60 s). For the efficient use of the fast-Fourier transform algorithm signals were zero-padded. Therefore, investigated EEG signals were zero padded to 2^{14} or 16384 samples. Spectral analysis has been applied using the Fieldtrip toolbox (Oostenveld *et al.* 2011).

Power spectral density was calculated for five frequency bands: theta (4–7 Hz), alpha (8–12 Hz), beta low (13–16 Hz), beta middle (17–20 Hz) and beta high (21–29 Hz). Median power of each frequency band range was used to represent frequency bands. EEG electrodes were manually clustered into ten regions of the brain for the analysis: left and right frontal, left and right central, left and right parietal, left and right occipital, left and right temporal ones (Andreassi 2010; Idris *et al.* 2014). Thus, for each subject, a total of 50 features were extracted to represent tendencies in terms of power for each brain region and frequency band.

2.2. Results of Sense of Presence Detection

In this section, the results of the theoretical investigation of the Sense of Presence Detection are provided. This section is divided into two subsections. The first subsection contains the results of the heart rate investigation. The second subsection contains the results of the brain activity investigation. Results are discussed in the following section.

2.2.1. Results of the Heart Rate Investigation

In this subsection results of the investigation of the heart rhythm with different levels of SoP are described. Heart rhythm was measured in bpm. Average heart rate for each session, ANOVA results, as well as box plot, are presented in the remaining of this subsection.

Average heart rate was calculated using RR intervals of the detected heartbeats; afterwards, a calculated heart rate was averaged over nine trials, then across 20 subjects. Therefore, in total 180 of observations were used to calculate average heart rate for each level of SoP. As a result, one-way ANOVA was conducted using a total of 540 observations with three groups.

Table 2.1 shows the average heart rate for each level of SoP. Subjects consuming the low level of SoP had an average heart rate of 70.80 bpm and the standard deviation was 5.59 bpm. The average heart rate of the subjects consuming the middle level of SoP was 69.04 bpm and having the standard deviation of 5.58 bpm. The average heart rate during the high level SoP session was 67.85 bpm and the standard deviation was 6.23 bpm. Presented values were rounded to two digits after the decimal point.

Table 2.1. Average heart rate during consumption of three different levels of sense of presence, with respective standard deviation. Results were rounded to two digits after the decimal point. Results are presented in beats per minute

Level of SoP	Low	Medium	High
Mean heart rate, bpm	70.80	69.04	67.85
Standard deviation, bpm	5.59	5.58	6.23

One-way ANOVA was used to investigate the effect of the heart rate on different levels of SoP. ANOVA results are shown in Table 2.2. ANOVA was conducted between: low and middle; middle and high; low and high; low, middle and high levels of SoP. A significant difference (significance level was 0.05) of a heart rate were found between low, middle and high levels of SoP ($p = 0.032$). Also, a significant difference in heart rate was found between low and high levels of SoP ($p = 0.008$). However, heart rate of the subjects was not significantly different between low and medium ($p = 0.15$) and between medium and high ($p = 0.249$) levels of SoP.

Box plot of the ANOVA results is shown in the Figure 2.6. Black circle markers denote the average values of each investigated SoP group. Horizontal lines denote medians of the SoP groups.

Table 2.2. ANOVA results of each group. Significant values are highlighted ($p < 0.05$). Results were rounded to three digits after the decimal point

Level of SoP	F statistic	p-value
Low and medium	2.09	0.150
Medium and high	1.34	0.249
Low and high	7.03	**0.008**
Low, medium and high	3.47	**0.032**

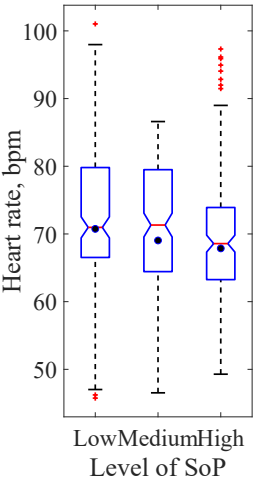

Fig. 2.6. Box plot of a heart rate collected during three different levels of sense of presence. Black circle marks the average value of each session. Each sense of presence level consisted of 180 observations during, involving 20 subjects and nine sessions

A difference between median values of low-level (70.97 bpm) and middle-level (71.32 bpm) SoP groups is 0.35 bpm. However, a difference between their average values is 1.76 bpm. Moreover, median value of middle-level SoP is higher than low-level SoP group. Median value of high-level SoP is 68.57 bpm and average value 67.85 bpm. The low-level group of SoP has three outliers, the middle-level group has no outliers, and the high-level SoP group has eight outliers, which all are above the upper adjacent.

2.2.2. Results of the Brain Activity Investigation

In this subsection results of the investigation of the brain activity with different levels of SoP are described. Brain activity was measured for ten regions using spectral analysis, distributing brain activity into five frequency bands, specifically:

theta, alpha, beta Low, beta middle, and beta high. Power spectral density of EEG signal during the consumption of different levels of SoP and ANOVA results are presented in this subsection.

Power spectral density was estimated for ten different regions: the left and right frontal, parietal, central, temporal and occipital regions. Each investigated region is illustrated in separate subfigures, shown in Fig. 2.7. The low level of SoP is represented using red color, the medium level of SoP is represented using green color, and the high level of SoP is represented using blue color.

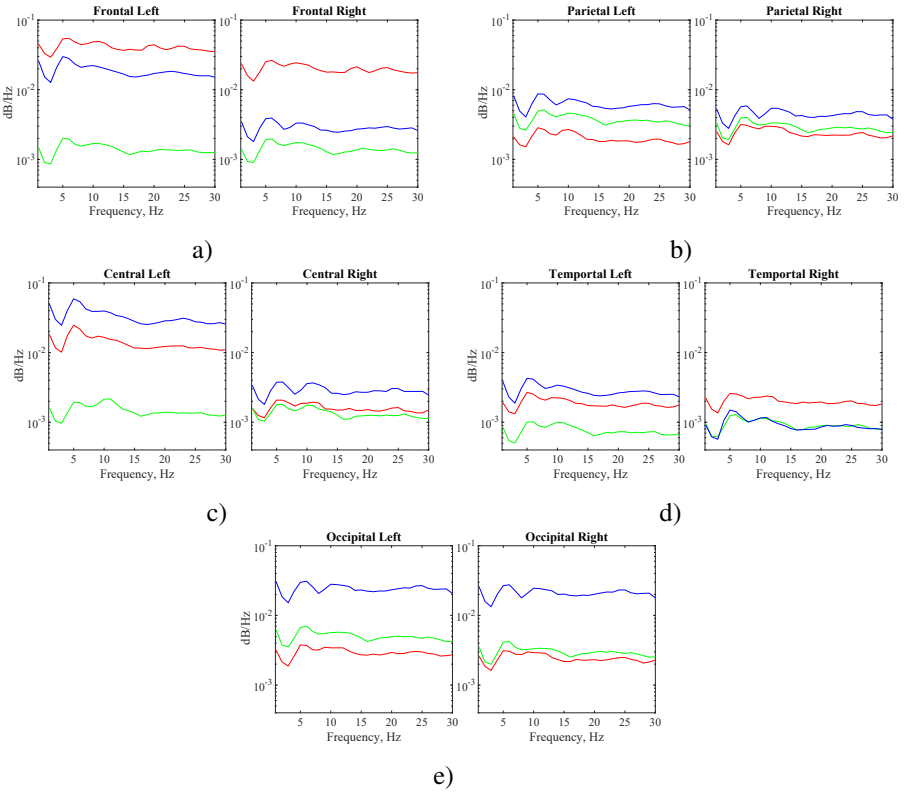

Fig. 2.7. Illustration of the power spectral density estimated using electroencephalogram signal during the consumption of three different levels of sense of presence. Brain activity of: a) frontal region; b) parietal region; c) central region; d) temporal region; e) occipital region

ANOVA analysis, comparing the effect of different level of SoP on the brain activity was carried out to the 50 brain band and region combinations. Each combination consisted of 540 observations (three sessions, twenty subjects, and nine

trails). Results are shown in Table 2.3. Presented values were rounded to three digits after the decimal point, significant values ($p < 0.05$) were highlighted, values less than 0.001 are presented as "<0.001".

Table 2.3. ANOVA results of electroencephalogram signals with significance level $\alpha = 0.05$, bold font denotes significant values. Results were rounded to three digits after the decimal point

Frequency band		Theta	Alpha	Beta low	Beta middle	Beta high
Frontal	Left	**<0.001**	**<0.001**	0.091	**<0.001**	0.283
	Right	**0.004**	**0.014**	**0.005**	**0.026**	0.104
Parietal	Left	**<0.001**	**0.002**	**<0.001**	0.191	**0.041**
	Right	**<0.001**	**0.009**	**<0.001**	0.680	**<0.001**
Central	Left	**0.004**	**<0.001**	0.770	0.230	0.334
	Right	**0.045**	**<0.001**	0.367	0.981	0.352
Temporal	Left	**<0.001**	0.182	**<0.001**	0.726	**<0.001**
	Right	**<0.001**	**0.009**	**<0.001**	0.466	**<0.001**
Occipital	Left	**0.027**	**<0.001**	0.739	0.751	0.789
	Right	**0.011**	**<0.001**	0.968	0.717	0.448

Based on the results of the statistical analysis, there is no significant difference ($p > 0.05$) in the beta high activity of the frontal region. However, this study have found a significant difference ($p < 0.05$) in theta, alpha, beta low and middle bands, except of the frontal left region in beta low frequencies where the p-value was 0.09, though the left frontal region showed lower p-values ($p < 0.001$) than those of the right region in theta, alpha, and mid beta frequencies.

Regarding the parietal region a significant difference ($p < 0.05$) was found in theta, alpha, beta low and beta high frequency bands, yet no significant difference ($p > 0.1$) was found in the beta middle oscillations of the parietal region.

Moreover, this study found that the different level of SoP significantly changes activity in theta and alpha bands of the central region ($p < 0.05$), but no significant difference ($p > 0.2$) was found in the beta oscillations.

The temporal region in theta, beta low and beta high-frequency band activity showed a significant difference ($p < 0.001$) when changing the level of SoP. Also, a significant difference ($p = 0.009$) was found in alpha band brain activity of the right temporal region. However, no significant difference was found in beta middle oscillations ($p > 0.4$) of the temporal region and alpha oscillations ($p = 0.18$) of the left temporal region.

Regarding the occipital region, there was a significant difference in alpha, and theta frequency bands found ($p < 0.01$) with the change SoP level and no significant difference ($p > 0.4$) in beta bands (low, medium and high).

2.2.3. Discussion of the Results

In this chapter, the relationship between different levels of SoP and the heart activity, measured using ECG signal, was investigated. Average heart rate calculated using ECG signals was analyzed, and significant changes were found when users were consuming content with different levels of SoP. ANOVA results revealed significant difference ($p = 0.008$) between low and high level of SoP. However, ANOVA did not show a significant difference in heart rate between low and medium or high and medium levels of SoP. It suggests that evaluating the level of SoP objectively is difficult, only profoundly separated levels of SoP shows a significant difference in the heart rate.

Moreover, this study showed, that average heart rate decreases when subjects are consuming content with higher levels of SoP. However, heart rate during the consumption of high level SoP had the highest standard deviation and eight outliers, all above upper adjacent. In comparison, the standard deviation of the heart rate was lower when medium and low SoP level content was consumed. Furthermore, only the low level of SoP had three outliers, while the medium level of SoP had no outliers. Thus, this effect may be interpreted in terms of user experience: as the level of SoP is getting higher, the consumed content tends to be more realistic and lifelike, therefore affecting subjects more prominently, raising a heart rate when consuming thrilling or stimulating content, and reducing heart rate when consuming relaxing, peaceful content.

Furthermore, in this study, the relationship between a different level of SoP and brain activity, measured using EEG signal, was investigated. A spectrum of EEG signals was analyzed, and significant changes were found in θ power for all investigated brain regions, specifically: the frontal, parietal, central, temporal and occipital. In literature, it is proposed that θ activity is related to the arousal and sensorimotor processing and its mechanisms to keep track the location within the environment. Also, it is linked to mechanisms of memory and learning. Thus, higher levels of SoP should induce different θ activity. However, this study has not found distinct regions of the theta activity with the respect of the SoP level.

In addition, a significant difference was found in α band activity of the frontal, parietal, central, occipital and right temporal regions. In literature α waves were shown to indicate brain activation during emotional processes, it implies that a higher level of SoP can induce greater emotional involvement.

Finally, a significant difference was found in β_{l} power of the frontal right, parietal and temporal regions. β_{m} activity showed a significant difference in the

frontal region. β_{m} oscillations are linked with enchanted mental activity. β_{h} band activity is associated with high levels of arousal, cognitive fatigue. Thus, results show that changes in β_{h} power of the temporal and parietal lobe might indicate cognitive fatigue due to the different level of SoP.

2.3. Conclusions of Chapter 2

1. According to the investigation, the electrocardiogram and electroencephalogram signal based features can be used for the SoP level detection of the presented audiovisual content.
2. Results of the heart rate investigation showed that the estimated heart rate from the electrocardiogram signal can be used as a feature to distinguish between low and high SoP level when there are three SoP levels of an audiovisual content presented to the user.
3. According to the brain activity investigation, power density spectrum of the electroencephalogram signal in the β frequency range should be divided into subranges of β_{l}, β_{m} and β_{h} in order to use β frequency range based features to distinguish between an audiovisual content with three SoP levels.
4. Based on the results of the statistical analysis, an electroencephalogram based features can be used to distinguish between three levels of SoP when a user is presented with an audiovisual content. Such features are:
   - 4.1. the relative α power of the frontal, parietal, central, occipital and right temporal regions;
   - 4.2. the relative β_{l} power of the frontal right, parietal or temporal regions;
   - 4.3. the relative β_{m} power of the frontal region;
   - 4.4. the relative β_{h} power of the temporal or parietal regions.

3

Experimental Research of Visual Comfort Detection

In this chapter the results of the second and third tasks are presented. The experimental research of visual discomfort detection using features obtain by measuring physiological signals are presented. This research aimed at finding how stereoscopic images with a different level of visual comfort affects brain activity and pupillometric features. Brain activity was measured as an EEG signal using a consumer-grade device, from the frontal lobe. Pupillometric features were estimated from gaze data, obtained using an eye tracker. Stereoscopic images used in this research were collected by Jung *et al.* (2013). Authors of the paper, through subjective measurements, showed that images have significantly different levels of visual comfort. In this experiment, the IVY LAB database (Jung *et al.* 2013) was extended with annotated single-sensor EEG data and gaze data collected from 28 control subjects. Additionally, subjects indicated a time of depth perception for each image and reevaluated the visual discomfort of the stereoscopic images.

The research results, presented in this chapter are published in three papers (Abromavičius *et al.* 2018; Abromavičius, Serackis 2018; Abromavičius, Serackis 2017;) and presented at international "DAMSS" (Druskininkai, 2017) and national "Science – Future of Lithuania" (Vilnius, 2018) scientific conferences.

3.1. Objectives of the Experiment

This investigation aimed at identifying a set of visual comfort-related features, which could be estimated using an eye-tracking device and a consumer-grade EEG sensing device. Research results on subjective evaluation of stereoscopic images, taken from IVY LAB 3D image database (Jung *et al.* 2014, 2013), were analyzed in several works (Shao *et al.* 2017; Xu *et al.* 2018; Zhang *et al.* 2016). In recent years, subjective evaluation was used as a reference for the development of objective assessment methods, based on the human visual system, binocular disparity evaluation, blur, spatial frequency (Jiang *et al.* 2016; Yang *et al.* 2019; Zhou *et al.* 2018). Jiang *et al.* (2017a,b), in their work, introduced disparity features, such as magnitude, contrast, dispersion, skewness, and also combined with the oscillatory activity of the middle temporal area, for the assessment of visual discomfort. Performance of their method was evaluated on NBU S3D-VCA (Jiang *et al.* 2015) and IVY LAB 3D (Jung *et al.* 2013) stereoscopic image databases.

Four objectives were formulated to achieve the aim of the investigation. The first objective was to estimate the number of focus points in an image for a user before the DPM occurs and how the number of focus points changes with the visual comfort level. The second objective was to determine a relative pupil size during analysis of the stereoscopic image of the investigated dataset, and how it varies with the visual comfort level, assigned to the image. The third objective was to examine the relationship between eye disparity, measured at the focus point, and image visual comfort level designated by the user. The fourth objective was to measure and analyze the EEG activity from the frontal lobe and investigate how this activity changes with the level of visual comfort. We predicted that the number of focus points, the pupil size, the eye disparity and the activity of EEG would be affected by different visual comfort levels since natural mechanisms of binocular vision are violated with the usage of artificial stereoscopic cues.

In the second section stimuli, subjects, signal acquisition, subjective assessment, signal processing methods applied in this research will be presented. Additionally, in the subsections of this section a procedure of the experiment, estimated features, and methods for analyzing these features will be discussed. In the third section, the results of the research will be presented. The presented results are divided into two subsections – the first subsection contains the results of the investigation with gaze signals, and the second subsection contains the results of the investigation with the EEG signals. The fourth section contains a discussion of the results. Finally, conclusions are presented in the last section.

3.2. Visual Comfort Detection Methods

In this investigation, a group of 28 volunteers was invited to perform a set of individual tests on the IVY LAB stereoscopic image dataset (Jung *et al.* 2013). This dataset of 120 stereoscopic images was selected in order to compare subjective evaluation results with other studies. During the experiment, each participant was asked to indicate the moment of the visually comfortable depth perception (DPM) and afterward rate the image comfort level from 1 to 5 (5 is for the highest visual comfort). Information about the time when the participant reaches a stable depth perception (identifies a stereoscopic depth of the stimulus) is relevant in situations when content is changed suddenly, or a different level of visual comfort is induced. In their study, Hoffman *et al.* (2008) showed that in addition to increased viewers fatigue and discomfort, distortions in 3D displays also increases the time required to identify a stereoscopic stimulus.

A contribution of this section is a systematic approach for the feature extraction from the EEG and gaze signals. An experiment was designed to measure physiological signals while subjects were consuming stereoscopic stimuli. Additionally, subjective evaluations of DPM and visual comfort were obtained. General outline of the experiment is illustrated in Fig. 3.1. Details about the methodology of the experiment, description of the stimuli, equipment used to collect the physiological signals, information about the participants and subjective assessment procedures are described in the following subsections. However, detailed information about the stereoscopic images can be found in the original paper by Jung *et al.* (2013).

3.2.1. Stereoscopic Visual Stimuli

The IVY LAB stereoscopic 3D image database (Jung *et al.* 2013) of 120 stereoscopic images was used for investigation. Level of the visual comfort of each image was rated by the subjects on a scale from 1 to 5 (extremely uncomfortable to very comfortable). This dataset contains stereoscopic images with urban, nature, indoor objects including humans and non-living entities, as shown in Fig. 3.2. Image resolution was 1920×1080 pixels with the magnitude of crossed disparity ranging from 0.11 to 5.07 degrees. Moreover, this dataset was used in other research works regarding visual comfort, e.g., Sohn *et al.* (2013) designed an object-dependent model to predict visual discomfort, Xu *et al.* (2018) introduced a visual discomfort prediction model based on the mechanisms of neural activity, Oh *et al.* (2017) introduced a process of blurring and parallax shift to reduce visual discomfort.

Stereoscopic visual stimuli were shown on a 1280×1024 resolution screen with a 60 Hz refresh rate. The stereoscopic 3D effect was produced by using anaglyph red and blue image encoding. Thus, to achieve the stereoscopic 3D effect,

the participants were wearing red-blue filter glasses. Encoded images are shown in Fig. 3.3. Images in Fig. 3.3a have lower stereoscopic disparity and most subjects evaluated such images as visually comfortable; images in Fig. 3.3c have larger disparity, therefore most subjects evaluated such images as visually uncomfortable.

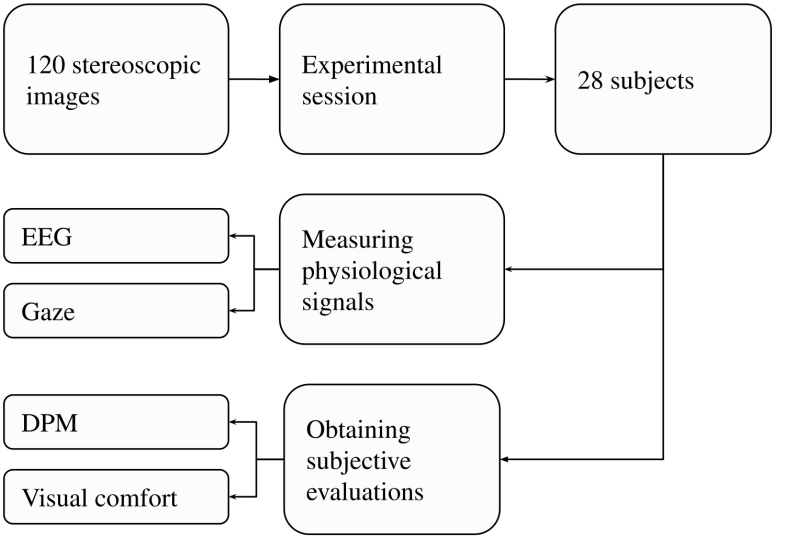

Fig. 3.1. Structure of the experiment. More detailed illustration of the experimental session is given in Fig. 3.4

Anaglyph technology is traditionally considered more prone to crosstalk, as shown in the study of Terzic, Hansard (2017). However, a study from 2013 claims that crosstalk is lower on passive displays than on active displays (Yun *et al.* 2013). Another study found no significant difference between active and passive stereo displays (Wang *et al.* 2011). Therefore, usage of the anaglyph system enables to accumulate more factors causing visual discomfort and visual fatigue. More factors increase the possibility to detect changes in the analyzed features.

3.2.2. Subjective Assessment

A group of 28 subjects (25 males and three females) participated in this experiment as volunteers. Subjects received no rewards or compensations for their participation. Their age varied between 19 and 37 years old, with an average of 22 (with a standard deviation of 4). All volunteers were informed about the procedure, goals, and the subjective assessment phase of the experiment. Furthermore, all subjects have signed consent forms and orally expressed that they were ready to begin the experimental session.

Fig. 3.2. Right eye stimuli of the IVY LAB stereoscopic 3D image database

The visually comfortable stereoscopic view is easy to find and quickly focuses on the point in the image at which depth perception is comfortable, as images in Fig. 3.3a. There is no object in such images, for which focusing is hard to complete. However, in some stereoscopic images, focusing on the object is challenging and takes more time, as shown in Fig. 3.3c. During the experiment, participants were asked not only to rate images according to the visual comfort but also to fix the moment at which focusing on the object was successful. The time when each subject registered this moment of focus was marked as a depth perception moment (DPM).

During each trial the DPM was collected in the first phase, to measure when the subjects achieved depth perception. The visual comfort score was collected in the 2nd phase – after each stimulus subjects were asked to assess the level of visual comfort. The subjective assessment was carried using the Single Stimuli adjectival categorical judgment method of ITU-R BT.500-13. Grade level of visual comfort was in five-grade scale from 1 (extremely uncomfortable) to 5 (very comfortable).

After the experiment, the reliability of the subjects was qualitatively evaluated by using the procedures described in ITU-R BT.500-13. Unreliable voting parameters were not found for any of the participants. However, four subjects' data were discarded due to faulty reference connection (for one subject), measurement

errors which led to substantially decreased sampling rates (for two subjects) and failure to pass the color blindness test (for one subject). Consequently, records of 24 subjects' were used for this study.

3.2.3. Setup of the Experiment

Subjects were seated in front of the 17-inch screen in which stereoscopic images were shown. Sitting distance from the screen was approximately 70–80 cm. To simulate real-life conditions, head and body motions were not restricted; when the instructions about the experiment were given, subjects also were reminded to sit freely and comfortably. Additionally, subjects were encouraged to wear corrective lenses. Furthermore, each volunteer, if desired, could select a musical background.

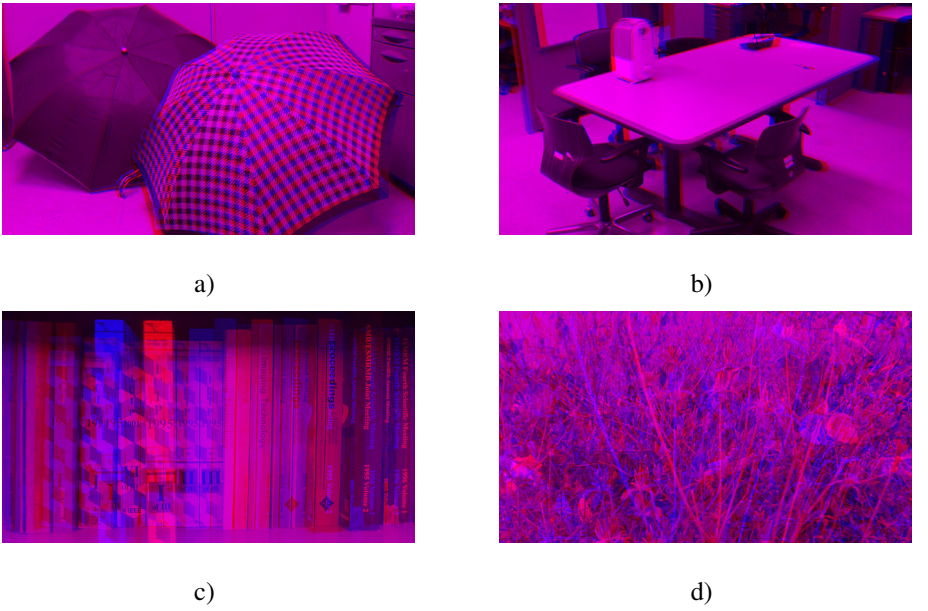

a) b) c) d)

Fig. 3.3. An example of the encoded stereo pairs of comfortable and uncomfortable stimuli: a) visually comfortable stimuli of indoors; b) visually comfortable stimuli of a table; c) visually uncomfortable stimuli of indoors; d) visually uncomfortable stimuli of outdoors

Structure of the conducted experiment is shown in Fig. 3.4. When subjects received information about the experiment, signed consent forms and vocally agreed to participate in the experiment the EEG sensor and glasses were mounted. All subjects were screened for normal color vision, and normal visual acuity, using

Ishihara Color Vision and Fine Stereopsis tests (ITU-R BT.2021-1), respectively. To stabilize the opinion of the subjects, a training session with five random presentations was introduced. The data received from this voting were not taken into account of the results. Afterward, the training session subjects were asked to complete the calibration procedures of the eye tracker, in order to receive accurate results for the experiment. Finally, before the test session, the individual baseline EEG activity of the subjects was measured.

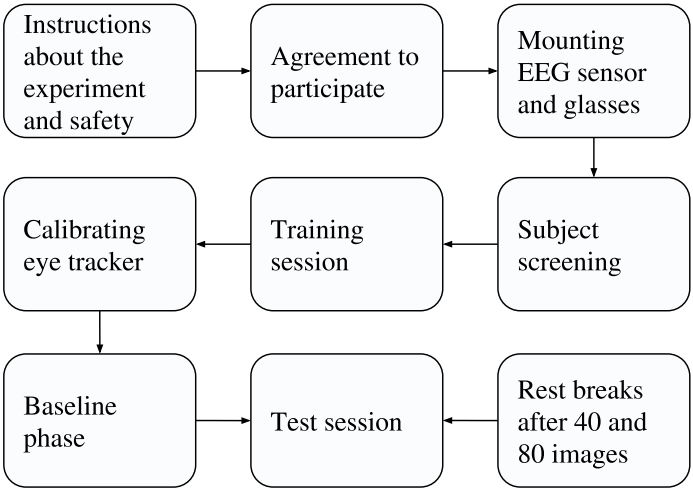

Fig. 3.4. Setup of the experiment

The test session of the experiment consisted of 120 trials. Order of the displayed images to the subjects during the experiment was randomized. A single trial of the test session is shown in Fig. 3.5.

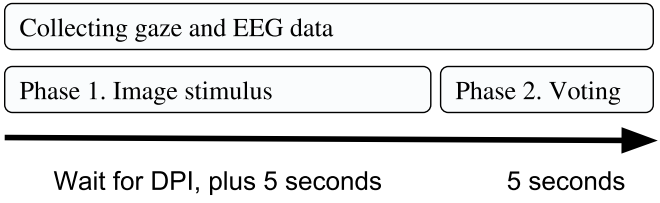

Fig. 3.5. A single trial of the test session

Physiological signals, specifically the eye tracker data and single-sensor EEG, were measured during the test session, except for the resting periods. The experiment is divided into two phases. During the first phase, participants were

instructed to press the spacebar key as soon as they had perceived the depth of the shown stereoscopic 3D content. A stereoscopic stimulus was displayed for the subject 5 seconds more after the DPM input. Directly after the first phase, an evaluation screen was shown to the subjects for 5 seconds. Subjects were informed that they can stop for a rest or quit the experiment at any time. Also, two resting periods of at least 30 seconds, after 40 and 80 images, was mandatory. The total duration of the experiment was approx. 40 minutes. The experimental procedure, anaglyph stereo rendering, timing, and keyboard input controls were implemented using Psychtoolbox software tools (Pelli 1997).

3.2.4. Eye Tracker Signal Preprocessing and Feature Extraction

A goal of this research was to investigate the effect of the EEG and gaze signal based features with different levels of visual comfort. Five feature sets were extracted from the gaze data, and their changes analyzed using statistical analysis tools. In this subsection feature extraction from eye tracker data and their processing will be presented.

Gaze signals were collected using Tobii T120 eye tracker. This eye tracker uses infrared illumination to create reflection patterns on the cornea and pupil of the eye, while image sensors capture images of the eyes and reflection patterns. Tracker supports binocular tracking and allows head movements within a certain area.

Knowing the size of the pupil and changes over time is often used when studying accommodation time to stimuli. The eye tracker used in this research allows measurements of the position of the eyes as well as the pupil size. The optical sensor registers an image of the eyes which then is used to calculate the eye model. As the eye model used by the eye tracker provides data about the distance between the eye and the sensor, the firmware can calculate the pupil size by measuring the diameter of the pupil on the image and multiply it with a scaling factor.

Several definitions exist regarding what should be defined as the size of the pupil. In the eye model used by Tobii Eye Tracker, the pupil size is defined as the actual, external physical size of the pupil. However, in most scientific research the actual size of the pupil is less important than its variations in size over time (Brisson *et al.* 2013; John *et al.* 2018; Ukai, Howarth 2008). Inoue, Ohzu (1997) found that changes in pupillary responses to a stereoscopic 3D display was elicited by convergence and moved to the stereoscopic distance on the 3D image.

In order to estimate a gaze point and gaze direction with high precision, the eye tracker firmware adapts the algorithms to the person sitting in front of the eye tracker. This adaptation is made during the calibration process when the user is looking at points located at known coordinates on display. Thus, each subject completed a calibration procedure with five calibration points. The calibration

points spanned the display area where the stimuli are to be shown in order to ensure proper interaction.

The eye tracker measured eye position, gaze point and pupil diameter of each eye at a rate of 60 Hz. Using these measurements following features were calculated for the investigation:

- gaze point – calculated as a center point of gaze coordinates of the individual measures taken from the left and right eye;
- the pupil size – the estimate of pupil diameter, calculated as a mean of the left and right eye, measured in millimeters;
- focus point – estimated from the spatial distribution of the gaze points. Each focus point was aggregated of gaze points which did not change their coordinates more than 5% of the screen dimensions over 0.2 seconds or more;
- binocular disparity – the horizontal distance between the left and right eye coordinates, calculated for each gaze point, measured as pixels; pixel size for our screen settings were 0.2634 mm;
- crossed disparity – the ratio of crossed gaze points to a total number of gaze points. Gaze point was marked as a crossed when the difference between horizontal gaze coordinates was negative. This ratio was calculated for each trial. It is more difficult to focus upon objects which require crossed disparity, objects with uncrossed disparity are less critical to visual attention Khaustova *et al.* (2014).

3.2.5. Electroencephalogram Signal Preprocessing and Analysis

The presented investigation aimed at indicating the dynamics in a single-sensor EEG signal activity before the user focuses on the point in the image at which the depth perception occurs and the EEG activity after that moment. Changes in the power spectrum of the EEG signals were analyzed at different frequency bands. The duration from the moment of a new image was presented to the user, the moment of focus, and successful depth perception varied from user to user and also depended on the visual comfort level for the image.

EEG signals were captured using consumer-oriented Neurosky Mindwave headset with a single electrode placed at the frontal lobe. This device is wireless, uses a dry sensor technology, therefore it is convenient to wear, to apply and to remove it. Neurosky Mindwave headset has been used in scientific research before, in areas, such as recognizing human emotions (Ursuţiu *et al.* 2018; Yoon *et al.* 2013), developing an attention aware system, which is capable of recognizing attention levels (Chen *et al.* 2017), detecting cognitive loading (Lin, Kao 2018). Further-

more, Maskeliunas *et al.* (2016) analyzed the abilities to use consumer-grade EEG units for control tasks and named some problems that should be taken into account before using them. In this investigation, it was analyzed EEG activity as a complementary feature for image comfort level classification. Therefore, the requirements for the accuracy of the headset was acceptable. Illustration of a raw ECG signal of a single trial is shown in Fig. 3.6. A trial consists of stimulus and voting phases, voting phase starts 5 s after the depth perception moment. Vertical line marks the depth perception moment, time is measured from the beginning of the experiment. Stimulus begins at the beginning of the plot (approx. at 346.2 s)

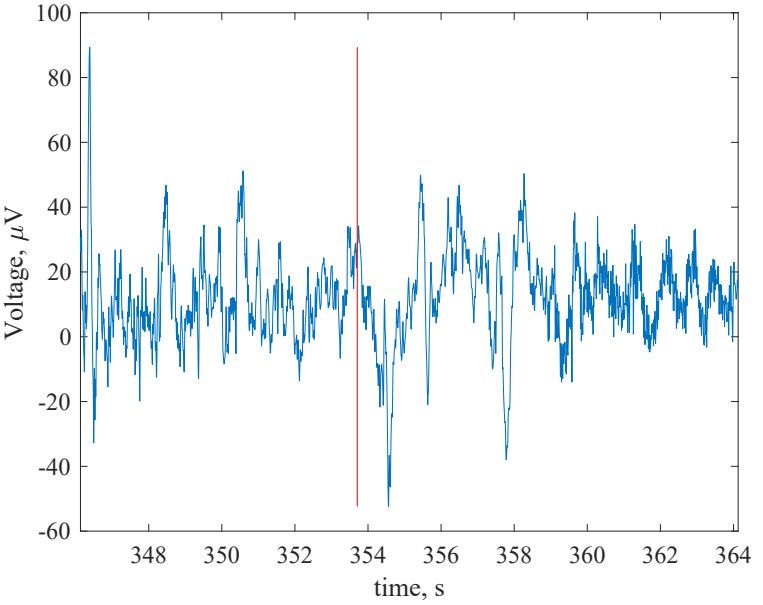

Fig. 3.6. Illustration of a raw electroencephalogram signal of a single trial

In addition to the features, estimated from the data provided by the eye-tracker, the dynamics in the single sensor EEG signal activity before the moment of DPM and after was evaluated. EEG signal activity as changes in the signal spectrum energy at different frequency bands was analyzed. The duration from the moment a new image was presented to the user to the moment the focusing, and successful depth perception varied from user to user and also depended on the image visual comfort level.

EEG is described regarding its frequency band. The varying amplitude and frequency of the wave represent various brain states (Carnegie, Rhee 2015), which depends on external stimulation and internal mental states (Terzic, Hansard 2017). The most common classification uses EEG waveform frequency (e.g., alpha, beta, theta, and delta). The signal captured from the headset had a sampling rate of 300 Hz and was additionally filtered using 4^{th} order digital Butterworth band-pass filter with cutoff frequencies between 0.01 Hz and 40 Hz. A filtered EEG signal is shown in Fig. 3.7. To remove ocular artifacts from the EEG signal, (wICA) based method (Castellanos, Makarov 2006). Based on visual inspection of the filtered signals, two minor modifications were made in the implementation of this method: reducing the threshold multiplier to 0.3 and selecting a fastICA algorithm for extraction of ICA components. Result of the ocular aftifact removal is shown in the Fig. 3.8.

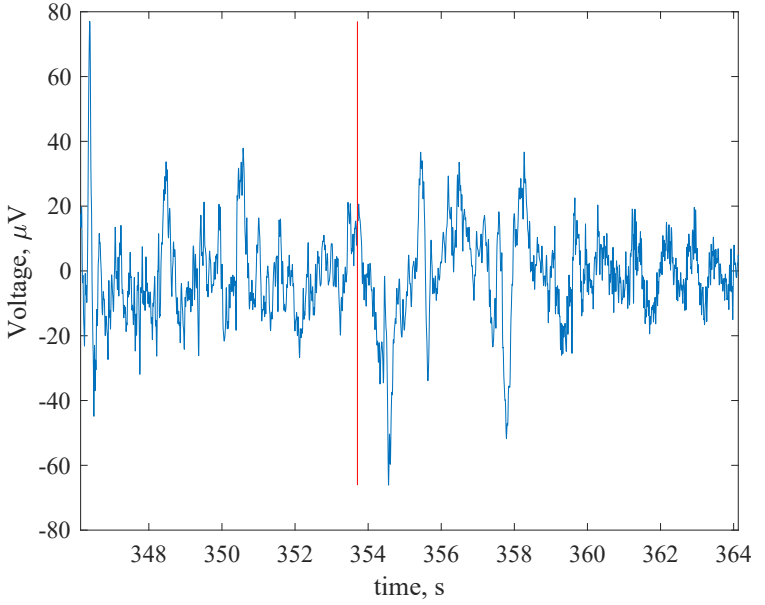

Fig. 3.7. Illustration of a band-pass filtered electroencephalogram signal of a single trial

For the time-frequency analysis of the single sensor EEG signal, the 'multitaper method' based on Slepian sequences as tapers was used. In this investigation the Oostenveld *et al.* (2011) implementation of this method was used. Frequency components in the range from 1 to 30 Hz with 1 s duration analysis time-frame was analyzed. Also, a 4 Hz spectral smoothing through multi-tapering was applied.

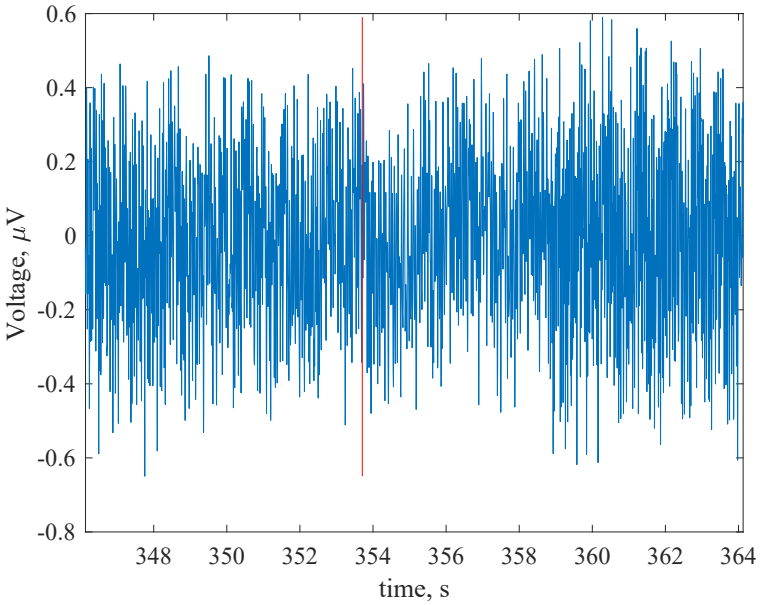

Fig. 3.8. Illustration of an electroencephalogram signal of a single trial, with ocular artifacts removed

Fig. 3.9 shows an EEG spectrogram of a single trial. Obtained frequency components were separated to theta (4–8 Hz), alpha (8–13 Hz), low beta (13–17 Hz), beta medium (17–21 Hz) and high beta (21–30 Hz) frequency bands. Afterwards, median power of each frequency band range was used to represent frequency bands.

3.2.6. Statistical Analysis Methods

The results of this experimental investigation from the viewpoint of the eye tracker based and EEG signal-based features to be used for automatic comfort level prediction was analyzed. Therefore, the time from image presentation start to the time DPM was indicated by the subject was compared, and the comparison of statistical similarity between the eye tracker and EEG signal features at different frequencies between different visual comfort levels was performed.

To accumulate the measurement results from different subjects on each image type (level of visual comfort), collected data was analyzed for six different time frames: “all pre-DPM”; 1, 2, 5 s pre-DPM; 5 s post-DPM and “full duration”. “All pre-DPM” time frame was used to analyze all data collected from the beginning of the stimuli to the moment of the DPM. This time frame is not consistent in

duration, which varies from a couple to tens of seconds, but it can describe eye activity features accumulated from the beginning of the stimuli to the moment of the DPM. “Full duration” time frame describes values for the whole duration of image presentation: from the beginning of the stimuli up to the subjective evaluation part.

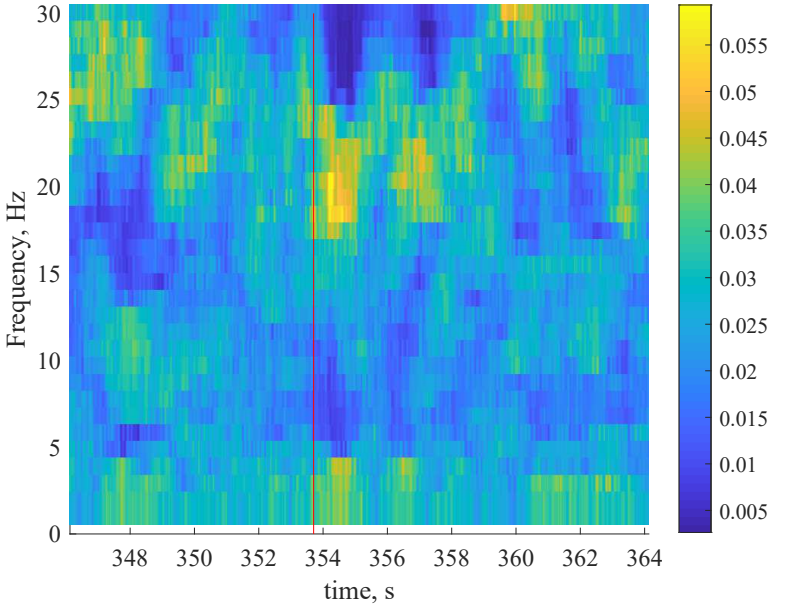

Fig. 3.9. Illustration of an electroencephalogram spectrogram of a single trial

Different visual comfort levels were investigated as an experimental parameter to find the changes in the brain activity and gaze features of the subjects. In the study, EEG signals were divided into five frequency bands. In order to find evidence of these changes one-way ANOVA, was performed. ANOVA uses F-tests to statistically test the equality of means, by measuring the ratio of group variances. Result of ANOVA analysis – F-statistic shows if the investigated groups are significantly different. The p-value measures the significance as a probability that the null hypothesis is correct. The small p-value, lower than the significance level, e.g., 0.05 or less shows that the null hypothesis should be rejected and it indicates that differences between group means are significant. In this experiment, the alpha significance level was set to 0.05.

3.3. Results of the Visual Comfort Detection

In this section, the results of the experimental investigation of the visual comfort detection methods are presented. This section is divided into three subsections. The first subsection contains subjective evaluation results. In the second subsection, the results of the eye tracker data investigation are presented. The third subsection contains the results of the brain activity investigation. Results are discussed in the following section.

3.3.1. Comparison of the Depth Perception Moment Time

During the experimental investigation, each subject was free to rate the stereoscopic images according to their personal experiences. The requirement of identifying the DPM by pressing a key was an additional stimulus to concentrate on each image evaluation and provided additional time to make a decision. The subjective assessment results of visual comfort showed that individual scores of 5 images varied from "very uncomfortable" (VUn) to "uncomfortable" (Un). The visual comfort of 21 images varied from Un to "mildly uncomfortable" (MdUn). The 58 images had variations between MdUn and "comfortable" (Co), and 36 images had visual comfort assessment variations between Co and "very comfortable" (VCo). Compared to the experiment of Jung *et al.* (2013), our experiment had two main differences between experimental conditions – to achieve stereoscopic depth effect different screen size and different technology (anaglyph) to display the stimuli, was used. The mean difference between subjective assessment results of two experiments were 0.061 (with a standard deviation of 0.42). Subjective image evaluation differences between ours and Jung *et al.* (2013) experiment are shown in Fig. 3.10. Our results of the subjective assessment are shown using a yellow bar with 95% confidence intervals. Teal dots represent mean opinion scores obtained from the Jung *et al.* (2013) experiment.

Data, collected during the experimental investigation, to find the features, which are statistically different for the images with a distinct visual comfort level was analyzed. Four hypotheses were tested in this investigation. One-way ANOVA was used to assess the effect of the focus points, pupil size, disparity and the activity of the EEG signal on the level of visual comfort.

The subjects spent approximately 4–6 seconds before indicating a DPM. The images with the VCo score showed the lowest average time (4.31 ± 2.8 seconds) to DPM. The longest time (6.12 ± 4.9 seconds) to DPM was found for the VUn rated images. Table 3.1 shows the results of mean DPM times at the different visual comfort levels. Note, that sample size is different for each group, e.g., only 5% of all stimuli were rated as very uncomfortable.

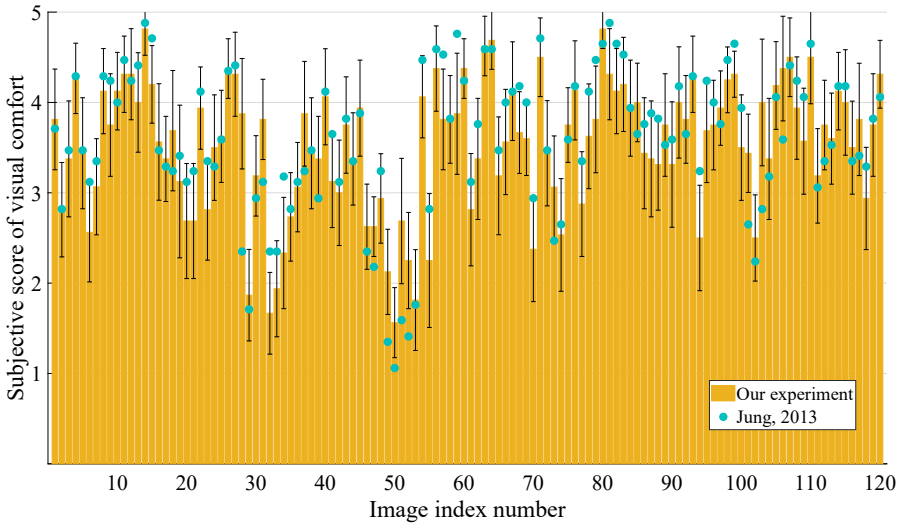

Fig. 3.10. Comparison of the subjective assessment results

Table 3.1. Mean values of the depth perception moment time in seconds with a standard deviation for each subjective assessment score

Assessment	DPM time, s
Very uncomfortable	6.12 ± 4.9
Uncomfortable	5.96 ± 4.0
Mildly uncomfortable	5.59 ± 3.6
Comfortable	5.54 ± 3.8
Very comfortable	4.31 ± 2.8

The DPM time of the subjects to the presented stereoscopic image possessed a high standard deviation from 2.8 seconds for the VCo images to 4.9 seconds for the VUn images. It should be noted, that for a set of images (usually rated as the VUn) the depth perception was not achieved at all, and in some cases, subjects spent up to 30 seconds trying to achieve the DPM. Therefore, we expected a different behavior of the eyes when comparing low and high visual comfort images.

In this investigation, the term pre-DPM time was used to indicate the duration between the start of the new stereoscopic image appears on the screen till the moment the user press spacebar as an moment, that the user achieved depth perception.

Histograms in Fig. 3.11 illustrates pre-DPM time statistics for images with different mean opinion scores. Histograms of 5 subjective assessment scores of visual comfort are shown. The abscissa represents DPM time with 0.5 s bin resolution. The number of samples (number of images) in each subjective assessment

group varies from 436 to 769. Therefore, normalization according to the probability density function of the histogram was applied. The resolution of the bins in the histogram is 0.5 s.

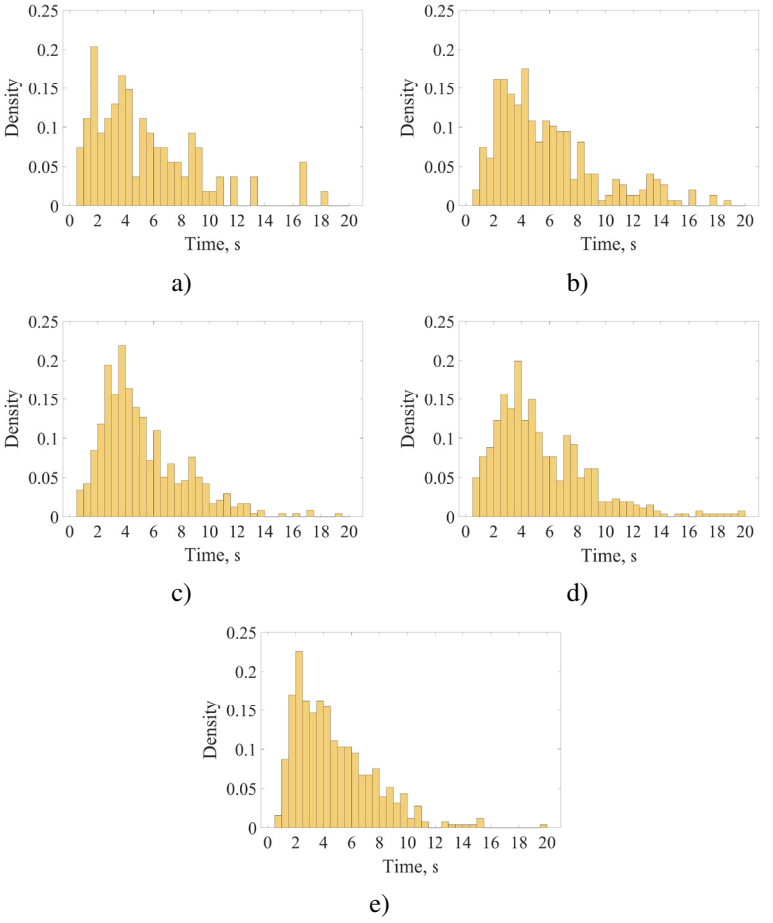

Fig. 3.11. Histograms of the time required to establish a stable depth perception (DPM): a) very uncomfortable; b) uncomfortable; c) mildly uncomfortable; d) comfortable; e) very comfortable

The mean value of pre-DPM time given in Table 3.1 shows that approx. 5–6 s were spent by the subjects to perceive the depth of the image and indicate it using the keyboard. The most visually comfortable images, those classified into the VCo group, required the shortest time for a decision with the smallest standard deviation. However, the mean value remained close to 5 s.

3.3.2. Results of the Eye Tracker Data Investigation

In the first hypothesis, it was investigated, if there is a statistically significant difference between visual comfort score and an estimated number of focus points in an image, measured in the fixed time frame. It was assumed whenever the subjects are looking at the visually uncomfortable stimuli they are searching for an object in the picture with the comfortable mapping of disparities which will ensure the comfortable depth perception. The low level of the visual comfort forces the users to explore more regions of the image for the possibility of finding the comfortable area or object, thus increasing the number of focus points in low scored images.

Change of the average number of focus points with different visual comfort scores for three investigated time frames is shown in Fig. 3.12. Visual comfort level gradually changes from 1 (very uncomfortable) to 5 (very comfortable). The error bar represents the standard error. An average number of focus points depends on the duration of the time frame.

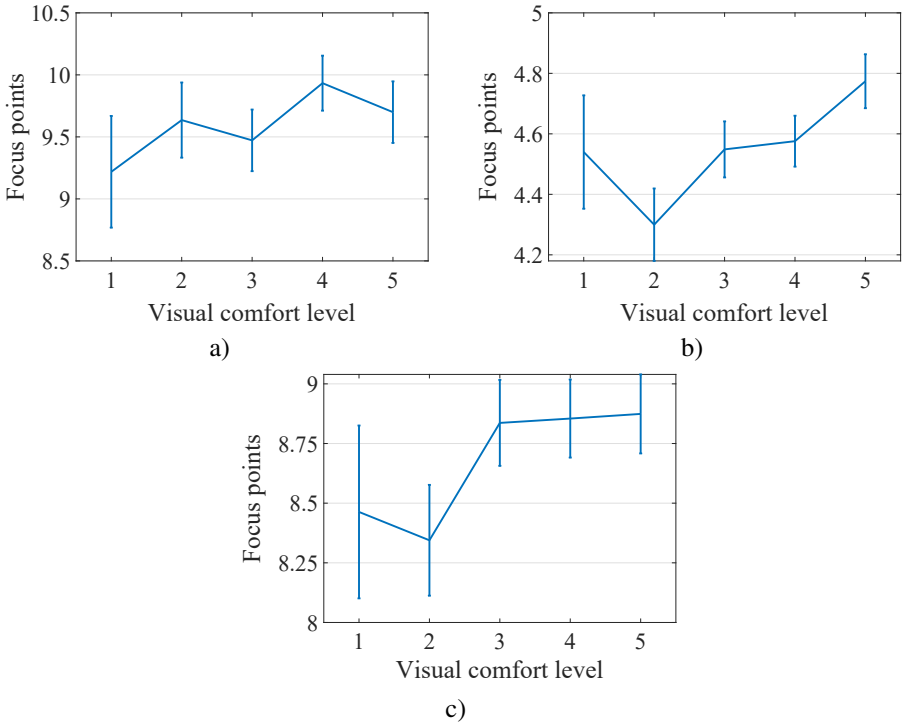

Fig. 3.12. Average number of focus points for each subjective assessment group using: a) 5 s pre-DPM time frame ($p = 0.545$); b) 2 s pre-DPM time frame ($p = 0.035$); c) 5 s post-DPM time frame ($p = 0.302$)

Using 2 s pre-DPM time frame lowest number of estimated focus points were for Un scored stimuli, highest for VCo scored stimuli, 4.30 and 4.77 respectively. Results showed that the average number of estimated focus points for the 5 s pre-DPM time frame were between 9.22 and 9.93, while for the 5 s post-DPM time frame the average number of estimated focus points were between 8.34 and 8.87. Additionally, subjects after the DPM maintains similar number of focus points for MdUn, Co and VCo visual comfort scores, 8.84, 8.85 and 8.87 respectively. However, a number of focus points for VUn, and Un scores was found lower – 8.46 and 8.34 respectively.

In the Fig. 3.12a, an average number of focus points using 5 s pre-DPM time frame is displayed. Average number of focus points changes from 9.22 (for VUn rated stimuli) to 9.70 (for VCo rated stimuli). However, the highest number of focus points were found for Co rated stimuli – 9.93. The standard error of the estimated number of focus points overlapped for all visual scores.

In the Fig. 3.12b, an average number of focus points using 5 s pre-DPM time frame is displayed. Average number of focus points changes from 9.22 (for VUn rated stimuli) to 9.70 (for VCo rated stimuli). However, the highest number of focus points were found for Co rated stimuli – 9.93. The standard error of the estimated number of focus points overlapped for all visual scores.

In the Fig. 3.12c, an average number of focus points using 5 s post-DPM time frame is displayed. Average number of focus points changes from 9.22 (for VUn stimuli) to 9.70 (for VCo stimuli). However, the standard error of the average number of focus points overlapped for all visual scores.

Table 3.2 shows results of the average number of focus points, received from each subjective assessment group (calculated using individual ratings of the subjects) and the ANOVA measures for the five groups of images. The results in Table 3.2 shows that the number of focus points changes with different visual comfort scores. The longest duration of investigated time frame was "full duration", the average number of focus points varied from 20.87 (for VCo stimuli) to 24.05 (for Co stimuli). Using the shortest time frame (1 s pre-DPM time frame), the average number of focus points was varying from 2.64 (for Un stimuli) to 2.84 (for VCo stimuli).

A significant difference, according to the estimated p-value (which should be less than 0.05 for significance indication), was found using 2 s ($p = 0.035$) pre-DPM analysis time frame window. Differences between the number of focus points for images with distinct subjective scores using 1 s pre-DPM ($p = 0.107$), 5 s pre-DPM ($p = 0.545$), "all pre-DPM" ($p = 0.097$), 5 s post-DPM ($p = 0.302$) and "full duration" ($p = 0.174$) time frame windows were not significant.

In the second hypothesis, it was investigated, if there is a statistically significant difference between visual comfort score and estimated pupil size in an image, estimated for the fixed time frame. Changes in pupil size with different visual

comfort scores for three investigated time frames are shown in Fig. 3.13. Visual comfort level gradually changes from 1 (very uncomfortable) to 5 (very comfortable). The error bar represents the standard error. Pupil size was found relatively similar for all investigated time frames, e.g., using 1 s pre-DPM time frame estimated pupil size was 4.06 mm, and using full duration time frame – 4.11 mm.

Table 3.2. An average number of focus points and their significance level for the different visual comfort scores during the investigated time frames. A bold font denotes significant values ($p < 0.05$)

Time frame	VUn	Un	MdUn	Co	VCo	F	Sig
All pre-DPM	12.14	13.32	13.52	14.64	11.76	1.977	0.097
1 s pre-DPM	2.69	2.64	2.74	2.81	2.84	1.907	0.107
2 s pre-DPM	4.54	4.30	4.55	4.58	4.77	2.597	**0.035**
5 s pre-DPM	9.22	9.64	9.47	9.93	9.70	0.770	0.545
5 s post-DPM	8.46	8.34	8.84	8.85	8.87	1.217	0.302
Full duration	21.17	22.28	22.68	24.05	20.87	1.596	0.174

In the Fig. 3.13a, an estimated pupil size, in millimeters, using 5 s pre-DPM time frame is shown. Pupil size of the subjects changed from 4.15 mm (for VUn rated stimuli) to 4.12 mm (for VCo rated stimuli). The highest pupil size were found for Un rated stimuli – 4.22 mm, lowest pupil size, 4.12 mm, was found for VCo rated stimuli. The standard error of the pupil size overlapped for all adjacent visual scores except for the VCo scored stimuli.

In the Fig. 3.13b, an estimated pupil size using 2 s pre-DPM time frame is shown. Pupil size of the subjects reduced from 4.26 mm (for Un rated stimuli) to 4.07 mm (for VCo rated stimuli). The pupil size estimated for the VUn rated stimuli was 4.14 mm, and had the highest standard error. The standard error of the pupil size overlapped for all adjacent visual scores except for the VCo and VUn rated stimuli.

In the Fig. 3.13c, an estimated pupil size using 5 s post-DPM time frame is shown. Pupil size of the subjects reduced from 4.32 mm (for Un rated stimuli) to 4.11 mm (for VCo rated stimuli). The pupil size estimated for the VUn rated stimuli was 4.17 mm, and had the highest standard error. The standard error of the pupil size of adjacent visual comfort scores overlapped only for the Un and MdUn rated stimuli.

A significant difference between visual comfort level of the image given during experimental investigation and estimated pupil size of the subject was found using 1 s pre-DPM ($p < 0.001$), 2 s pre-DPM ($p = 0.001$), "all pre-DPM" ($p = 0.036$), 5 s post-DPM ($p < 0.001$) and "full duration" ($p = 0.015$) time frames (see Table 3.3). There were no significant changes found using 5 s pre-DPM time frame ($p = 0.158$). The estimated pupil size was highest for the stimuli

scored as the Un, this result was consistent in all investigated time frames. Lowest pupil size was found for the images with the VCo ratings. In most cases, the mean pupil size of the VUn rated images was found lower than Co rated images, however having a higher standard error, as shown in Fig. 3.13.

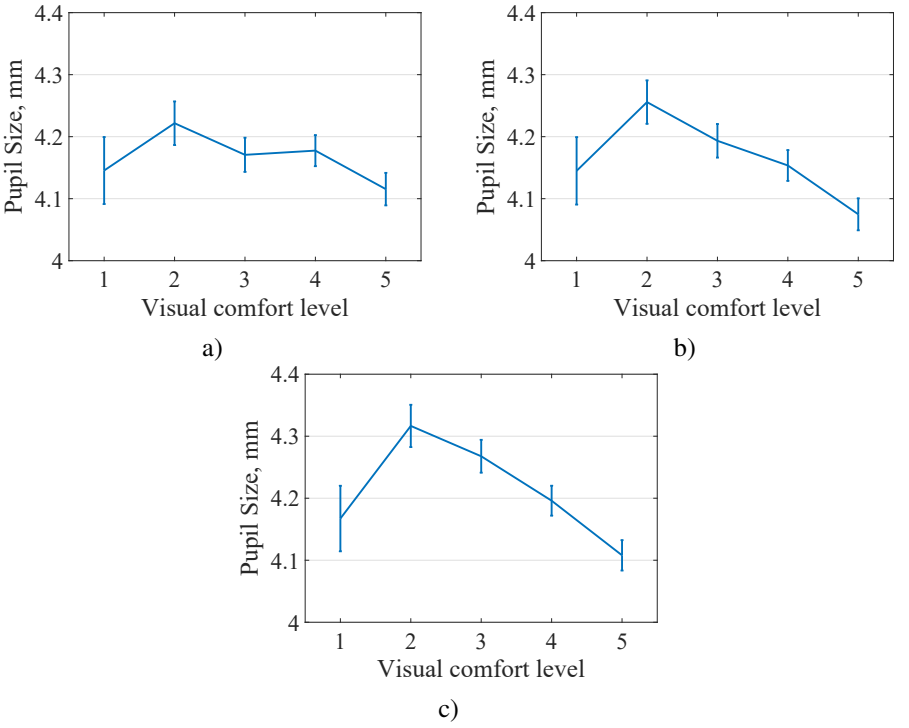

Fig. 3.13. Average pupil size for each subjective assessment group using: a) 5 s pre-DPM time frame ($p = 0.158$); b) 2 s pre-DPM time frame ($p = 0.001$); c) 5 s post-DPM time frame ($p = 0.000$)

In the third hypothesis, it was investigated, if there is a statistically significant difference between visual comfort rating and mean gaze disparity, estimated during the fixed period. Changes in disparity with different visual comfort scores for three investigated time frames are shown in Fig. 3.14. Visual comfort level gradually changes from 1 (very uncomfortable) to 5 (very comfortable). The error bar represents the standard error. Gaze disparity was measured in pixels, the size of the pixel was 0.2634 mm. An estimated number of pixels for different duration time frames were relatively similar. However, estimated disparity changed with the level of visual comfort, e.g., disparity of 1 s pre-DPM time frame was lowest for the VCo scored stimuli (73.1 pixels), highest – Un scored stimuli (84.3 pixels),

and disparity of full duration time frame was lowest for the VCo scored stimuli (74.1 pixels), highest – Un scored stimuli (83.5 pixels), respectively.

Table 3.3. Mean pupil size (in millimeters) and its significance level for the different visual comfort scores during the investigated time frames. A bold font denotes significant values ($p < 0.05$)

Time frame	VUn	Un	MdUn	Co	VCo	F	Sig
All pre-DPM	4.22	4.25	4.18	4.18	4.11	2.579	**0.036**
1 s pre-DPM	4.12	4.23	4.19	4.14	4.06	5.424	**0.000**
2 s pre-DPM	4.14	4.26	4.19	4.15	4.07	4.990	**0.001**
5 s pre-DPM	4.15	4.22	4.17	4.18	4.12	1.653	0.158
5 s post-DPM	4.17	4.32	4.27	4.20	4.11	8.170	**0.000**
Full duration	4.21	4.27	4.18	4.18	4.11	3.098	**0.015**

In the Fig. 3.14a, an estimated disparity using 5 s pre-DPM time frame is shown. Disparity of the subjects gaze fluctuated from 83 pixels (for VUn rated stimuli) to 70.9 pixels (for VCo rated stimuli). The highest gaze disparity was found for Un rated stimuli – 85.8 pixels, lowest gaze disparity – 70.9 pixels, was found for VCo rated stimuli. The standard error of the gaze disparity did not overlap between VCo and VUn, Un, Co scored stimuli.

In the Fig. 3.14b, an estimated disparity using 2 s pre-DPM time frame is shown. Disparity of the subjects gaze fluctuated from 82.4 pixels (for VUn rated stimuli) to 71.1 pixels (for VCo rated stimuli). The highest gaze disparity was found for Un rated stimuli – 83.3 pixels, lowest gaze disparity – 71.1 pixels, was found for VCo rated stimuli. The standard error of the gaze disparity did not overlap only of VCo and all other (VUn, Un, MdUn and Co) stimuli.

In the Fig. 3.14c, an estimated disparity using 5 s post-DPM time frame is shown. Disparity of the subjects gaze fluctuated from 83.6 pixels (for VUn rated stimuli) to 75.6 pixels (for VCo rated stimuli). The highest gaze disparity was found for Un rated stimuli – 85.8 pixels, lowest gaze disparity – 75.6 pixels, was found for VCo rated stimuli. The standard error of the gaze disparity for post-DPM time frame overlapped for all adjacent visual comfort scores. However, the standard error did not overlap between VCo and Un, MdUn visual comfort scores.

ANOVA results of the effects of disparity for the different visual comfort levels are shown in Table 3.4. Results of disparity values were rounded to one number after the decimal point. Significant difference was found using 5 s pre-DPM time frame ($p = 0.041$). However, no significant difference was found between subjective assessment groups using 1 s pre-DPM ($p = 0.176$), 2 s pre-DPM ($p = 0.079$), "all pre-DPM" ($p = 0.292$), 5 s post-DPM ($p = 0.152$) and "full duration" ($p = 0.502$) time frames. Results indicated a reduced gaze disparity when observing images with high visual comfort scores.

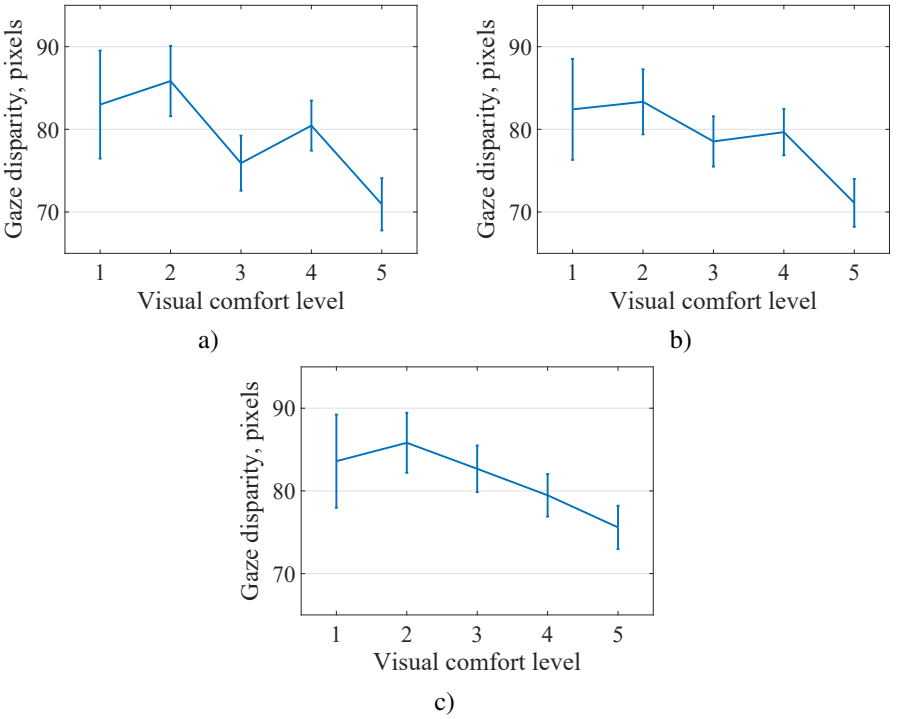

Fig. 3.14. Average binocular disparity for each subjective assessment group using: a) 5 s pre-DPM time frame ($p = 0.041$); b) 2 s pre-DPM time frame ($p = 0.079$); c) post-DPM time frame ($p = 0.152$)

A ratio between crossed and uncrossed disparity was investigated for different visual comfort values. Changes in the estimate of this ratio for three investigated time frames are shown in Fig. 3.15. Visual comfort level gradually changes from 1 (very uncomfortable) to 5 (very comfortable). The error bar represents the standard error.

The ratio of crossed disparity for time frames with different duration was relatively similar. However, estimated ratio changed with the level of visual comfort, e.g., ratio of crossed disparity using 1 s pre-DPM time frame was lowest for the MdUn scored stimuli (0.33), highest – VUn scored stimuli (0.39), and estimated ratio using full duration time frame was lowest for the VCo scored stimuli (0.29), highest – VUn scored stimuli (0.36), respectively. A higher value in this ratio indicates that a larger number of focus points required crossed disparity to perceive stereoscopic depth.

In the Fig. 3.15a, an estimated ratio of crossed disparity using 5 s pre-DPM time frame is shown. Ratio of crossed disparity fluctuated from 0.4 (for VUn rated

stimuli) to 0.32 (for VCo rated stimuli). The highest ratio was found for VUn rated stimuli – 0.40, lowest ratio – 0.31, was found for MdUn rated stimuli. However, ratio of Un, MdUn, Co and VCo had differences below 0.02 between scores. The standard error of the estimated ratio did not overlap only between VUn and all other (Un, MdUn, Co and VCo) rated stimuli.

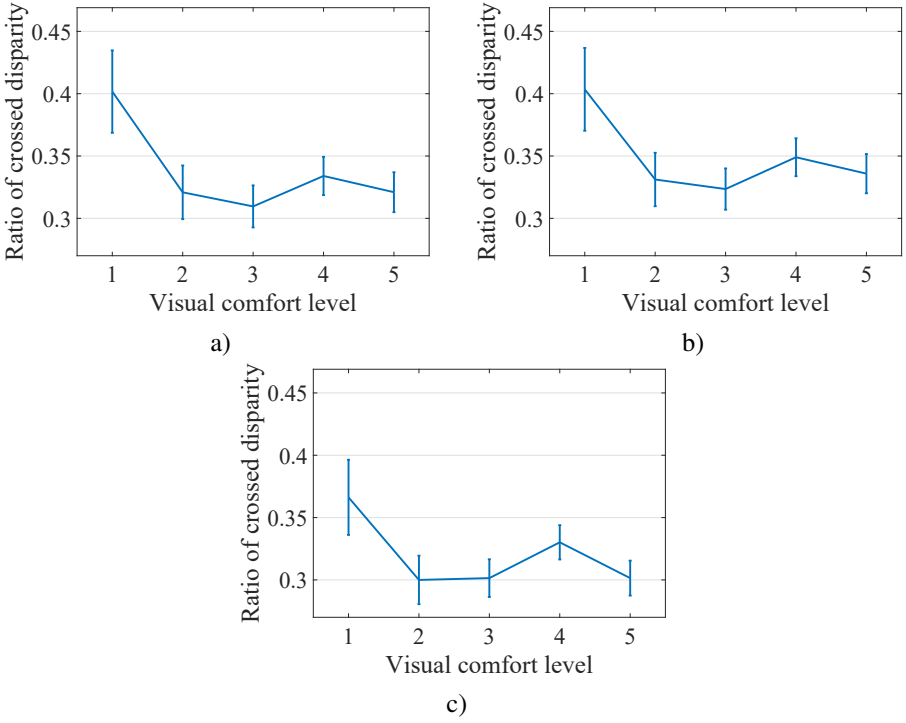

Fig. 3.15. Crossed disparity ratio for each subjective assessment group: a) 5 sec. pre-DPM time frame ($p = 0.159$); b) 2 sec. pre-DPM time frame ($p = 0.264$); c) post-DPM time frame ($p = 0.172$)

In the Fig. 3.15b, an estimated ratio of crossed disparity using 2 s pre-DPM time frame is shown. Ratio of crossed disparity fluctuated from 0.4 (for VUn rated stimuli) to 0.34 (for VCo rated stimuli). The highest ratio was found for VUn rated stimuli – 0.40, lowest ratio – 0.32, was found for MdUn rated stimuli. However, ratio of Un, MdUn, Co and VCo had differences below 0.03 between scores. The standard error of the estimated ratio did not overlap only between VUn and all other (Un, MdUn, Co and VCo) rated stimuli.

In the Fig. 3.15c, an estimated ratio of crossed disparity using 5 s post-DPM time frame is shown. Ratio of crossed disparity fluctuated from 0.37 (for VUn

rated stimuli) to 0.30 (for VCo rated stimuli). The highest ratio was found for VUn rated stimuli – 0.37, lowest ratio – 0.30, was found for Un, MdUn and VCo rated stimuli. The standard error of the estimated ratios did not overlap only between VUn and Un, MdUn and VCo rated stimuli.

Table 3.4. Mean binocular disparity (in pixels) and its significance level for the different visual comfort scores during the investigated time frames. A bold font denotes significant values ($p < 0.05$)

Time frame	VUn	Un	MdUn	Co	VCo	F	Sig
All pre-DPM	80.5	82.3	76.6	79.9	71.2	1.239	0.292
1 s pre-DPM	81.3	84.3	78.3	79.4	73.1	1.583	0.176
2 s pre-DPM	82.4	83.3	78.5	79.7	71.1	2.095	0.079
5 s pre-DPM	83	85.8	75.9	80.5	70.9	2.502	**0.041**
5 s post-DPM	83.6	85.8	82.7	79.5	75.6	1.679	0.152
Full duration	82.3	83.5	78.9	80.3	74.1	0.836	0.502

Table 3.5. Crossed disparity (results are shown as a proportion of both crossed and uncrossed disparities) within the investigated time frame for the different visual comfort score

Time frame	VUn	Un	MdUn	Co	VCo	F	Sig
All pre-DPM	0.35	0.30	0.29	0.31	0.31	0.643	0.632
1 s pre-DPM	0.39	0.34	0.33	0.36	0.34	0.687	0.601
2 s pre-DPM	0.40	0.33	0.32	0.35	0.34	1.310	0.264
5 s pre-DPM	0.40	0.32	0.31	0.33	0.32	1.651	0.159
5 s post-DPM	0.37	0.30	0.30	0.33	0.30	1.598	0.172
Full duration	0.36	0.30	0.30	0.31	0.29	0.866	0.483

The analysis of gaze data showed the highest ratio of the crossed disparity at the focus points for the images with the lowest (VUn) visual comfort scores (see Fig. 3.15). However, ANOVA analysis found no significant difference between visual comfort scores and ratio of the crossed disparity in all investigated time frames, as shown in Table 3.5.

3.3.3. Results of the Brain Activity Investigation

A selection of a pre-DPM time for analysis of spectral components is important for the EEG signal-based feature estimation. To ensure that the EEG spectral components carry statistically separable data, we have compared EEG activity between images grouped to five comfort levels at different time frames: 0.5, 1, 3, 4, 5 6, 7, and 10 seconds before the DPM.

A selection of frequency band for EEG activity analysis plays a vital role in the comfort level prediction capabilities. Since frequency bands (alpha, beta, theta) have a tendency to contradict each other, e.g., Cheng *et al.* (2007), in their study, not only used EEG power analysis in specific frequency bands but also used different combinations to estimate relative power between different bands (e.g., theta/alpha, beta/alpha, etc.). Similarly, Zou *et al.* (2015) evaluated six types of band ratios during repetitive random dot stereogram based task, results showed significant differences for all investigated ratios, alpha activity was found as most promising indicator in their experiment. In this study brain activity was separated to: theta (θ) 4–8 Hz, alpha (α) 8–13 Hz, low beta (β_l) 13–17 Hz, beta medium (β_m) 17–21 Hz and high beta (β_h) 21–30 Hz frequency bands (Dunbar *et al.* 2007). In addition to commonly used band ratios (Cheng *et al.* 2007; Hsu, Wang 2013; Zou *et al.* 2015), sub-beta oscillations (β_l, β_m, β_h) were investigated, making a total set of seven different frequency band ratios for the investigation: α/β; $(\alpha+\theta)/\beta$; α/θ; θ/β; α/β_l; α/β_m; α/β_h.

Table 3.6 presents the results of ANOVA measures for the five groups of images with different visual comfort level on investigated brain activity band at particular pre-DPM time. θ, α and β_l frequencies showed no statistically significant differences for all investigated pre-DPM time frames. A significant difference was found for β_m frequency band using 6 s pre-DPM time frame ($p = 0.017$), and for β_h frequency band using 2, 3, 4, 5, 6 and 7 s pre-DPM time frames, with significance levels (rounded to three digits after the decimal point) of 0.014, 0.002, 0.002, 0.000, 0.000 and 0.008, respectively.

Table 3.6. One-way ANOVA results of the visual comfort scores for oscillatory activity at investigated time frame before depth perception moment. Significant values ($p < 0.05$) were highlighted

pre-DPM time, s	θ	α	β_l	β_m	β_h
0.5	0.273	0.550	0.259	0.054	0.429
1	0.241	0.617	0.199	0.126	0.330
2	0.169	0.906	0.176	0.189	**0.014**
3	0.436	0.347	0.242	0.133	**0.002**
4	0.276	0.173	0.362	0.129	**0.002**
5	0.223	0.231	0.280	0.061	**0.000**
6	0.273	0.917	0.231	**0.017**	**0.000**
7	0.299	0.664	0.203	0.162	**0.008**
10	0.217	0.432	0.556	0.598	0.277

Table 3.7 presents the results of ANOVA measures for the five groups of images with different visual comfort levels on ratios of the investigated brain activity bands at particular pre-DPM time. θ/β, $(\theta+\alpha)/\beta$, α/β and α/β_l frequency band

ratios showed no statistically significant differences for all investigated pre-DPM time frames. A significant difference was found for θ/α ratio using 0.5, 1, 2, 3, 4 and 5 s pre-DPM time frames, with significance levels of 0.031, 0.020, 0.026, 0.005, 0.002 and 0.002, respectively. Additionally, a significant difference was found for θ/β_{m} ratio using 6 s pre-DPM time frame ($p = 0.028$), and for θ/β_{h} ratio significance levels were 0.005, 0.000, 0.000, 0.000, 0.000 and 0.020, using 2, 3, 4, 5, 6 and 7- s pre-DPM time frames, respectively.

Table 3.7. One-way ANOVA results of the visual comfort scores for ratios of the oscillatory activity at investigated time frame before depth perception moment. Significant values ($p < 0.05$) are highlighted

pre-DPM time, s	θ/α	θ/β	$(\theta+\alpha)/\beta$	α/β	α/β_{l}	α/β_{m}	α/β_{h}
0.5	**0.031**	0.244	0.233	0.365	0.229	0.088	0.392
1	**0.020**	0.084	0.178	0.438	0.232	0.287	0.050
2	**0.026**	0.599	0.543	0.330	0.190	0.288	**0.005**
3	**0.005**	0.936	0.564	0.162	0.296	0.154	**0.000**
4	**0.002**	0.772	0.499	0.114	0.381	0.274	**0.000**
5	**0.002**	0.543	0.372	0.087	0.537	0.221	**0.000**
6	0.103	0.396	0.819	0.936	0.665	**0.028**	**0.000**
7	0.104	0.548	0.755	0.893	0.252	0.104	**0.020**
10	0.068	0.460	0.707	0.786	0.681	0.598	0.055

Multiple comparison tests using the Tukey-Kramer ($\alpha = 0.05$) method was used to investigate ANOVA results which showed significant effects. Results of the post-hoc Tukey's test at 4, 5, and 6 s pre-DPM times are given in Tables 3.8, 3.9, and 3.10. Brain activities and their ratios investigated using Tukey's test were conducted for the significant values shown in Tables 3.6 and 3.7. Tukey-Kramer's post-hoc tests revealed significant differences between subjective assessment value pairs.

Table 3.8 presents the results of Tukey's test pairwise comparison of brain activity for the five groups of images with different visual comfort levels. Tukey's test was conducted to investigate β_{h} brain activity band, θ/α and α/β_{h} brain activity ratios using 4 s pre-DPM time frame. At the 4 s pre-DPM time, significant difference between VUn and Un ($p = 0.046$), MdUn ($p = 0.005$), Co ($p = 0.000$), VCo ($p = 0.000$) groups were observed in α/β_{h} ratio. Additionally, significant difference were found in θ/α oscillatory activity ratio between VUn and VCo ($p = 0.045$), and Un and VCo ($p = 0.002$) pairs. Furthermore, the test results showed that the β_{h} activity at 4 s pre-DPM time for VUn was significantly different from Co ($p = 0.022$) and VCo ($p = 0.004$) visual comfort levels. The post-hoc test revealed no significant difference between other visual comfort pairs using 4 s pre-DPM time frame.

Table 3.8. Summary of the p-values using a post-hoc Tukey's test for the significant differences in oscillatory activity, calculated using 4 s time frame before depth perception moment. Significant values ($p < 0.05$) are highlighted

β_{h}	θ/α	α/β_{h}	Group	vs. group
0.350	0.998	**0.046**	VUn	Un
0.273	0.486	**0.005**	VUn	MdUn
0.022	0.631	**0.000**	VUn	Co
0.004	**0.045**	**0.000**	VUn	VCo
1.000	0.280	0.897	Un	MdUn
0.465	0.467	0.302	Un	Co
0.120	**0.002**	**0.044**	Un	VCo
0.415	0.994	0.791	MdUn	Co
0.083	0.297	0.222	MdUn	VCo
0.900	0.116	0.839	Co	VCo

The effect of visual comfort for oscillatory activity using 4 s pre-DPM time frame is shown in Figure 3.16. The abscissa represents visual comfort level from 1 – very uncomfortable to 5 – very comfortable. The error bar represents the standard error. Relative α power level (see Fig. 3.16a) of the subjects decreased from 0.956 to 0.927 with higher visual comfort level, while the relative activity β_{h} power (see Fig. 3.16b) increased from 1.040 to 1.123 with the higher visual comfort. Therefore, the α/β_{h} ratio (see Fig. 3.16c) decreased from 0.981 to 0.849, when visual comfort level increased. The standard error of the α level did not overlap between VCo and other (VUn, Un, MdUn, Co) rated stimuli (Fig. 3.16a). The standard error of the β_{h} level did not overlap between VUn and other (Un, MdUn, Co, VCo) rated stimuli, and the standard error of VCo and Co did not overlap with lower visual comfort levels (Fig. 3.16b). The standard error of the α/β_{h} ratio did not overlap between VUn and other (Un, MdUn, Co, VCo) rated stimuli, and the standard error of VCo did not overlap with lower visual comfort levels (VUn, Un, MdUn). However, visual comfort of other adjacent scores overlapped (Fig. 3.16c).

Results of Tukey's test pairwise comparison of brain activity for the five groups of images with different visual comfort levels are shown in Table 3.9. Tukey's test was conducted to investigate brain activity of the β_{h} band and brain activity of the θ/α and α/β_{h} ratios using 5 s pre-DPM time frame. Post-hoc analysis indicated significant difference between VUn and Co ($p = 0.021$), VUn and VCo ($p = 0.002$), Un and VCo ($p = 0.042$), MdUn and VCo ($p = 0.014$) visual comfort scores at β_{h} frequency. Additionally, significant difference were observed between Un and VCo ($p = 0.002$) scores at the θ/α ratio. Moreover, significant differences were found between VUn and all four visual comfort groups: Un ($p = 0.026$), MdUn ($p = 0.007$), Co ($p < 0.001$), VCo ($p < 0.001$), and between VCo and Un ($p = 0.027$), VCo and MdUn ($p = 0.042$) visual comfort scores at α/β_h frequency

ratio. However, the post-hoc test revealed no significant difference between other visual comfort pairs using 5 s pre-DPM time frame.

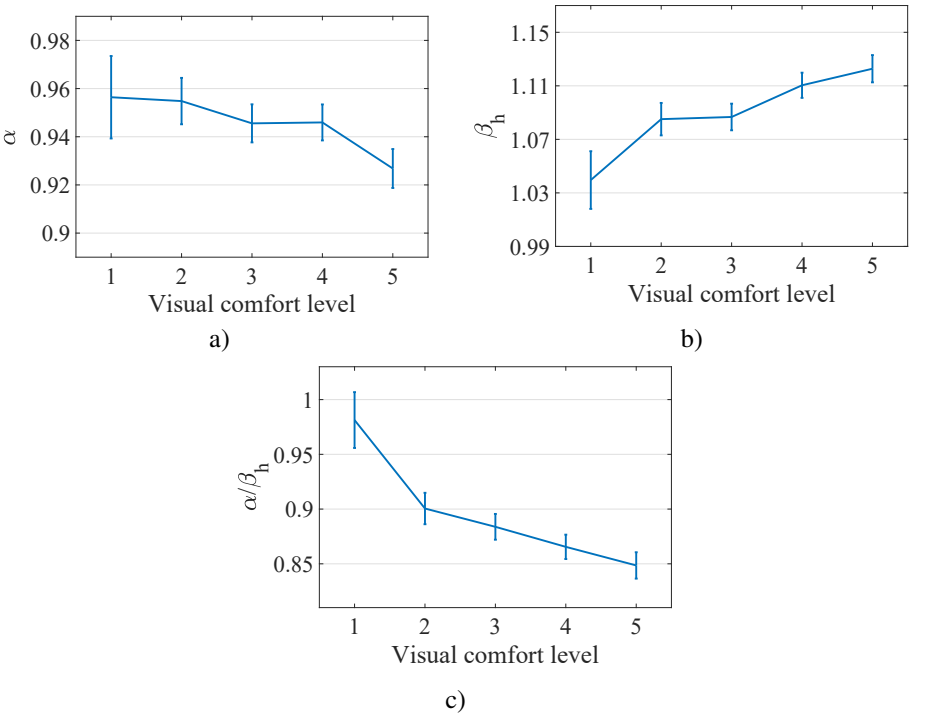

Fig. 3.16. Relative electroencephalogram activity of the subjects using 4 s time frame before depth perception moment: a) relative α level ($p = 0.173$); b) relative β_{h} level ($p = 0.002$); c) ratio of $\alpha/\beta_{\mathrm{h}}$ levels ($p = 0.000$)

The effect of visual comfort for oscillatory activity using 5 s pre-DPM time frame is shown in Figure 3.17. The abscissa represents visual comfort level from 1 – very comfortable to 5 – very comfortable. The error bar represents the standard error. Relative level of the α power (see Fig. 3.17a) decreased from 0.960 to 0.925 with higher visual comfort levels, while the relative level of the β_{h} power (see Fig. 3.17b) increased from 1.039 to 1.136 with the higher visual comfort. Therefore, the ratio of the $\alpha/\beta_{\mathrm{h}}$ waves (see Fig. 3.17c) decreased from 0.983 to 0.834, when the level of visual comfort increased. The standard error of the α level did not overlap between VCo and other (VUn, Un, MdUn, Co) rated stimuli (Fig. 3.17a). The standard error of the β_{h} level did not overlap between VUn and other (Un, MdUn, Co, VCo) rated stimuli, and the standard error of VCo and Co did not overlap with lower visual comfort levels (Fig. 3.17b). The standard error

of the α/β_{h} ratio did not overlap between VUn and other (Un, MdUn, Co, VCo) rated stimuli, and the standard error of VCo and Co did not overlap with lower visual comfort levels (VUn, Un, MdUn). However, visual comfort of other adjacent scores overlapped (Fig. 3.17c).

Table 3.9. Summary of the p-values using a post-hoc Tukey's test for the significant differences in oscillatory activity, calculated using 5 s time frame before depth perception moment. Significant values ($p < 0.05$) are highlighted

β_{h}	θ/α	α/β_{h}	Group	vs. group
0.436	1.000	**0.026**	VUn	Un
0.430	0.563	**0.007**	VUn	MdUn
0.021	0.546	**0.000**	VUn	Co
0.002	0.069	**0.000**	VUn	VCo
1.000	0.192	0.994	Un	MdUn
0.370	0.165	0.337	Un	Co
0.042	**0.002**	**0.027**	Un	VCo
0.224	1.000	0.499	MdUn	Co
0.014	0.401	**0.042**	MdUn	VCo
0.751	0.365	0.682	Co	VCo

The post-hoc results using the 6 s pre-DPM time are shown in Table 3.10. The post-hoc tests were conducted using Tukey's pairwise method. Tukey's tests were conducted to investigate brain activity of the β_{m} and β_{h} bands and brain activity of the α/β_{h} and α/β_{h} ratios. Post-hoc analysis indicated significant difference between VUn and VCo ($p = 0.016$) visual comfort scores at β_{m} frequency. Additionally, significant effects of visual comfort was observed in β_{h} frequency band between VUn and Co ($p = 0.017$), VUn and VCo ($p = 0.001$), VCo and Un ($p = 0.021$), VCo and MdUn ($p = 0.008$) scores. Moreover, significant differences were found at α/β_m frequency ratio between VCo and MdUn ($p = 0.044$) visual comfort scores, and at α/β_h ratio between VUn and other four visual comfort rating pairs: Un ($p = 0.022$), MdUn ($p = 0.016$), Co ($p = 0.001$), VCo ($p < 0.001$). However, the post-hoc test revealed no significant difference between other visual comfort pairs using 6 s pre-DPM time frame.

The effect of visual comfort in oscillatory activity using 6 s pre-DPM time frame is shown in Figure 3.18. The abscissa represents visual comfort level from 1 – very comfortable to 5 – very comfortable. The error bar represents the standard error. Relative α power level (see Fig. 3.18a) of the subjects decreased from 0.957 to 0.938 with higher visual comfort level, while the relative activity β_{h} power (see Fig. 3.18b) increased from 1.029 to 1.145 with the higher visual comfort. Therefore, the α/β_{h} ratio (see Fig. 3.18c) decreased from 0.989 to 0.841, when visual comfort level increased. The standard error of the α level overlaped between all visual comfort scores (Fig. 3.18a). The standard error of the β_{h} level did not

overlap between VUn and all other (Un, MdUn, Co, VCo) rated stimuli, and the standard error of VCo and Co did not overlap with lower visual comfort levels (Fig. 3.18b). The standard error of the $\alpha/\beta_{\mathrm{h}}$ ratio did not overlap between VUn and other (Un, MdUn, Co, VCo) rated stimuli, and the standard error of the VCo did not overlap with lower rated stimuli of VUn, Un and MdUn.

3.3.4. Discussion of the Results

In this study, the effect of visual comfort for gaze and EEG features, collected using eye tracker and consumer grade EEG device, was investigated. Additionally, the time of stable depth perception for various stereoscopic images was measured.

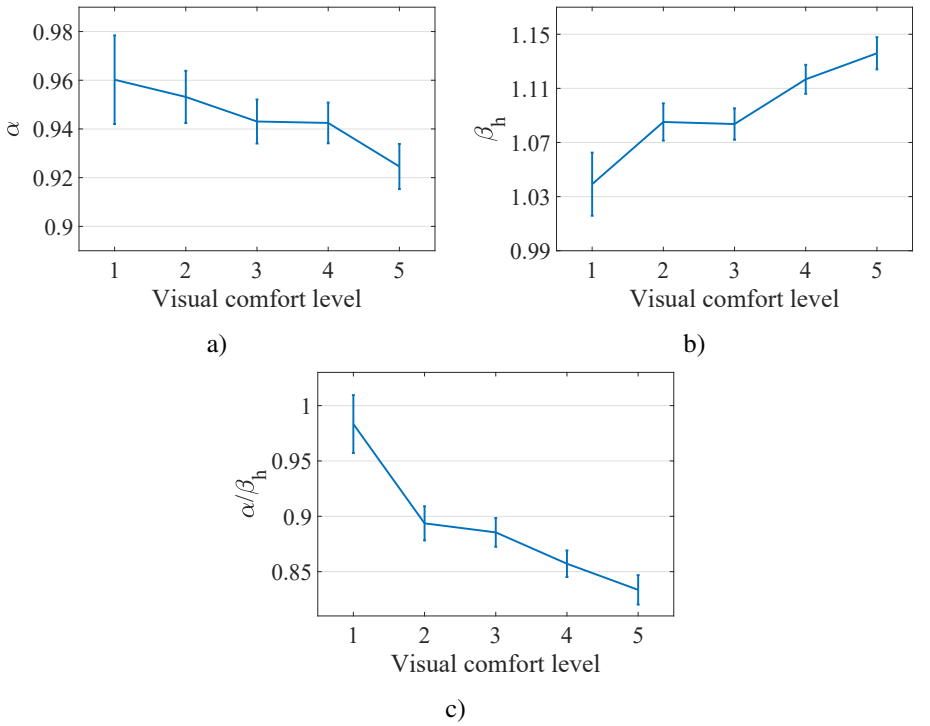

Fig. 3.17. Relative electroencephalogram activity of the subjects using 5 s time frame before depth perception moment: a) relative alpha level ($p = 0.231$); b) relative high beta level ($p = 0.000$); c) ratio of alpha and high beta levels ($p = 0.000$)

Depth perception of images rated as VCo showed shortest DPM time (4.31 s). Images rated as VUn showed highest DPM time (6.12 s). Such tendency may give

assumption, that the DPM time correlates with the visual comfort level. However, very high standard deviation, from 2.8 s (VCo) to 4.9 s (VUn) was observed in the results (Table 3.1). This may indicate that behavior of the subjects depends on other underlying factors, which can be unique to the shown content, individual experience of the subjects or the limits of the ability to focus on the object in the image. This investigation supports and extends a research by Hoffman *et al.* (2008), which showed that minimum time of 400–500 ms was required to identify a stereoscopic stimulus when the vergence-accommodation conflict was zero, and that 3D displays, in comparison to the real-life scenes, increases the time required to identify a stereoscopic stimulus and a level of visual fatigue and discomfort.

Table 3.10. Summary of the p-values using a post-hoc Tukey's test for the significant differences in oscillatory activity, calculated using 6 s time frame before depth perception moment. Significant values ($p < 0.05$) are highlighted

β_{m}	β_{h}	$\alpha/\beta_{\mathrm{m}}$	$\alpha/\beta_{\mathrm{h}}$	Group	vs. group
0.082	0.381	0.716	**0.022**	VUn	Un
0.394	0.380	0.985	**0.016**	VUn	MdUn
0.063	**0.017**	0.379	**0.001**	VUn	Co
0.016	**0.001**	0.143	**0.000**	VUn	VCo
0.722	1.000	0.791	1.000	Un	MdUn
1.000	0.363	0.956	0.765	Un	Co
0.944	**0.021**	0.577	0.287	Un	VCo
0.649	0.239	0.250	0.711	MdUn	Co
0.212	**0.008**	**0.044**	0.222	MdUn	VCo
0.902	0.582	0.890	0.875	Co	VCo

A significant difference between a number of focus points (see Table 3.2), pupil size (see Table 3.3) and binocular disparity (see Table 3.4) to a different level of visual comfort was found. The experimental data were analyzed using different time frames, including time frames taken before the moment of DPM and after the DPM. Time frame windows with the significant effects were not consistent across different gaze features, e.g., significant effect in binocular disparity was found using 5 s pre-DPM time frame, an effect in focus points – using 2 s pre-DPM time frame, an effect in pupil size – with all investigated time frames, except with the 5 s pre-DPM time frame. Pupil size correlations with arousal, memory activities, brain processing tasks were showed in early studies (Beatty 1982). Porter *et al.* (2007) in their investigation showed that visual search tasks using distractors that increase difficulty of target recognition lead to increases in pupil diameter. Furthermore, in their work Suryakumar (2005), used pupillometry to investigate illumination effects on visual discomfort level.

Ratio of crossed disparity (Table 3.5) showed no significant effect for all investigated time frames, it could be interpreted as different visual comfort levels

have a similar ratio of crossed and uncrossed disparity, and this feature is not an important factor for subjects to rate comfort level of a stimulus.

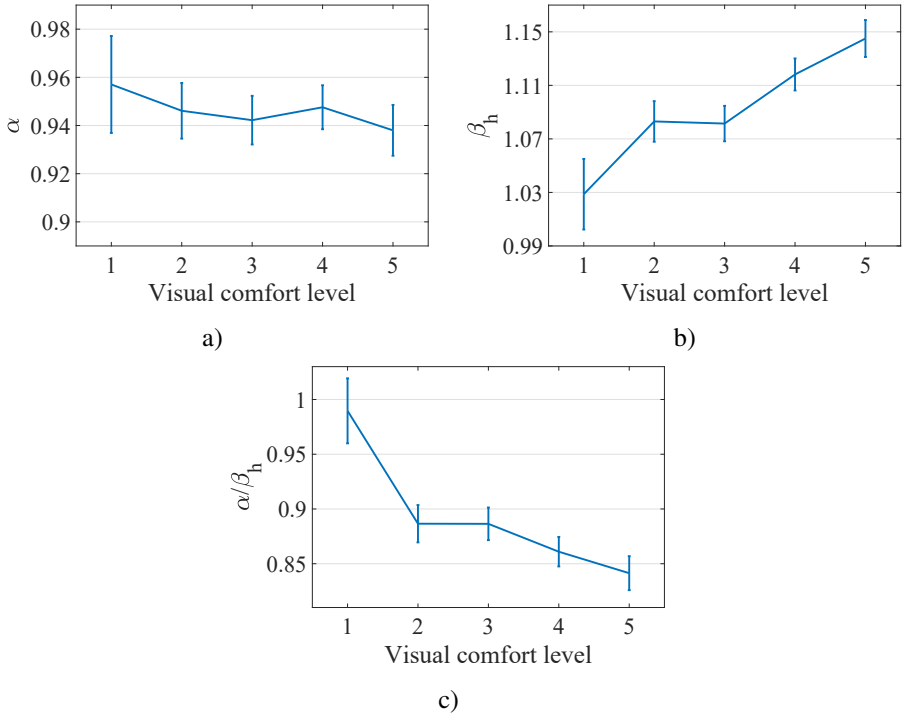

Fig. 3.18. Relative electroencephalogram activity of the subjects using 6 s time frame before depth perception moment: a) relative alpha level ($p = 0.917$); b) relative high beta level ($p = 0.000$); c) ratio of alpha and high beta levels ($p = 0.000$)

An interesting fact was found – features calculated for the VUn rated images had values similar to the Co or VCo rated images, e.g., lowest number of focus points (shown in Fig. 3.12) using 2 s pre-DPM time frame ($p = 0.035$), was found for the Un rated stimuli (4.3 focus points), while for the VUn and Co rated images average number of focus points was approx. 4.5, VCo rated stimuli had highest number of focus points – 4.8; the pupil size of the VUn visual comfort rating (shown in Fig. 3.13) was 4.15 mm (using 2 s pre-DPM time frame), similar to the Co rating – 4.15 mm, highest pupil size (4.27 mm) was found for the Un visual comfort rating, lowest – for the VCo rating (4.08 mm); estimated disparity (shown in Fig. 3.14) using 5 s pre-DPM time frame ($p = 0.041$) was largest for Un rated images (85.84 pixels), and smallest for the VCo rated images (71 pixel). We

assume that subjects rated images as VUn, when the stereoscopic perception was not achieved. Therefore, experimental investigation results tend to look similar to the high visual comfort scores.

Additional estimated feature – the ratio of crossed disparity (shown in Fig. 3.15) was used for complementary analysis of the results. The calculated ratio of crossed disparity, received using images with different comfort levels, was highest for the VUn visual comfort scores (0.40). By comparison, this ratio for the other four visual comfort levels varied from 0.31 to 0.33. However, this difference was found not significant using any of the investigated time frames (shown in Table 3.5). Therefore, crossed disparity could not be used as a standalone feature, but it may be used as a supplementary feature for the classification of the lowest rated images (VUn) because other estimates of the gaze features for the lowest rated images were mixed with Co and VCo scores. Probably, images rated as VUn were too difficult to focus on, resulting in controversial gaze features, except the ratio of crossed disparity. Thus, more experimental investigations are needed with subject behavior for VUn stereoscopic stimuli.

Multiple studies using multi-channel EEG measurements investigated visual fatigue for 2D and 3D content. For example, Chen *et al.* (2013) showed decreases in power spectral entropy. Similar study, using non-consumer grade EEG device (Chen *et al.* 2014) compared energy values in several EEG bands with four discomfort-related parameters – significant changes were found in all bands, except θ band. In our investigation, oscillatory activity of θ, α and β_{l} frequency bands showed no significant difference in all investigated pre-DPM time durations (as shown in Table 3.6). In the Figures 3.16a, 3.17a and 3.18a, the relative mean power of α activity is illustrated, α activity reduced when the level of visual comfort increased. In the Figures 3.16b, 3.17b and 3.18b, the relative mean power of β_{h} activity is illustrated, β_{h} activity increased when the level of visual comfort increased. Therefore, the ratio of $\alpha/\beta_{\mathrm{h}}$ (shown in Figures 3.16c, 3.17c and 3.18c) decreased with higher visual comfort levels. The post-hoc tests showed that $\alpha/\beta_{\mathrm{h}}$ ratio is statistically different for the VUn group and all other visual comfort groups using 4, 5 and 6 s pre-DPM time frames (as shown in Tables 3.8, 3.9 and 3.10). This shows that using the $\alpha/\beta_{\mathrm{h}}$ ratio, as a feature, it is possible to recognize stereoscopic views in the image, specially ones which are VUn for the subjects.

Additionally, the estimation of the different ratios of the EEG band activity showed strong significant differences in the θ/α and $\alpha/\beta_{\mathrm{m}}$ ratios (see Table 3.7). This phenomenon was expected to take into account. Chen *et al.* (2013) published results, where authors used the β frequency range for the ratio estimation. However, in this study, it was noticed that α ratio for visual comfort level classification should be estimated in respect to β_h frequency range. Taking the whole β frequency range no significant differences were found (see Table 3.7). Additionally, after the experimental session, some of the subjects informed that several images

were too difficult to focus and the DPM was not achieved for these images. Therefore, when interpreting the results of this investigation, it would be useful to consider that VUn may indicate a visual comfort level which is too low for the subjects to reach the depth perception.

Developers of virtual reality headsets are implementing EEG and eye tracking sensors in their newest devices (Enhancing AR/VR Devices; FMCG Packaging A-B Testing). Physiological data based calibration of head-mounted displays, compared to the standard subjective assessment methods, is more comfortable and acceptable for the user. Main issues of the objective based calibration of a device are accuracy, reliability, and comfortability. Our proposed technique can be used towards solving these issues. Using DPM time and EEG data an algorithm can be developed, which could be able to detect individual sensation of visual discomfort and calibrate head-mounted display individually for each user without spending a considerable amount of time.

In this investigation, the results of the experimental tests with 28 subjects to evaluate the differences in EEG activity and gaze data was used. Subjects were asked to look at stereoscopic images, and rate their visual comfort using five levels grading system. Additionally, subjects marked a time of achieved depth perception. With such additional markers, the IVY LAB database, by Jung *et al.* (2013), was extended with annotated single-sensor EEG data, gaze data and subjective DPM information. Using these additional markers user behavior during stereoscopic perception was analyzed.

3.4. Conclusions of Chapter 3

1. According to the experimental investigation, the power density spectrum of the EEG signal in the β frequency range should be divided into subranges of β_{l}, β_{m} and β_{h} in order to use β frequency range based features to detect visual discomfort before the DPM.
2. Detection of visual discomfort using features obtained from EEG signal before DPM is dependent on investigated window frame size. Visual discomfort can be detected using β_{h} frequency range of EEG spectrum with analysis window sizes from 2 to 7 s before the DPM.
3. Relative α level of the brain activity increases with higher visual discomfort level, and relative β_{h} level decreases with higher visual discomfort level. Therefore, visual discomfort can be detected using a ratio of $\alpha/\beta_{\mathrm{h}}$ as a feature, when using frame durations from 2 to 7 s before the DPM.
4. Experimental results showed that θ and α waves of the brain activity cannot be used as a feature to detect visual discomfort before the DPM. How-

ever, visual discomfort can be detected using EEG signal when a ratio of θ/α waves is used as a feature with 0.5 or 1 s analysis frame size before the DPM.

5. Depth perception moment time is different for each level of visual discomfort. It increases from 4.31 ± 2.8 s (for images rated as very comfortable) to 6.12 ± 4.9 s (for images rated as very uncomfortable).
6. A number of focus points changes with level of visual discomfort before the DPM. An average number of focus points can be used as a feature to detect visual discomfort when using 2 s time frame before the DPM. Using 2 s time frame, the number of focus points increases by 10% for the images scored from "uncomfortable" to "very comfortable".
7. Pupil size can be used as a feature to detect visual discomfort when using 1, 2 s pre-DPM or 5 s post-DPM time frame windows.
8. Level of binocular disparity, measured at the focus point, decreases by 14.9 pixels in average with higher levels of visual comfort. Binocural disparity can be used as a feature to detect visual discomfort when 5 s pre-DPM time frame is used.
9. Crossed disparity ratio was highest for images rated as "extremely uncomfortable" by approximately 6% compared to other four groups. However, crossed disparity cannot be used as a feature to detect visual discomfort.

General Conclusions

1. The ECG and EEG signal based features can be used for the SoP level detection of the presented audiovisual content:
   1.1. the estimated heart rate from the electrocardiogram signal can be used as a feature to distinguish between low and high SoP level when there are three SoP levels of an audiovisual content presented to the user;
   1.2. features estimated from the electroencephalogram signal can be used to distinguish between an audiovisual content with three SoP levels. However, the β frequency range should be divided into subranges of β_{l}, β_{m} and β_{h}.
2. The EEG signal based features obtained using consumer grade single sensor EEG device placed on the frontal region can be used to detect visual discomfort of the stereoscopic images before the moment of depth perception:
   2.1. visual discomfort can be detected using β_{h} frequency range or the ratio of $\alpha/\beta_{\mathrm{h}}$ of EEG spectrum with analysis window sizes from 2 to 7 s before the DPM;
   2.2. visual discomfort can be detected using EEG signal when a ratio of θ/α waves is used as a feature with 0.5 or 1 s analysis frame size before the DPM.

3. Features obtained using eye tracker data can be used to detect visual discomfort of the stereoscopic images before the moment of depth perception:
   3.1. an average number of focus points can be used as a feature to detect visual discomfort when using 2 s time frame before the DPM;
   3.2. pupil size can be used as a feature to detect visual discomfort when using 1, 2 s pre-DPM or 5 s post-DPM time frame windows;
   3.3. binocular disparity, measured at the focus point can be used as a feature to detect visual discomfort when 5 s pre-DPM time frame is used.

References

Ando, T.; Tanaka, A.; Fukasaku, S.; Takada, R.; Okada, M.; Ukai, K.; Shizuka, K.; Oyamada, H.; Toda, H.; Taniyama, T.; *et al.* 2002. Pupillary and cardiovascular responses to a video movie in senior human subjects, *Autonomic Neuroscience* 97(2): 129–135. [see 9 p.]

Andreassi, J. L. 2010. *Psychophysiology: Human behavior and physiological response*. Psychology Press. 66-70 p. [see 29 p.]

Arndt, S.; Brunnström, K.; Cheng, E.; Engelke, U.; Möller, S.; Antons, J.-N. 2016. Review on using physiology in quality of experience, *Electronic Imaging* 2016(16): 1–9. [see 16 p.]

Aston-Jones, G.; Cohen, J. D. 2005. An integrative theory of locus coeruleus-norepinephrine function: adaptive gain and optimal performance, *Annu. Rev. Neurosci.* 28: 403–450. [see 14 p.]

Barkowsky, M.; Bialkowski, J.; Eskofier, B.; Bitto, R.; Kaup, A. 2009. Temporal trajectory aware video quality measure, *IEEE Journal of Selected Topics in Signal Processing* 3(2): 266–279. [see 13 p.]

Barkowsky, M.; Cousseau, R.; Le Callet, P. 2011. Is visual fatigue changing the perceived depth accuracy on an autostereoscopic display?, in *Stereoscopic Displays and Applications XXII*, vol. 7863, International Society for Optics and Photonics, 78631V. [see 8 p.]

Barreda-Ángeles, M.; Pépion, R.; Bosc, E.; Le Callet, P.; Pereda-Baños, A. 2014. Exploring the effects of 3d visual discomfort on viewers' emotions, in *Image Processing (ICIP), 2014 IEEE International Conference on*, IEEE, 753–757. [see 17 p.]

Beatty, J. 1982. Task-evoked pupillary responses, processing load, and the structure of processing resources, *Psychological bulletin* 91(2): 276. [see 15, 67 p.]

Berger, H. 1929. Über das elektrenkephalogramm des menschen, *European archives of psychiatry and clinical neuroscience* 87(1): 527–570. [see 15 p.]

Bernhard, M.; Dell'mour, C.; Hecher, M.; Stavrakis, E.; Wimmer, M. 2014. The effects of fast disparity adjustment in gaze-controlled stereoscopic applications, in *Proceedings of the Symposium on Eye Tracking Research and Applications*, ACM, 111–118. [see 8 p.]

Birch, J. 1997. Efficiency of the ishihara test for identifying red-green colour deficiency, *Ophthalmic and Physiological Optics* 17(5): 403–408. [see 23 p.]

Bosse, S.; Müller, K.-R.; Wiegand, T.; Samek, W. 2016. Brain-computer interfacing for multimedia quality assessment, in *2016 IEEE International Conference on Systems, Man, and Cybernetics (SMC)*, IEEE, 002 834–002 839. [see 16 p.]

Bouma, H.; Baghuis, L. 1971. Hippus of the pupil: Periods of slow oscillations of unknown origin, *Vision Research* 11(11): 1345–1351. [see 9 p.]

Brisson, J.; Mainville, M.; Mailloux, D.; Beaulieu, C.; Serres, J.; Sirois, S. 2013. Pupil diameter measurement errors as a function of gaze direction in corneal reflection eyetrackers, *Behavior research methods* 45(4): 1322–1331. [see 44 p.]

Bronzino, J. D. 1999. *Biomedical engineering handbook*. CRC press. [see 26 p.]

Bryant, J.; Oliver, M. B. 2009. *Media effects: Advances in theory and research*. Routledge. [see 17 p.]

Carnegie, K.; Rhee, T. 2015. Reducing visual discomfort with hmds using dynamic depth of field, *IEEE computer graphics and applications* 35(5): 34–41. [see 47 p.]

Castellanos, N. P.; Makarov, V. A. 2006. Recovering eeg brain signals: artifact suppression with wavelet enhanced independent component analysis, *Journal of neuroscience methods* 158(2): 300–312. [see 29, 47 p.]

Castellar, E. N.; Oksanen, K.; Van Looy, J. 2014. Assessing game experience: Heart rate variability, in-game behavior and self-report measures, in *2014 Sixth International Workshop on Quality of Multimedia Experience (QoMEX)*, IEEE, 292–296. [see 17 p.]

Chen, C.; Li, K.; Wu, Q.; Wang, H.; Qian, Z.; Sudlow, G. 2013. Eeg-based detection and evaluation of fatigue caused by watching 3dtv, *Displays* 34(2): 81–88. [see 16, 69 p.]

Chen, C.; Wang, J.; Li, K.; Wu, Q.; Wang, H.; Qian, Z.; Gu, N. 2014. Assessment visual fatigue of watching 3dtv using eeg power spectral parameters, *Displays* 35(5): 266–272. [see 69 p.]

Chen, C.-M.; Wang, J.-Y.; Yu, C.-M. 2017. Assessing the attention levels of students by using a novel attention aware system based on brainwave signals, *British Journal of Educational Technology* 48(2): 348–369. [see 45 p.]

Cheng, S.; Lee, H.; Shu, C.; Hsu, H. 2007. Electroencephalographic study of mental fatigue in visual display terminal tasks, *Journal of Medical and Biological Engineering* 27(3): 124. [see 61 p.]

Cho, S.-H.; Kang, H.-B. 2014. Prediction of visual discomfort in watching 3d video using multiple features, in *2014 Southwest Symposium on Image Analysis and Interpretation*, IEEE, 65–68. [see 11, 16 p.]

Cohen, H. W. 2011. P values: use and misuse in medical literature, *American journal of hypertension* 24(1): 18–23. [see 24 p.]

Daly, I.; Nicolaou, N.; Nasuto, S. J.; Warwick, K. 2013. Automated artifact removal from the electroencephalogram: a comparative study, *Clinical EEG and neuroscience* 44(4): 291–306. [see 28 p.]

Daly, I.; Pichiorri, F.; Faller, J.; Kaiser, V.; Kreilinger, A.; Scherer, R.; Müller-Putz, G. 2012. What does clean eeg look like?, in *Engineering in Medicine and Biology Society (EMBC), 2012 Annual International Conference of the IEEE*, IEEE, 3963–3966. [see 28 p.]

Dettmann, A.; Bullinger, A. C. 2018. Autostereoscopic displays for in-vehicle applications, in *Congress of the International Ergonomics Association*, Springer, 457–466. [see 8 p.]

Drachen, A.; Nacke, L. E.; Yannakakis, G.; Pedersen, A. L. 2010. Correlation between heart rate, electrodermal activity and player experience in first-person shooter games, in *Proceedings of the 5th ACM SIGGRAPH Symposium on Video Games*, ACM, 49–54. [see 17 p.]

Dunbar, G.; Boeijinga, P.; Demazieres, A.; Cisterni, C.; Kuchibhatla, R.; Wesnes, K.; Luthringer, R. 2007. Effects of tc-1734 (azd3480), a selective neuronal nicotinic receptor agonist, on cognitive performance and the eeg of young healthy male volunteers, *Psychopharmacology* 191(4): 919–929. [see 61 p.]

Emoto, M.; Niida, T.; Okano, F. 2005. Repeated vergence adaptation causes the decline of visual functions in watching stereoscopic television, *Journal of display technology* 1(2): 328. [see 9 p.]

Emoto, M.; Nojiri, Y.; Okano, F. 2004. Changes in fusional vergence limit and its hysteresis after viewing stereoscopic tv, *Displays* 25(2-3): 67–76. [see 9 p.]

Engelke, U.; Barkowsky, M.; Le Callet, P.; Zepernick, H.-J. 2010a. Modelling saliency awareness for objective video quality assessment, in *Quality of Multimedia Experience (QoMEX), 2010 Second International Workshop on*, IEEE, 212–217. [see 13 p.]

Engelke, U.; Darcy, D. P.; Mulliken, G. H.; Bosse, S.; Martini, M. G.; Arndt, S.; Antons, J.-N.; Chan, K. Y.; Ramzan, N.; Brunnström, K. 2017. Psychophysiology-based qoe assessment: A survey, *IEEE Journal of Selected Topics in Signal Processing* 11(1): 6–21. [see 10, 11, 12, 14 p.]

Engelke, U.; Kaprykowsky, H.; Zepernick, H.-J.; Ndjiki-Nya, P. 2011. Visual attention in quality assessment, *IEEE Signal Processing Magazine* 28(6): 50–59. [see 12 p.]

Engelke, U.; Liu, H.; Wang, J.; Le Callet, P.; Heynderickx, I.; Zepernick, H.-J.; Maeder, A. 2013. Comparative study of fixation density maps, *IEEE Transactions on Image Processing* 22(3): 1121–1133. [see 13 p.]

Engelke, U.; Maeder, A.; Zepernick, H.-J. 2009. Visual attention modelling for subjective image quality databases, in *Multimedia Signal Processing, 2009. MMSP'09. IEEE International Workshop on*, IEEE, 1–6. [see 12 p.]

Engelke, U.; Pepion, R.; Le Callet, P.; Zepernick, H.-J. 2010b. Linking distortion perception and visual saliency in h. 264/avc coded video containing packet loss, in *Visual Communications and Image Processing 2010*, vol. 7744, International Society for Optics and Photonics, 774406. [see 12, 13 p.]

Enhancing AR/VR Devices with EEG and ECG Biosensors [interactive]. 2018.]. Available online at: http://neurosky.com/2018/01/enhancing-arvr-devices-with-eeg-and-ecg-biosensors. [see 70 p.]

Fernandes, A. S.; Feiner, S. K. 2016. Combating vr sickness through subtle dynamic field-of-view modification, in *2016 IEEE Symposium on 3D User Interfaces (3DUI)*, IEEE, 201–210. [see 8 p.]

Fischmeister, F. P. S.; Bauer, H. 2006. Neural correlates of monocular and binocular depth cues based on natural images: A loreta analysis, *Vision research* 46(20): 3373–3380. [see 8 p.]

FMCG Packaging A-B Testing using VR and Emotiv Mobile EEG Headsets [interactive]. 2016.]. Available online at: https://www.emotiv.com/blog/fmcg-packaging-a-b-testing-using-vr-and-emotiv-mobile-eeg-headsets/. [see 70 p.]

Freund, R. J.; Littell, R. C. 1981. *SAS for linear models: a guide to the ANOVA and GLM procedures*. Sas Institute Cary. [see 24 p.]

Frey, J.; Appriou, A.; Lotte, F.; Hachet, M. 2016. Classifying eeg signals during stereoscopic visualization to estimate visual comfort, *Computational intelligence and neuroscience* 2016: 7. [see 8, 9 p.]

Goncharova, I. I.; McFarland, D. J.; Vaughan, T. M.; Wolpaw, J. R. 2003. Emg contamination of eeg: spectral and topographical characteristics, *Clinical neurophysiology* 114(9): 1580–1593. [see 28 p.]

Gramfort, A.; Luessi, M.; Larson, E.; Engemann, D. A.; Strohmeier, D.; Brodbeck, C.; Parkkonen, L.; Hämäläinen, M. S. 2014. Mne software for processing meg and eeg data, *Neuroimage* 86: 446–460. [see 29 p.]

Grand View Research, 2018. Visualization and 3d rendering software market size, share and trends analysis report by application, 2018 – 2025. 2018. [see 2 p.]

Gupta, R.; Arndt, S.; Antons, J.-N.; Schleicher, R.; Möller, S.; Falk, T. H.; *et al.* 2013. Neurophysiological experimental facility for quality of experience (qoe) assessment, in *Integrated Network Management (IM 2013), 2013 IFIP/IEEE International Symposium on*, IEEE, 1300–1305. [see 8 p.]

Guyon, I.; Elisseeff, A. 2003. An introduction to variable and feature selection, *Journal of machine learning research* 3(Mar): 1157–1182. [see 24 p.]

Harezlak, K.; Kasprowski, P.; Stasch, M. 2014. Towards accurate eye tracker calibration–methods and procedures, *Procedia Computer Science* 35: 1073–1081. [see 12 p.]

Haykin, S.; *et al.* 2005. Cognitive radio: brain-empowered wireless communications, *IEEE journal on selected areas in communications* 23(2): 201–220. [see 29 p.]

Hoffman, D. M.; Girshick, A. R.; Akeley, K.; Banks, M. S. 2008. Vergence–accommodation conflicts hinder visual performance and cause visual fatigue, *Journal of vision* 8(3): 33–33. [see 39, 67 p.]

Howarth, P.; Costello, P. 1997. The occurrence of virtual simulation sickness symptoms when an hmd was used as a personal viewing system, *Displays* 18(2): 107–116. [see 8 p.]

Hsu, B.-W.; Wang, M.-J. J. 2013. Evaluating the effectiveness of using electroencephalogram power indices to measure visual fatigue, *Perceptual and motor skills* 116(1): 235–252. [see 61 p.]

Hua, H. 2017. Enabling focus cues in head-mounted displays, *Proceedings of the IEEE* 105(5): 805–824. [see 9 p.]

Hyvarinen, A. 1999. Fast and robust fixed-point algorithms for independent component analysis, *IEEE transactions on Neural Networks* 10(3): 626–634. [see 29 p.]

Hyvärinen, A.; Oja, E. 2000. Independent component analysis: algorithms and applications, *Neural networks* 13(4-5): 411–430. [see 29 p.]

Iatsun, I.; Larabi, M.-C.; Fernandez-Maloigne, C. 2015. Investigation and modeling of visual fatigue caused by s3d content using eye-tracking, *Displays* 39: 11–25. [see 8, 10 p.]

Idris, Z.; Muzaimi, M.; Ghani, R. I.; Idris, B.; Kandasamy, R.; Abdullah, J. M. 2014. Principles, anatomical origin and applications of brainwaves: A review, our experience and hypothesis related to microgravity and the question on soul, *Journal of Biomedical Science and Engineering* 7(08): 435. [see 29 p.]

Inoue, T.; Ohzu, H. 1997. Accommodative responses to stereoscopic three-dimensional display, *Applied optics* 36(19): 4509–4515. [see 44 p.]

iPad (4th generation) - Technical Specifications [interactive]. 2019. "Apple" [viewed on March 15th, 2019]. Available online at: https://support.apple.com/kb/SP662?locale=en_GB. [see 23 p.]

iPhone 5 - Technical Specification [interactive]. 2019. "Apple" [viewed on March 15th, 2019]. Available online at: https://support.apple.com/kb/SP655?locale=en_GB. [see 23 p.]

ITU-R BT.2021-1 2015. Subjective methods for the assessment of stereoscopic 3dtv systems . [see 43 p.]

ITU-R BT.2022. General viewing conditions for subjective assessment of quality of sdtv and hdtv television pictures on flat panel displays. 2012. [see 23 p.]

ITU-R BT.500-13. Methodology for the subjective assessment of the quality of television pictures. 2012. [see 23, 41 p.]

ITU-T Rec. P.910. Subjective video quality assessment methods for multimedia applications. 2008. [see 23 p.]

Jaschinski, W.; Bonacker, M.; Alshuth, E. 1996. Accommodation, convergence, pupil diameter and eye blinks at a crt display flickering near fusion limit, *Ergonomics* 39(1): 152–164. [see 9 p.]

Jepma, M.; Nieuwenhuis, S. 2011. Pupil diameter predicts changes in the exploration–exploitation trade-off: Evidence for the adaptive gain theory, *Journal of cognitive neuroscience* 23(7): 1587–1596. [see 15 p.]

Jiang, Q.; Shao, F.; Jiang, G.; Yu, M.; Peng, Z. 2015. Three-dimensional visual comfort assessment via preference learning, *Journal of Electronic Imaging* 24(4): 043 002. [see 38 p.]

Jiang, Q.; Shao, F.; Jiang, G.; Yu, M.; Peng, Z. 2017a. Leveraging visual attention and neural activity for stereoscopic 3d visual comfort assessment, *Multimedia Tools and Applications* 76(7): 9405–9425. [see 38 p.]

Jiang, Q.; Shao, F.; Jiang, G.; Yu, M.; Peng, Z. 2017b. Visual comfort assessment for stereoscopic images based on sparse coding with multi-scale dictionaries, *Neurocomputing* 252: 77–86. [see 38 p.]

Jiang, Q.; Shao, F.; Lin, W.; Jiang, G. 2016. On predicting visual comfort of stereoscopic images: a learning to rank based approach, *IEEE Signal Processing Letters* 23(2): 302–306. [see 11, 38 p.]

John, B.; Raiturkar, P.; Banerjee, A.; Jain, E. 2018. An evaluation of pupillary light response models for 2d screens and vr hmds, in *Proceedings of the 24th ACM Symposium on Virtual Reality Software and Technology*, ACM, 19. [see 44 p.]

Johnson, C.; Moorhead, R.; Munzner, T.; Pfister, H.; Rheingans, P.; Yoo, T. S. 2005. Nih-nsf visualization research challenges report, Institute of Electrical and Electronics Engineers. [see 2 p.]

Joshi, S.; Li, Y.; Kalwani, R. M.; Gold, J. I. 2016. Relationships between pupil diameter and neuronal activity in the locus coeruleus, colliculi, and cingulate cortex, *Neuron* 89(1): 221–234. [see 14 p.]

Jung, Y.; Sohn, H.; Lee, S.-i.; Ro, Y. 2014. Visual comfort improvement in stereoscopic 3d displays using perceptually plausible assessment metric of visual comfort, *IEEE Transactions on Consumer Electronics* 60(1): 1–9. [see 38 p.]

Jung, Y. J.; Sohn, H.; Lee, S.-I.; Park, H. W.; Ro, Y. M. 2013. Predicting visual discomfort of stereoscopic images using human attention model, *IEEE transactions on circuits and systems for video technology* 23(12): 2077–2082. [see 37, 38, 39, 50, 70 p.]

Kahneman, D.; Beatty, J. J. 1966. Pupil diameter and load on memory., *Science* 154 3756: 1583–5. [see 15 p.]

Kennedy, R. S.; Lane, N. E.; Berbaum, K. S.; Lilienthal, M. G. 1993. Simulator sickness questionnaire: An enhanced method for quantifying simulator sickness, *The international journal of aviation psychology* 3(3): 203–220. [see 8 p.]

Khaustova, D.; Fournier, J.; Wyckens, E.; Le Meur, O. 2014. An investigation of visual selection priority of objects with texture and crossed and uncrossed disparities, in *Human Vision and Electronic Imaging XIX*, vol. 9014, International Society for Optics and Photonics, 90140D. [see 45 p.]

Kim, H.; Lee, S.; Bovik, A. C. 2014. Saliency prediction on stereoscopic videos, *IEEE Transactions on Image Processing* 23(4): 1476–1490. [see 11 p.]

Klamm, J.; Tarnow, K. G. 2015. Computer vision syndrome: a review of literature, *Medsurg Nursing* 24(2): 89. [see 9 p.]

Koelstra, S.; Muhl, C.; Soleymani, M.; Lee, J.-S.; Yazdani, A.; Ebrahimi, T.; Pun, T.; Nijholt, A.; Patras, I. 2012. Deap: A database for emotion analysis; using physiological signals, *IEEE transactions on affective computing* 3(1): 18–31. [see 10 p.]

Krishnan, S. R.; Seelamantula, C. S. 2013. On the selection of optimum savitzky-golay filters, *IEEE transactions on signal processing* 61(2): 380–391. [see 26 p.]

Kroupi, E.; Hanhart, P.; Lee, J.-S.; Rerabek, M.; Ebrahimi, T. 2014. Predicting subjective sensation of reality during multimedia consumption based on eeg and peripheral physiological signals, in *2014 IEEE International Conference on Multimedia and Expo (ICME)*, IEEE, 1–6. [see 17 p.]

Lambooij, M.; Fortuin, M.; Heynderickx, I.; IJsselsteijn, W. 2009. Visual discomfort and visual fatigue of stereoscopic displays: A review, *Journal of Imaging Science and Technology* 53(3): 30 201–1. [see 7, 8, 9 p.]

Lambooij, M. T.; IJsselsteijn, W. A.; Heynderickx, I. 2007. Visual discomfort in stereoscopic displays: a review, in *Stereoscopic Displays and Virtual Reality Systems XIV*, vol. 6490, International Society for Optics and Photonics, 64900I. [see 7, 8, 9 p.]

Lascu, M.; Lascu, D. 2008. Electrocardiogram compression and optimal ecg filtering algorithms, *WSEAS Transactions on Computers* 7(4): 155–164. [see 26 p.]

Le Callet, P.; Niebur, E. 2013. Visual attention and applications in multimedia technologies, *Proceedings of the IEEE* 101(9): 2058–2067. [see 12 p.]

Le Meur, O.; Ninassi, A.; Le Callet, P.; Barba, D. 2010a. Do video coding impairments disturb the visual attention deployment?, *Signal Processing: Image Communication* 25(8): 597–609. [see 13 p.]

Le Meur, O.; Ninassi, A.; Le Callet, P.; Barba, D. 2010b. Overt visual attention for free-viewing and quality assessment tasks: Impact of the regions of interest on a video quality metric, *Signal Processing: Image Communication* 25(7): 547–558. [see 13 p.]

Lee, J.-S.; De Simone, F.; Ebrahimi, T. 2009. Influence of audio-visual attention on perceived quality of standard definition multimedia content, in *Quality of Multimedia Experience, 2009. QoMEx 2009. International Workshop on*, IEEE, 13–18. [see 13 p.]

Lee, S.-i.; Lee, S. H.; Plataniotis, K. N. K.; Ro, Y. M. 2016. Experimental investigation of facial expressions associated with visual discomfort: feasibility study toward an objective measurement of visual discomfort based on facial expression, *Journal of Display Technology* 12(12): 1785–1797. [see 8 p.]

Lin, F.-R.; Kao, C.-M. 2018. Mental effort detection using eeg data in e-learning contexts, *Computers & Education* 122: 63–79. [see 8, 45 p.]

Liu, H.; Engelke, U.; Wang, J.; Le Callet, P.; Heynderickx, I. 2013. How does image content affect the added value of visual attention in objective image quality assessment?, *IEEE Signal Processing Letters* 20(4): 355–358. [see 13 p.]

Liu, H.; Heynderickx, I. 2011. Visual attention in objective image quality assessment: Based on eye-tracking data, *IEEE Transactions on Circuits and Systems for Video Technology* 21(7): 971–982. [see 13 p.]

Luz, E. J. d. S.; Schwartz, W. R.; Cámara-Chávez, G.; Menotti, D. 2016. Ecg-based heartbeat classification for arrhythmia detection: A survey, *Computer methods and programs in biomedicine* 127: 144–164. [see 26 p.]

Maskeliunas, R.; Damasevicius, R.; Martisius, I.; Vasiljevas, M. 2016. Consumer-grade eeg devices: are they usable for control tasks?, *PeerJ* 4: e1746. [see 46 p.]

Mertler, C. A.; Reinhart, R. V. 2016. *Advanced and multivariate statistical methods: Practical application and interpretation*. Routledge. 12-20 p. [see 24 p.]

Minguillon, J.; Lopez-Gordo, M. A.; Pelayo, F. 2017. Trends in eeg-bci for daily-life: Requirements for artifact removal, *Biomedical Signal Processing and Control* 31: 407–418. [see 28 p.]

Moon, S.-E.; Lee, J.-S. 2017. Implicit analysis of perceptual multimedia experience based on physiological response: a review, *IEEE Transactions on Multimedia* 19(2): 340–353. [see 8 p.]

Murata, A.; Uetake, A.; Otsuka, M.; Takasawa, Y. 2001. Proposal of an index to evaluate visual fatigue induced during visual display terminal tasks, *International Journal of Human-Computer Interaction* 13(3): 305–321. [see 9 p.]

Muthukumaraswamy, S. 2013. High-frequency brain activity and muscle artifacts in meg/eeg: a review and recommendations, *Frontiers in human neuroscience* 7: 138. [see 28 p.]

Ninassi, A.; Le Meur, O.; Le Callet, P.; Barba, D. 2007. Does where you gaze on an image affect your perception of quality? applying visual attention to image quality metric, in *Image Processing, 2007. ICIP 2007. IEEE International Conference on*, vol. 2, IEEE, II–169. [see 13 p.]

Norcia, A. M.; Appelbaum, L. G.; Ales, J. M.; Cottereau, B. R.; Rossion, B. 2015. The steady-state visual evoked potential in vision research: a review, *Journal of vision* 15(6): 4–4. [see 17 p.]

Ogdon, D. C. 2019. Hololens and vive pro: Virtual reality headsets, *Journal of the Medical Library Association: JMLA* 107(1): 118. [see 4 p.]

Oh, H.; Kim, J.; Kim, J.; Kim, T.; Lee, S.; Bovik, A. C. 2017. Enhancement of visual comfort and sense of presence on stereoscopic 3d images, *IEEE Transactions on Image Processing* 26(8): 3789–3801. [see 39 p.]

Oostenveld, R.; Fries, P.; Maris, E.; Schoffelen, J.-M. 2011. Fieldtrip: open source software for advanced analysis of meg, eeg, and invasive electrophysiological data, *Computational intelligence and neuroscience* 2011: 1. [see 29, 47 p.]

Oppenheim, A. V.; Schafer, R. W. 2014. *Discrete-time signal processing*. Pearson Education. [see 26 p.]

Pan, J.; Tompkins, W. J. 1985. A real-time qrs detection algorithm, *IEEE Trans. Biomed. Eng* 32(3): 230–236. [see 26 p.]

Partala, T.; Surakka, V. 2003. Pupil size variation as an indication of affective processing, *International journal of human-computer studies* 59(1-2): 185–198. [see 14 p.]

Pelli, D. G. 1997. The videotoolbox software for visual psychophysics: Transforming numbers into movies, *Spatial vision* 10(4): 437–442. [see 44 p.]

Perrin, A.-F.; Řeřábek, M.; Ebrahimi, T. 2016. Towards prediction of sense of presence in immersive audiovisual communications, *Electronic Imaging* 2016(16): 1–8. [see 3, 10, 21, 22, 23, 24, 25, 29 p.]

PnS Market Research, 2017. Global advanced visualization market size, share, development, growth and demand forecast to 2023. 2017. [see 2 p.]

Porter, G.; Troscianko, T.; Gilchrist, I. D. 2007. Effort during visual search and counting: Insights from pupillometry, *The Quarterly Journal of Experimental Psychology* 60(2): 211–229. [see 15, 67 p.]

Read, J. C.; Bohr, I. 2014. User experience while viewing stereoscopic 3d television, *Ergonomics* 57(8): 1140–1153. [see 2 p.]

Saito, S. 1992. Does fatigue exist in a quantitative measurement of eye movements?, *Ergonomics* 35(5-6): 607–615. [see 9 p.]

Savitzky, A.; Golay, M. J. 1964. Smoothing and differentiation of data by simplified least squares procedures., *Analytical chemistry* 36(8): 1627–1639. [see 26 p.]

Semmlow, J. L.; Griffel, B. 2014. *Biosignal and medical image processing*. CRC press. [see 26 p.]

Shao, F.; Jiang, Q.; Fu, R.; Yu, M.; Jiang, G. 2016. Optimizing visual comfort for stereoscopic 3d display based on color-plus-depth signals, *Optics express* 24(11): 11 640–11 653. [see 7 p.]

Shao, F.; Lin, W.; Li, Z.; Jiang, G.; Dai, Q. 2017. Toward simultaneous visual comfort and depth sensation optimization for stereoscopic 3-d experience, *IEEE transactions on cybernetics* 47(12): 4521–4533. [see 38 p.]

Sohn, H.; Jung, Y. J.; Lee, S.-i.; Ro, Y. M. 2013. Predicting visual discomfort using object size and disparity information in stereoscopic images, *IEEE Transactions on Broadcasting* 59(1): 28–37. [see 39 p.]

Solimini, A. G. 2013. Are there side effects to watching 3d movies? a prospective crossover observational study on visually induced motion sickness, *PloS one* 8(2): e56 160. [see 2 p.]

Song, J.; Yang, F.; Zhou, Y.; Wan, S.; Wu, H. R. 2016. Qoe evaluation of multimedia services based on audiovisual quality and user interest, *IEEE Transactions on Multimedia* 18(3): 444–457. [see 8 p.]

Sood, M.; Kumar, V.; Bhooshan, S. V. 2013. Review of state of art in electrooculogram artifact removal from electroencephalogram signals, *International Journal of Enhanced Research in Science Technology & Engineering* 2(4): 32–41. [see 28 p.]

56-inch Quad Full HD Reference LCD monitor - Technical Specifications [interactive]. 2019. "Sonny" [viewed on March 15th, 2019]. Available online at: https://pro.sony/en_IE/products/broadcastpromonitors/srm-l560. [see 23 p.]

Suryakumar, R. 2005. Study of the dynamic interactions between vergence and accommodation . [see 67 p.]

Terzic, K.; Hansard, M. 2017. Causes of discomfort in stereoscopic content: a review, *arXiv preprint arXiv:1703.04574* 1–22. [see 40, 47 p.]

Thompson, H. S.; Kardon, R. H. 2006. Irene e. loewenfeld, phd physiologist of the pupil, *Journal of Neuro-ophthalmology* 26(2): 139–148. [see 14 p.]

Thomson, D. J. 1982. Spectrum estimation and harmonic analysis, *Proceedings of the IEEE* 70(9): 1055–1096. [see 29 p.]

Trani, A.; Verhaeghen, P. 2018. Foggy windows: Pupillary responses during task preparation, *Quarterly Journal of Experimental Psychology* 71(10): 2235–2248. [see 13 p.]

Uetake, A.; Murata, A.; Otsuka, M.; Takasawa, Y. 2000. Evaluation of visual fatigue during vdt tasks, in *Smc 2000 conference proceedings. 2000 ieee international conference on systems, man and cybernetics.'cybernetics evolving to systems, humans, organizations, and their complex interactions'(cat. no. 0*, vol. 2, IEEE, 1277–1282. [see 9 p.]

Ukai, K.; Howarth, P. A. 2008. Visual fatigue caused by viewing stereoscopic motion images: Background, theories, and observations, *Displays* 29(2): 106–116. [see 9, 44 p.]

Urigüen, J. A.; Garcia-Zapirain, B. 2015. Eeg artifact removal—state-of-the-art and guidelines, *Journal of neural engineering* 12(3): 031 001. [see 15, 28 p.]

Ursuţiu, D.; Samoilă, C.; Drăgulin, S.; Constantin, F. A. 2018. Investigation of music and colours influences on the levels of emotion and concentration, in *Online Engineering & Internet of Things*, Springer, 910–918. [see 45 p.]

Urvoy, M.; Barkowsky, M.; Le Callet, P. 2013. How visual fatigue and discomfort impact 3d-tv quality of experience: a comprehensive review of technological, psychophysical, and psychological factors, *annals of telecommunications-annales des télécommunications* 68(11-12): 641–655. [see 8, 9 p.]

Van Rijn, H.; Dalenberg, J. R.; Borst, J. P.; Sprenger, S. A. 2012. Pupil dilation co-varies with memory strength of individual traces in a delayed response paired-associate task, *PLoS One* 7(12): e51 134. [see 15 p.]

Varazzani, C.; San-Galli, A.; Gilardeau, S.; Bouret, S. 2015. Noradrenaline and dopamine neurons in the reward/effort trade-off: a direct electrophysiological comparison in behaving monkeys, *Journal of Neuroscience* 35(20): 7866–7877. [see 14 p.]

Vos, D. M.; Riès, S.; Vanderperren, K.; Vanrumste, B.; Alario, F.-X.; Huffel, V. S.; Burle, B. 2010. Removal of muscle artifacts from eeg recordings of spoken language production, *Neuroinformatics* 8(2): 135–150. [see 28 p.]

Wang, L.; Teunissen, K.; Tu, Y.; Chen, L.; Zhang, P.; Zhang, T.; Heynderickx, I. 2011. Crosstalk evaluation in stereoscopic displays, *Journal of display technology* 7(4): 208–214. [see 40 p.]

Wang, X.; Qian, Z.; Xing, L.; Jin, S.; Liu, B.; Li, Z.; Yin, J. 2015. The study of human health effect induced by depth information of stereo vision film, *Journal of Innovative Optical Health Sciences* 8(05): 1550 011. [see 9 p.]

Wann, J. P.; White, A. D.; Wilkie, R. M.; Culmer, P. R.; Lodge, J. P. A.; Mon-Williams, M. 2014. Measurement of visual aftereffects following virtual environment exposure: Implications for minimally invasive surgery, in *Handbook of Virtual Environments*, CRC Press, 812–834. [see 8 p.]

Whitham, E. M.; Lewis, T.; Pope, K. J.; Fitzgibbon, S. P.; Clark, C. R.; Loveless, S.; DeLosAngeles, D.; Wallace, A. K.; Broberg, M.; Willoughby, J. O. 2008. Thinking activates emg in scalp electrical recordings, *Clinical neurophysiology* 119(5): 1166–1175. [see 28 p.]

Whitham, E. M.; Pope, K. J.; Fitzgibbon, S. P.; Lewis, T.; Clark, C. R.; Loveless, S.; Broberg, M.; Wallace, A.; DeLosAngeles, D.; Lillie, P.; *et al.* 2007. Scalp electrical recording during paralysis: quantitative evidence that eeg frequencies above 20 hz are contaminated by emg, *Clinical Neurophysiology* 118(8): 1877–1888. [see 28 p.]

Winkler, S.; Subramanian, R. 2013. Overview of eye tracking datasets, in *2013 Fifth International Workshop on Quality of Multimedia Experience (QoMEX)*, IEEE, 212–217. [see 10 p.]

Xu, H.; Jiang, G.; Yu, M.; Luo, T.; Peng, Z.; Shao, F.; Jiang, H. 2018. 3d visual discomfort predictor based on subjective perceived-constraint sparse representation in 3d display system, *Future Generation Computer Systems* 83: 85–94. [see 38, 39 p.]

Yang, J.; Zhao, Y.; Zhu, Y.; Xu, H.; Lu, W.; Meng, Q. 2019. Blind assessment for stereo images considering binocular characteristics and deep perception map based on deep belief network, *Information Sciences* 474: 1–17. [see 38 p.]

Yano, S.; Ide, S.; Mitsuhashi, T.; Thwaites, H. 2002. A study of visual fatigue and visual comfort for 3d hdtv/hdtv images, *Displays* 23(4): 191–201. [see 8 p.]

Yoon, H.; Park, S.-W.; Lee, Y.-K.; Jang, J.-H. 2013. Emotion recognition of serious game players using a simple brain computer interface, in *ICT Convergence (ICTC), 2013 International Conference on*, IEEE, 783–786. [see 45 p.]

Yoshitomi, T.; Ito, Y.; Inomata, H. 1985. Adrenergic excitatory and cholinergic inhibitory innervations in the human iris dilator, *Experimental eye research* 40(3): 453–459. [see 14 p.]

Yun, J. D.; Kwak, Y.; Yang, S. 2013. Evaluation of perceptual resolution and crosstalk in stereoscopic displays, *Journal of Display Technology* 9(2): 106–111. [see 40 p.]

Yuval-Greenberg, S.; Tomer, O.; Keren, A. S.; Nelken, I.; Deouell, L. Y. 2008. Transient induced gamma-band response in eeg as a manifestation of miniature saccades, *Neuron* 58(3): 429–441. [see 28 p.]

Zekveld, A. A.; Kramer, S. E.; Festen, J. M. 2010. Pupil response as an indication of effortful listening: The influence of sentence intelligibility, *Ear and hearing* 31(4): 480–490. [see 15 p.]

Zhang, W.; Luo, T.; Jiang, G.; Jiang, Q.; Ying, H.; Lu, J. 2016. Using saliency-weighted disparity statistics for objective visual comfort assessment of stereoscopic images, *3D Research* 7(2): 17. [see 38 p.]

Zheng, W.-L.; Lu, B.-L. 2015. Investigating critical frequency bands and channels for eeg-based emotion recognition with deep neural networks, *IEEE Transactions on Autonomous Mental Development* 7(3): 162–175. [see 10 p.]

Zhou, J.; Gu, X.; Zhang, Y. 2017. On evaluation the quality of subjective s3d comfort assessment, in *2017 IEEE International Symposium on Broadband Multimedia Systems and Broadcasting (BMSB)*, IEEE, 1–6. [see 8 p.]

Zhou, Y.; Chen, Z.; Li, W. 2018. Hybrid distortion aggregated visual comfort assessment for stereoscopic image retargeting, *arXiv preprint arXiv:1811.12687* . [see 38 p.]

Zou, B.; Liu, Y.; Guo, M.; Wang, Y. 2015. Eeg-based assessment of stereoscopic 3d visual fatigue caused by vergence-accommodation conflict, *Journal of Display Technology* 11(12): 1076–1083. [see 61 p.]

List of Scientific Publications by the Author on the Topic of the Dissertation

Papers in the Reviewed Scientific Journals

Abromavičius, V.; Serackis, A.; Plonis, D; Katkevičius, A. 2018. Evaluation of EEG-based Complementary Features for Assessment of Visual Discomfort Based on Stable Depth Perception Time, *The Radioengineering* 27(4): 1138–1146. ISSN 1210-2512. IF=0.967.

Abromavičius, V.; Serackis, A. 2018. Eye and EEG Activity Markers for Visual Comfort Level of Images, *Biocybernetics and Biomedical Engineering* 38(4): 810–818. ISSN 0208-5216. IF=2.159.

Abromavičius, V. 2017. Patirtos kokybės tyrimas taikant ECG požymius stebint audiovizualinį turinį, *Mokslas: Lietuvos ateitis: Elektronika ir elektrotechnika* 9(3): 340–344. ISSN 2029-2341.

Other Papers

Abromavičius, V.; Serackis, A. 2017. Stereoscopic Focus Moment Identification Based on Pupil Dynamics Measures, in *2017 5th IEEE Workshop on Advances in Information, Electronic and Electrical Engineering (AIEEE)*, 1–4.

Abromavičius, V.; Gedminas, A.; Serackis, A. 2017. Detecting Sense of Presence Changes in EEG Spectrum During Perception of Immersive Audiovisual Content, in *2017 Open Conference of Electrical, Electronic and Information Sciences (eStream)*, 1–4.

Serackis, A.; Abromavičius, V.; Gudiškis, A. 2015. Identification of ECG Signal Pattern Changes to Reduce the Incidence of Ventricular Tachycardia False Alarms, in *2015 Computing in Cardiology Conference (CinC)*, 1193–1196.

Summary in Lithuanian

Įvadas

Problemos formulavimas

Virtualios realybės turiniui peržiūrėti skirti atvaizdavimo įrenginiai praktikoje naudojami mažai ne dėl aukštos jų kainos ar nepakankamos vaizdo kokybės, o neretai dėl dažnai sukeliamo regos diskomforto. Regos diskomforto lygis yra individualus kiekvienam naudotojui, todėl reikalingos techninės priemonės, leidžiančios aptikti pirmuosius regos diskomforto požymius naudojant virtualiosios realybės akinius. Rinkoje jau pasirodė virtualiosios realybės akiniai su integruota akių sekimo įranga, taip pat akinių gamintojai bendradarbiauja su elektroencefalogramų nuskaitymo įrenginius gaminančiomis įmonėmis. Tačiau nėra sukurti būdai regos diskomfortui aptikti naudojant akių aktyvumo ar elektroencefalogramų registravimo įrenginius. Siekiant aptikti akių diskomfortą sąlygojančias situacijas vaizdo peržiūros metu, disertacijoje sprendžiama vaizdo pojūčių kiekybinio įvertinimo problema.

Problemai išspręsti disertacijoje naudoti viešuose duomenų rinkiniuose esantys elektrokardiogramų, elektroencefalogramų signalai, vaizdų rinkiniai. Papildomai buvo atliktas eksperimentinis tyrimas, kurio metu buvo matuojamos ne tik elektroencefalogramos, tačiau registruojamas ir akių aktyvumas naudojant specializuotą akių sekimo įrenginį. Tyrimo dalyviai žiūrėjo į vaizdus turinčius stereoskopinį efektą, bei turėjo subjektyviai vertinti patiriamą regos diskomfortą. Buvo tikimasi, kad surinktuose signaluose galima išskirti požymius, kurie leis atskirti skirtingą regos diskomfortą sukeliančius vaizdus.

Mokslo problemos aktualumas

Nuo 1987 m. JAV National Science Foundation (NSF) pripažino vizualizavimo mokslą strategine nacionalinio proveržio kryptimi. Po iš esmės sėkmingos ir 25 metus trukusios šios mokslo krypties vystymosi istorijos lieka nemažai aktualių ir neišspręstų problemų. Tarp aktualiausiųjų probleminių vizualizavimo uždavinių (angl. *Visualization Research Challenges*) įvardinamas vizualizavimas, kuris skirtomas į tyrimų tematikas, susijusias su vizualizavimu: 1) skirtu žiūrovui (angl. *view-dependent*), 2) grįstu vaizdo turiniu (angl. *image-based rendering*), 3) naudojant skirtingas vaizdo skyras (angl. *multiresolution*), 4) grįstu svarba (angl. *importance-based*), 5) naudojančiu adaptyvius ir išteklius tausojančius algoritmus (angl. *adaptive resource-aware algorithms*). Teigiama, kad šie uždaviniai turi būti sprendžiami įvertinant konkrečios taikomosios srities keliamus reikalavimus.

Analizuojant trimačio vizualizavimo sistemų ateities perspektyvas yra atliktos kelios trimačio vizualizavimo rinkos vystymosi prognozės-studijos. Industry Reports 2017 metais prognozavo 3D vizualizavimo rinkos augimą iki 4,03 mlrd. JAV dolerių 2023 metais. PnS Market Research 2019 metais atlikto tyrimo duomenimis, trimačio sutapdinimo ir modeliavimo rinka turėtų pasiekti 3,84 mlrd. JAV dolerių iki 2023 metų.

Doktorantūros metu buvo tiriami požymiai susiję su regos diskomfortu (angl. *visual discomfort*), su vizualizavimu sietinu akių nuovargiu (angl. *gaze fatigue*), akių įtampa (angl. *eyestrain*), klaidingu gylio suvokimu ir ilgu žmogaus prisitaikymo prie vaizdo laiku (angl. *depth perception time*). Yra žinoma, kad stereoskopinio vizualizavimo metu suaktyvėja žmogaus akių judėjimą valdančios smegenų sritys (angl. *oculomotor nerve*), kurių aktyvumas pastebimas EEG signaluose. Disertacijoje buvo siekiama ištirti esamų metodų EEG signalams analizuoti efektyvumą naudotojui stebint stereoskopinį turinį ir pasiūlyti požymius, regos diskomforto lygiui matuoti. Tyrimai buvo atliekami naudojant viešai prieinamą stereoskopinių vaizdų rinkinį. Buvo registruojami abiejų akių judesiai ir matuojamos elektroencefalogramos.

Tyrimų objektas

Tyrimų objektras yra paieška išmatuojamų kiekybinių parametrų, kurie leistų atpažinti, kada žmogus stebi vaizdus neįtempdamas akių judesius valdančius raumenis, atskirti, kada vaizdo gylio suvokimui akys yra tinkamoje padėtyje, o kada gylio suvokimui tinkamos akių padėties ilgai nepavyksta rasti.

Darbo tikslas

Disertacijos tikslas – pasiūlyti naujus požymius, tinkamus regos diskomfortui aptikti ištiriant pokyčius elektroencefalogramose ir akių judesių sekimo metu gautuose signaluose.

Darbo uždaviniai

Disertacijos hipotezėms patikrinti suformuluoti trys uždaviniai:

1. Ištirti stebimo audiovizualaus turinio poveikį signalų požymiams, gautiems iš matuojamų elektroencefalogramų ir elektrokardiogramų.
2. Ištirti skirtingo lygio stereoskopinį gylį formuojančių vaizdų įtaką elektroencefalogramoms ir pasiūlyti požymius regos diskomforto simptomus sąlygojančių būsenų atpažinimui.
3. Ištirti akių sekimo metu gaunamų signalų požymius, leidžiančius aptikti regos diskomforto simptomus stereoskopinių vaizdų stebėjimo metu.

Tyrimų metodika

Disertacijoje atlikti tyrimai suskirstyti į dvi grupes. Pirmojoje grupėje naudojami Perrin *et al.* (2016) autoriaus tyrimų metu išmatuoti signalai. Autoriaus atlikto tyrimo metu 20 savanorių grupė stebėjo trijų kokybės lygių vaizdo įrašus naudodami skirtingo dydžio vaizduoklius. Tyrimo metu išmatuotos elektrokardiogamos ir elektroencefalogramos buvo analizuojamos naudojant skaitmeninio signalų apdorojimo priemones bei statistinę signalų požymių analizę. Antrojojedisertacijos tyrimų grupėje naudojami 120 stereoskopinių vaizdų, kuriuos paruošė ir subjektyvaus vertinimo eksperimentiniame tyrime naudojo ir kiti autoriai Jung *et al.* (2013). Disertacijos rengimo metu buvo surinkta papildoma 28 savanorių grupė. Eksperimentiniame tyrime dalyvavę savanoriai, kaip ir kitų autorių tyrimuose, subjektyviai vertino stereoskopinius vaizdus į penkias klases. Papildomai eksperimento metu buvo matuojami savanorių elektroencefalogramų signalai, registruojami akių judesiai, vyzdžio dydžio dinaminiai pokyčiai bei fiksuotas momentas, kuomet akys pasiekia patogią padėtį gyliui stereoskopiniuose vaizduose suvokti.

Darbo mokslinis naujumas

1. Pasiūlyti požymiai įvertinti patirtą kokybę matuojant elektroencefalogramos signalus, esant trims skirtingiems patirtos kokybės lygiams.
2. Pasiūlyti požymiai leidžiantys taikyti akių sekimo įrenginus stereoskopinių vaizdų sukeltam regos diskomfortui įvertinti.
3. Pasiūlyti požymiai stereoskopinių vaizdų sukeltam regos diskomfortui įvertinti matuojant elektroencefalogramos signalus.

Darbo rezultatais yra siekiama pakeisti įprastus vidutinės nuomonės įverčius, kuriais vertinamas vartotojo regos diskomfortas. Požymiai išskirti iš išmatuotų fiziologinių signalų yra individualūs, todėl gali išreikšti kiekvieno vartotojo regos diskomfortą stebint stereoskopinį turinį.

Darbo rezultatų praktinė reikšmė

Požymiai išskirti iš išmatuotų fiziologinių signalų yra individualūs, todėl gali išreikšti kiekvieno vartotojo pojūtį stebint stereoskopinį turinį, taip pat ir regos diskomfortą. Akių judesių sekimo analizei pasiūlyti sprendimai gali būti pritaikyti virtualios realybės sistemose registruojančiose akių judesius ir vyzdžio dydį. Elektroencefalogramų analizei pasiūlyti

sprendimai tinkami naudoti virtualios realybės sistemose, kur yra galimybė naudoti tik vieną jutiklį, integruotą akiniuose.

Ginamieji teiginiai

1. Naudojant kaip požymius iš EEG signalų išskirtus aukštus ir žemus beta dažnius, išmatuotus momens ir smilkinio srityse, galima įvertinti patirtą kokybę audiovizualinio turinio stebėjimo metu.
2. Elektroencefalogramos 8–13 Hz ir 21–30 Hz dažnių ruožuose apskaičiuotų signalų spektro galios santykis yra požymis stereoskopiniams vaizdams aptikti, kai žiūrovui nepavyksta parinkti akių padėties tinkamam gylio vaizde suvokimui.
3. Taškų, į kuriuos sutelkiamas dėmesys skaičius yra požymis aptikti stereoskopinio gylio suvokimo momentą, jei naudojamas 2 s trukmės signalo analizės kadras.
4. Akies vyzdžio dydis yra požymis aptikti stereoskopinio gylio suvokimo momentą, tačiau naudojant 5 s trukmės signalo analizės kadrą kaip požymis turi būti pasirenkamas akių paralaksas.

Darbo rezultatų aprobavimas

Darbo rezultatai paskelbti šešiuose moksliniuose straipsniuose:

- dvi publikacijos atspausdintos žurnaluose, įtrauktuose į Thomson Reuters Web of Science sąrašą ir turinčiuose citavimo indeksą (Abromavičius *et al.* 2018, Abromavičius, Serackis 2018);
- viena publikacija atspausdinta recenzuojamame mokslo žurnale, įtrauktame į Index Copernicus duomenų bazę (Abromavičius 2017);
- trys publikacijos atspausdintos tarptautinių konferencijų straipsnių rinkiniuose, cituojamuose ISI Proceedings duomenų bazėje (Abromavičius, Serackis 2017, Abromavičius *et al.* 2017, Serackis *et al.* 2015)

Pagrindiniai disertacijos rezultatai paskelbti aštuoniuose mokslinėse konferencijose:

- 2015 m. tarptautinėje konferencijoje „Computing in Cardiology CINC“, Prancūzijoje, Nicoje;
- 2016–2018 m. respublikinėse konferencijose „Science – Future of Lithuania“, Lietuvoje, Vilniuje;
- 2017 m. tarptautinėje konferencijoje „Electrical, Electronic and Information Sciences (eStream)“, Lietuvoje, Vilniuje;
- 2017 m. tarptautinėje konferencijoje „Advances in Information, Electronic and Electrical Engineering AIEEE“, Latvijoje, Rygoje;
- 2017–2018 m. tarptautinėse konferencijose „Data Analysis Methods for Software Systems“, Lietuvoje, Druskininkuose;

Disertacijos struktūra

Disertaciją sudaro: įvadas, trys skyriai, bendrosios išvados. Darbo apimtis yra 106 puslapiai kuriuose yra pateikta: 28 paveikslai ir 21 lentelė. Disertacijoje remtasi 158 kitų autorių literatūros šaltiniais.

1. Literatūros šaltinių apie regos diskomforto radimą metodų apžvalga

Įprastai Patirta kokybė (angl. *sense of presence* – SoP) matuojama klausimynais, kai vartotojas dažniausiai pagal 5 ar 10 balų sistemą įvertina matytą audiovizualinį turinį Song *et al.* (2016). Į klausimynus įtraukiami klausimai apie garso kokybę, vaizdo kokybę, įsijautimą į turinį, aplinkos suvokimą. Šiuos subjektyvius matavimus bandoma pakeisti objektyviais kokybės įvertinimo būdais, kurie grindžiami žmogaus fiziologine ir kognityvine informacija Gupta *et al.* (2013).

Fiziologiniai metodai leistų įvertinti SoP realiuoju laiku. Širdies ritmas ar jo pokytis gali būti vienas iš požymių, padedančių objektyviai įvertinti SoP. Širdies ritmo mažėjimas sietinas su kognityvine veikla, o jaudinantys potyriai didina širdies ritmą (Bryant, Oliver 2009). Priklausomybė tarp širdies ritmo ir SoP nustatyta žaidžiant kompiuterinius žaidimus Castellar *et al.* (2014); Drachen *et al.* (2010). Barreda-Ángeles *et al.* (2014) tyrinėjo regos diskomfortą (angl. *visual discomfort*) stereoskopiniuose 3D vaizduose esant įvairioms subjekto emocinėms būsenoms. Subjektyvūs savęs įvertinimai nerodė jokio poveikio regos diskomfortui, tačiau buvo rasta koreliacija tarp regos diskomforto ir fiziologinių matavimų širdies ritmo elektrokardiogramos (ECG) signale, taip pat rasta koreliacija tarp elektromiografijos ir odos galvaninių reakcijų (angl. *electrodermal activity*).

Naujausios technologijos ir infrastruktūra pritaikytos vaizdą perduoti ne tik į stacionarius įrenginius, bet ir į mobiliuosius telefonus, planšetinius ar nešiojamuosius kompiuterius. Objektyviam SoP įvertinimo patobulinimui pasiūlytas fiziologinių signalų rinkinys, susidedantis iš EEG, ECG, kvėpavimo signalų ir subjektyvių matavimų (Perrin *et al.* 2016). Autoriai SoP įvertinti naudoja skirtingos raiškos ir garso kokybės audiovizualinį turinį. Signalų rinkinys yra viešai prieinamas. Kadangi pateikti duomenys yra įvertinti subjektyviai, galima ieškoti panašumo tarp subjektyvių ir objektyvių SoP matavimų.

Regos diskomforto vertinimas gali būti atliekamas dvejopai: naudojant subjektyvias arba objektyvias priemones. Atliekant subjektyvų vertinimą, savanoriams yra pateikiamas klausimynas (eksperimento metu arba po jo), kuriame yra prašoma įvertinti patirtą regos diskomfortą, pykinimą, akių komfortą, patirtą kokybę stebint rodomą vaizdo medžiagą. Objektyviais metodais siekiama rasti biologinių signalų pokytį keičiant stereoskopinio turinio parametrus. Atliekant objektyvų vertinimą yra stebimas savanorių biologinis atsakas į rodomą turinį. Stebint biologinių signalų pokytį dažniausiai yra naudojama akių sekimo įranga (Bernhard *et al.* 2014; Iatsun *et al.* 2015; Lin, Kao 2018), bei smegenų aktyvumo matavimo įranga (Fischmeister, Bauer 2006; Frey *et al.* 2016; Moon, Lee 2017). Žinoma, yra ieškoma ir kitų objektyvių būdų vertinti regos diskomfortą, savo tyrime, Lee *et al.* 2016 parodė, kad regos diskomfortą galima vertinti remiantis veido išraiškomis.

2. Patirtos kokybės matavimo metodų teoriniai tyrimai

Tyrimui atlikti naudotas Perrin *et al.* (2016) duomenų rinkinys, kuris buvo sudarytas atlikus trijų matavimo sesijų eksperimentą. Kiekvienai sesijai naudoti skirtingi prietaisai, kuriais vartotojams buvo pateikiama vaizdo ir garso medžiaga. Tokiu būdu buvo subjektyviai nustatytas SoP lygio pokytis per kiekvieną sesiją. Pirmąją sesiją (žemo SoP lygio) vizualinė medžiaga buvo rodoma naudojant iPhone5 kartu su stereogarso signalu. Antrajai tyrimo sesijai (vidutinio SoP lygio) panaudota iPad4 ir stereogarso signalas. Trečiajai tyrimo sesijai (aukšto SoP lygio) panaudoti 5.1 erdvinio garso signalai ir taikyta ultraaukštos raiškos vaizdo sistema. Tyrime dalyvavo 20 subjektų (10 vyrų ir 10 moterų), kurių amžius buvo svyravo 18 iki 25 metų (vidutinis amžius – 21 metai esant 2,2 metų standartiniam nuokrypiui). Per kiekvieną sesiją parodyti 9 epizodai, kurių metu išmatuoti fiziologiniai signalai. Tyrime naudotų epizodų trukmė buvo 1 minutė. Po kiekvieno epizodo SoP įvertinta subjektyviai – klausimynu. Tyrimo subjektai pagal 9 balų skalę nuo 1 (žemas kriterijus) iki 9 (aukštas kriterijus) įvertino SoP atsakydami į šešis klausimus. Perrin *et al.* (2016) atlikta subjektyvių rezultatų analizė parodė, kad kiekvienas tirtas prietaisas skirtingai paveikė SoP lygį. Tyrimo metu buvo matuoti ECG, EEG ir kvėpavimo signalai, jie įtraukti į duomenų rinkinį.

Remiantis pateiktais signalais buvo siekiama patikrinti dvi hipotezes. Pirmoji – ar širdies ritmą veikia skirtingi SoP lygiai. Antroji – ar smegenų aktyvumą veikia skirtingi SoP lygiai. Tyrimo metu esant skirtingiems SoP lygiams ECG signaluose buvo matuojamas vidutinis širdies ritmas, o panaudojant EEG signalus – skaičiuojamas ir analizuojamas smegenų aktyvumo spektras.

Širdies ritmas ECG signale apskaičiuotas matuojant laiko trukmę tarp gretimų R tipo dantelių (RR intervalų). Q, R ir S tipo danteliai sudaro QRS kompleksą. Šis kompleksas yra lengvai aptinkamas požymis ECG signale. Todėl remiantis QRS kompleksu širdies ritmo skaičiavimas tiriant įprastus, neturinčius anomalijų ECG signalus, yra patikimas. Tyrime vidutinis širdies ritmas skaičiuotas kiekvienam rodytam 60 s trukmės epizodui, dūžiais per minutę (bpm. Gauti rezultatai palyginti su subjektyviu SoP įvertinimu.

ECG signalo diskretizavimo dažnis 250 Hz, pateikti signalai buvo padalinti į 70 s trukmės intervalus – atitinkamai kiekvienam subjekto žiūrėtam epizodui. Pirmos 10 s skirtos nuolatinei dedamajai nustatyti ir nebuvo naudojamos QRS pikų detektoriuje.

Signalui filtruoti buvo naudojamas ECG signalų triukšmo šalinimo, glaudinimo ir glodinimo Savitzky ir Golay filtras (Lascu, Lascu 2008). Savitzky ir Golay filtrai dažniausiai naudojami triukšmingiems signalams, turintiems platų dažnių ruožą, glodinti. Šie filtrai yra efektyvesni nei įprasti ribotos impulsinės reakcijos filtrai, nes leidžia pašalinti triukšmą ir išsaugoti reikalingą aukštojo dažnio turinį signale (Krishnan, Seelamantula 2013). Remiantis Krishnan, Seelamantula (2013) ir gautais eksperimentiniais rezultatais mūsų naudojamam Savitzky ir Golay filtrui parinkta 8 filtro eilė ir 31 atskaitos ilgio kadras. Maitinimo linijos triukšmai pašalinti juostiniu 50 Hz begalinės impulsinės reakcijos filtru, o filtro kokybę rodantis parametras Q yra lygus 30.

QRS kompleksams aptikti buvo naudotas pikų detektorius, grįstas Pan, Tompkins (1985) pasiūlytu algoritmu, pakeitus slenkstinę ribą, nuo kurios aptinkami QRS pikai, iki 0,35 santykinių vienetų. Intervalas tarp gretimų pikų parinktas standartinis – 0,25 s trukmės. Pikų detektoriaus veikimas pavaizduotas S2.1 paveiksle. Apskritimai žymi aptiktus širdies dūžius. Epizodas pradėtas rodyti ties 0 s riba. Pikų detektoriaus rezultatai buvo

patikrinti vizualiai. 10 % atsitiktinai pasirinktų ECG signalų pikų detektoriaus tikslumas viršijo 99,9 %.

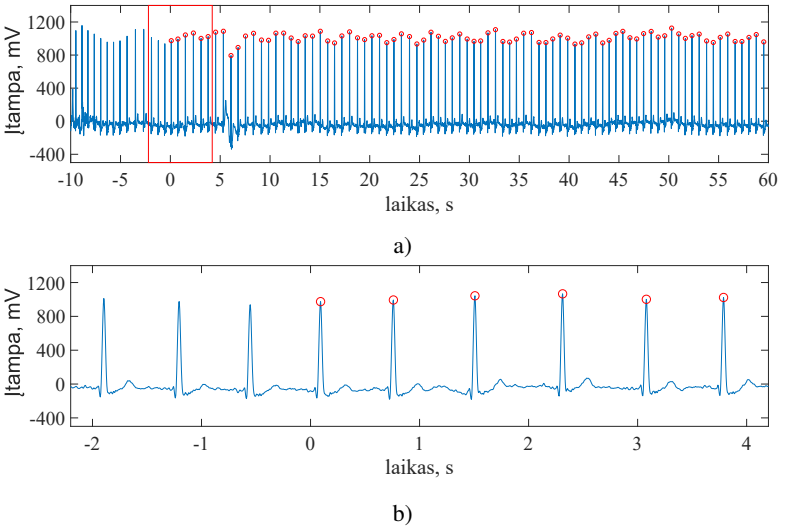

S2.1 pav. Elektrokardiogramos signalas: a) vieno epizodo trukmės elektrokardiogramos signalas; b) jo 6 s trukmės kadras

Remiantis aptiktais QRS pikais kiekvienam epizodui buvo skaičiuojamas vidutinis širdies ritmas. Vidutinio širdies ritmo matavimo rezultatai, gauti per kiekvieną sesiją (9 epizodų metu, dalyvaujant 20 subjektų), yra pateikti S2.1 lentelėje.

S2.1 lentelė. Vidutinis širdies ritmas ir jo standartinis nuokrypis esant trims skirtingiems patirtos kokybės lygiams. Rezultatai pateikti dūžiais per minutę

SoP lygis	Žemas	Vidutinis	Aukštas
Vidutinis širdies ritmas, bpm	70,80	69,04	67,85
Standartinis nuokrypis, bpm	5,59	5,58	6,23

Vidutinis širdies ritmas taikant žemo SoP lygio prietaisų konfigūraciją buvo 70,8 bpm, jo standartinis nuokrypis 5,59 bpm. Taikant vidutinio SoP lygio prietaisų konfigūraciją vidutinis širdies ritmas sumažėjo iki 69,04 bpm, standartinis nuokrypis – 5,58 bpm. Taikant aukšto SoP lygio konfigūraciją – vidutinis širdies ritmas sumažėjo iki 67,85 bpm, standartinis nuokrypis – 6, 23 bpm.

EEG signalo dažnių juostos ribos yra nuo 0,01 iki maždaug 100 Hz, jo amplitudė kinta nuo kelių mikrovoltų iki 100 μV, žinoma signalo amplitudė gali būti ir žymiai didesnė, esant pašalinio triukšmo poveikiui. Tiriant SoP poveikį smegenų aktyvumui gamma bangos (30–100 Hz) dažniausiai nėra nagrinėjamos dėl didelės matavimo netikslumų tikimybės ir kitų priežasčių (Whitham *et al.* 2008, 2007; Yuval-Greenberg *et al.* 2008).

EEG signalai buvo matuoti, stiprinti ir skaitmenizuoti naudojant *EGI Geodesic EEG System 300*. EEG duomenys rinkti naudojant 256 elektrodus, jos montuojant standartinėse pozicijose ant galvos. EEG signalų diskretizavimo dažnis 250 Hz. Elektrodai, kurių impedansas buvo didesnis nei 50 Ω buvo pašalinti iš tolimesnio apdorojimo. Signalams filtruoti buvo naudojamas 4 eilės skaitmeninis Batervorto filtras, kurio pralaidumo juosta buvo nuo 0,01 iki 40 Hz. Signalų atskaitos potencialui buvo naudojamas Cz elektrodas, po to signalų potencialai vėliau buvo dar kartą atskaityti pagal EEG signalų bendrą vidurkį. Artefaktams pašalinti buvo naudotas wavelet ICA metodas (Castellanos, Makarov 2006). Naudojant šį metodą buvo pakeisti du pradiniai parametrai: slenkstinis daugiklis sumažintas iki 0,5 ir ICA komponentams išskirti naudotas fastICA algoritmas (Hyvarinen 1999; Hyvärinen, Oja 2000).

Gautų signalų spektrinė analizė atlikta naudojant daugiakūginę (angl. *multi-taper*) Furjė transformaciją (Thomson 1982). Šis metodas naudoja ortogonalių langa funkcijų rinkinį, dar vadinamą Slepian kūgiais, ir vėliau apskaičiuoja gauto spektro svertinį vidurkį (Gramfort *et al.* 2014). Kūgio rinkinio naudojimas (vietoj įprastos langa funkcijos) leidžia sumažinti spektro įverčių dispersiją (Haykin *et al.* 2005). Spektrinė analizė buvo taikoma visam 60 s trukmės epizodui. Norint efektyviai panaudoti greitąją Furjė transformaciją signalai buvo prailginti nuliais. Taigi, tirti EEG signalai buvo prailginti iki 2^{14} matavimo imčių. Spektrinė analizė buvo atlikta naudojant Fieldtrip įrankį (Oostenveld *et al.* 2011).

Gautas EEG signalų spektras skirstytas į 5 dažnių ruožus: teta (4–7 Hz), alfa (8–12 Hz), žemos beta (13–16 Hz), vidutinės beta (17–20 Hz) ir aukštos beta (21–29 Hz) bangos. Tolimesnei analizei 256 EEG elektrodai buvo suskirstyti į 10 smegenų aktyvumo sričių: kairę ir dešinę kaktinę, kairę ir dešinę centrinę, kairę ir dešinę momeninę, kairę ir dešinę pakaušinę, kairę ir dešinę smilkininę (Andreassi 2010; Idris *et al.* 2014). Taigi, kiekvienam subjektui buvo apskaičiuota 50 skirtingų požymių atitinkančių kiekvieno regiono dažnių ruožus.

Tiriant SoP lygio poveikį širdies ritmui ir smegenų aktyvumui buvo atlikta dvimatė ir trimatė vieno faktoriaus dispersinė analizė (ANOVA). Tyrimo metu patikrinta ar gauti ECG ir EEG signalų požymiai reikšmingai skiriasi esant skirtingiems SoP lygiams. Rezultatų reikšmingumui įvertinti taikoma p vertė. p vertė rodo tikimybę gauti F statistinio kriterijaus vertę, kuri bus didesnė už tikrąją kriterijaus statistikos F vertę ar jai lygi. Maža p vertė, pvz., mažesnė nei 0,05, rodo, kad skirtumai tarp tiriamų grupių vidurkių yra statistiškai reikšmingi.

Širdies ritmo ANOVA analizės rezultatai pateikti S2.2 lentelėje. Rezultatai suapvalinti iki trijų skaičių po kablelio. Gautų rezultatų analizė parodė, kad yra artimas statistiškai reikšmingumo ribai ryšys tarp žemo ir vidutinio SoP lygių (F = 2,09, p = 0,15). Statistiškai reikšmingas skirtumas nebuvo gautas tarp vidutinio ir aukšto SoP lygių (F = 1,34, p = 0,25), t. y. širdies ritmas esant vidutinio ir aukšto SoP lygių konfigūracijai skiriasi nereikšmingai. Nustatytas statistiškai reikšmingas ryšys tarp žemo ir aukšto SoP lygių (F = 7,03, p = 0,008). Gavus trimatės ANOVA analizės rezultatus buvo nustatytas statistiškai reikšmingas ryšys tarp visų trijų SoP lygių ir širdies ritmo (F = 3,47, p = 0,032).

Smegenų aktyvumo ANOVA analizės rezultatai pateikti S2.3 lentelėje. Apskaičiuotos reikšmės suapvalintos iki trijų skaičių po kabelio, statistiškai reikšmingi rezultatai ($p < 0{,}05$) paryškinti, reikšmės mažesnės už 0,001 pažymėtos kaip „<0,001“.

Gautų rezultatų analizė parodė, kad aukštas beta bangų aktyvumas kaktinėje srityje nėra statistiškai reikšmingas ($p > 0{,}05$), tačiau tyrimo metu nustatytas statistiškai reikšmingas skirtumas ($p < 0{,}05$) teta, alfa, žemame ir vidutiniame beta bangų ruožuose.

S2.2 lentelė. ANOVA analizės rezultatai vertinant širdies ritmo pokytį esant skirtingiems patirtos kokybės lygiams. Statistiškai reikšmingi rezultatai ($p < 0{,}05$) yra paryškinti

SoP lygis	F kriterijus	p vertė
Žemas – vidutinis	2,09	0,150
Vidutinis – aukštas	1,34	0,249
Žemas – aukštas	7,03	**0,008**
Žemas – vidutinis – aukštas	3,47	**0,032**

Momeninėje srityje statistiškai reikšmingi skirtumai ($p < 0{,}05$) esant skirtingam SoP lygiui nustatyti teta, alfa, žemame ir aukštame beta ruože. Reikšmingų skirtumų ($p > 0{,}1$) nerasta vidutiniame beta ruože. Taip pat tyrimo metu nustatytas reikšmingas skirtumas ($p < 0{,}05$) centrinio regiono teta ir alfa dažnių ruožuose.

Smilkininėje srityje teta, žemi ir aukšti beta dažniai parodė statistiškai reikšmingus skirtumus ($p < 0{,}001$) esant skirtingiems SoP lygiams. Taip pat, reikšmingas skirtumas ($p = 0{,}009$) rastas alfa dažnių ruože dešiniajame smilkininėje srityje. Tačiau, statistiškai reikšmingi skirtumai nenustatyti smilkininėje srityje vidutiniams beta virpesiams ($p > 0{,}4$), ir kairėje smilkininėje srityje alfa virpesiams ($p = 0{,}18$).

S2.3 lentelė. ANOVA analizės rezultatai vertinant smegenų aktyvumo pokytį esant trims skirtingiems patirtos kokybės lygiams. Statistiškai reikšmingi rezultatai ($p < 0{,}05$) yra paryškinti

Smegenų bangos		Teta	Alfa	Žemos beta	Vidutinės beta	Aukštos beta
Kaktinė	Kairė	**<0,001**	**<0,001**	0,091	**<0,001**	0,283
	Dešinė	**0,004**	**0,014**	**0,005**	**0,026**	0,104
Momeninė	Kairė	**<0,001**	**0,002**	**<0,001**	0,191	**0,041**
	Dešinė	**<0,001**	**0,009**	**<0,001**	0,680	**<0,001**
Centrinė	Kairė	**0,004**	**<0,001**	0,770	0,230	0,334
	Dešinė	**0,045**	**<0,001**	0,367	0,981	0,352
Smilkininė	Kairė	**<0,001**	0,182	**<0,001**	0,726	**<0,001**
	Dešinė	**<0,001**	**0,009**	**<0,001**	0,466	**<0,001**
Pakaušinė	Kairė	**0,027**	**<0,001**	0,739	0,751	0,789
	Dešinė	**0,011**	**<0,001**	0,968	0,717	0,448

Pakaušinėje srityje, tarp skirtingų SoP lygių statistiškai reikšmingas skirtumas ($p < 0{,}01$) nustatytas alfa ir teta dažnių ruožams. Reikšmingų skirtumų ($p > 0{,}4$) nerasta beta (žemuose, vidutiniuose ir aukštuose) dažnių ruožuose.

3. Regos diskomforto radimo stereovaizduose metodų eksperimentiniai tyrimai

Tyrimui atlikti surinktas žvilgsnio ir EEG duomenų rinkinys. Tyrime dalyvavo 28 tyrimo subjektai, kuriems buvo rodomas 120 stereoskopinių paveikslų rinkinys. Eksperimento metu tyrimo subjektai buvo prašomi įvertinti patiriamą regos diskomfortą 5 balų skalėje, nuo 1 iki 5 (didžiausias regos komfortas) ir pažymėti kuomet pavyksta suvokti stereo gylį vaizduose (angl. *depth perception moment* – DPM). Atlikto eksperimento struktūra pavaizduota S3.1 paveiksle. Eksperimento metu 120 stereoskopinių vaizdų parodyta 28 tyrimo subjektams. Tyrimo subjektai įvertino patirtą regos diskomfortą ir gylio suvokimo momentą. Eksperimento metu buvo matuojami fiziologiniai signalai.

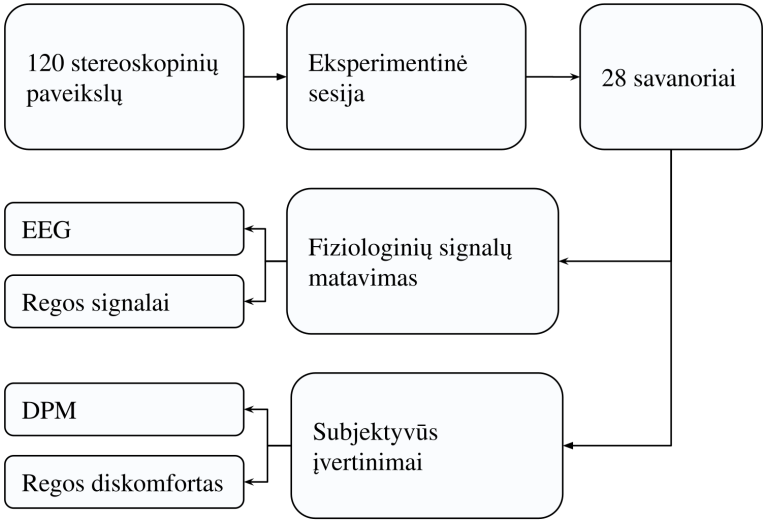

S3.1 pav. Eksperimento struktūra

Tyrimui atlikti buvo naudota *IVY LAB* surinkta stereoskopinių 3D vaizdų duomenų bazė, publikuota Jung *et al.* (2013) autorių. Vaizdų rinkinį sudaro vaizdai turintys gamtos, miesto, vidaus, žmonių ir daiktų objektų. Vaizdų skiriamoji geba 1920×1080 pikseliai, turintys nesugretinimą kintantį nuo 0,11 iki 5,07 laipsnių. Paveikslai buvo rodomi naudojant 1280×1024 taškų raiškos ekraną dirbantį 60 Hz atnaujinimo dažniu. Stereoskopinis 3D efektas buvo gaunamas naudojant anaglifo technologiją. Tyrimo subjektai dėvėjo akinius su raudonos ir mėlynos spalvos filtrais.

Tyrimo dalyviai buvo savanoriai (25 vyrai ir 3 moterys), kurių amžius svyravo nuo 19 iki 37 metų. Savanoriams nebuvo jokiais būdais atlyginamą už dalyvavimą eksperimente. Prieš prasidedant eksperimentui visi jo dalyviai buvo supažindinti su tyrimo procedūromis, tikslu, subjektyvaus vertinimo kriterijais, matuojamais duomenimis, galimu pavoju sveikatai. Taip pat tyrimo subjektai žodžiu ir raštu davė sutikimą dalyvauti eksperimente.

Tyrimo subjektams paveikslai buvo rodomi naudojant 17 colių ekraną. Sėdėjimo atstumas buvo 70–80 cm. Natūralių sąlygų atkūrimui galvos ir kūno judesiai nebuvo varžomi, taip pat savanoriai galėjo dėvėti regą koreguojančius prietaisus. Eksperimento pradžioje kiekvienas subjektas turėjo atlikti stereo suvokimo (ITU-R BT.2021-1) ir daltonizmo testus (*Isihara Color Vision test*). Taip pat, prieš prasidedant bandymams tyrimo subjektams buvo rodomi 5 atsitiktiniai paveikslai. Buvo prašoma juos įvertinti. Tokiu būdu buvo stabilizuojami nuomonės įverčiai. Po šio žingsnio buvo kalibruojami akių sekimo ir EEG matavimo įrenginiai.

Kiekvienas eksperimentas susidėjo iš dviejų dalių (S3.2 pav.). Pirmoje bandymo dalyje buvo rodomas stereoskopinis paveikslas, ir tyrimo subjektai turėjo nuspausti klaviatūros mygtuką, kuomet jie suvokė rodomo paveikslo stereoskopinį gylį, paveikslas buvo rodomas dar 5 s. Antra dalis buvo balsavimas, kuomet tyrimo subjektai turėjo įvertinti patirtą regos diskomfortą penkių balų skalėje, naudojant *Single Stimulus* kategorinį vertinimo metodą ITU-R BT.500-13. Kiekvienas eksperimentas susidėjo iš 120 tokių bandymų. Kiekvieno bandymo metu buvo matuojami fiziologiniai singalai. Vidutinė eksperimento trukmė buvo apie 40 minučių.

Po eksperimento subjektyvių duomenų patikimumui įvertinti buvo taikomos procedūros aprašytos ITU-R BT.500-13 standarte. Nepatikimų įverčių nebuvo rasta, tačiau iš eksperimento buvo pašalinta keturių tyrimo subjektų fiziologiniai duomenys, dėl blogo matavimo tikslumo (1 subjektas), matavimo klaidų, susijusių su mažu kvantavimo dažniu (2 subjektai), ir vienas subjektas neatliko daltonizmo testo.

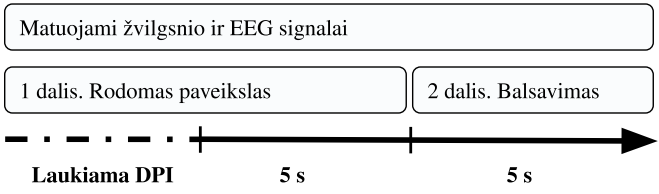

S3.2 pav. Vieno bandymo struktūra

Regos signalai buvo matuoti *Tobii T120* įranga. Įranga buvo kalibruojama kiekvienam subjektui atskirai, naudojant 5 taškus ant ekrano. Taškai buvo tolygiai paskirstyti ekrane. Įranga matavo akių poziciją, žvilgsnio poziciją, vyzdžio diametrą. Matavimo dažnis buvo 60 Hz. Pagal surinktus matavimo duomenis buvo formuojami požymiai:

- žvilgsnio taškas – apskaičiuojamas kaip centrinis taškas tarp kairės ir dešinės akių žvilgsnio koordinačių ekrane;
- vyzdžio dydis – apskaičiuojamas, kaip vidurkis tarp kairės ir dešinės akių išmatuotų vyzdžio diametrų, matuojamas milimetrais;
- dėmesio taškas – apskaičiuojamas pagal erdvini žvilgsnio taškų išsidėstymą. Kiekvienas dėmesio taškas yra žvilgsnio taškų rinkinys, kurių koordinatės nepakeitė daugiau nei 5% ekrano ploto per 0,2 s ar daugiau;

- regos nesugretinamumas – horizontalus atstumas tarp kairės ir dešinės akių žvilgsnio koordinačių, apskaičiuojamas kiekvienam žvilgsnio taškui, matuojamas pikseliais; pikselio dydis su naudota įranga buvo $0{,}2634$ mm;
- kryžminės regos santykis – teigiamų ir neigiamų regos nesugretinamumų santykis, apskaičiuojamas kiekvienam bandymui.

Norint įvertinti skirtumą tarp regos diskomforto grupių gauti požymiai buvo tiriami naudojant skirtingos trukmės kadrus. Buvo suformuoti 6 skirtingos trukmės kadrai: „visas iki DPM“, 1, 2, 5 s iki DPM, 5 s po DPM ir „pilnos trukmės“. „Pilnos trukmės“ kadrui buvo naudojami požymiai surinkti per visą vieno bandymo trukmę, nuo vaizdo pasirodymo iki subjektyvaus vertinimo dalies. „Visas iki DPM“ kadras tiria laiką nuo vaizdo pasirodymo iki DPM įvedimo. Šis kadras nėra pastovios trukmės, jo trukmė kinta nuo kelių sekundžių iki dešimties, tačiau juo galima įvertinti regos aktyvumą nuo vaizdo rodymo pradžios iki gylio suvokimo įvesties (DPM).

S3.1 lentelėje pateikti vidutinis dėmesio taškai skaičius kiekvienai regos diskomforto grupei, naudojant skirtingos trukmės kadro ilgį ir jų ANOVA rezultatai. Iš pateiktų rezultatų matyti, kad vidutinis dėmesio taškų skaičius priklauso nuo kadro trukmės ir nuo regos diskomforto. Taškų skaičius naudojant ilgiausios trukmės kadrą – „pilnos trukmės“ buvo gautas nuo $20{,}87$ (VCo diskomforto lygiui) iki $24{,}05$ (Co diskomforto lygiui). Naudojant trumpiausią kadro ilgį (1 s iki DPM) taškų skaičius buvo gautas nuo $2{,}64$ (Un lygiui) iki $2{,}84$ (VCo lygiui). Reikšmingas dėmesio taškų skirtumas gautas tik naudojant 2 s iki DPM langą ($p = 0{,}035$).

S3.2 lentelėje pateiktas vidutinis vyzdžio dydis kiekvienai regos diskomforto grupei, naudojant skirtingos trukmės kadro ilgį ir jų ANOVA rezultatai. Iš pateiktų rezultatų matyti, kad vyzdžio dydis nebuvo priklausomas nuo tiriamo kadro trukmės. Reikšmingi vyzdžio dydžio skirtumai gauti naudojant 1 s iki DPM ($p < 0{,}001$), 2 s iki DPM ($p = 0{,}001$), „visas iki DPM“ ($p = 0{,}036$), 5 s po DPM ($p < 0{,}001$) ir „pilnos trukmės“ ($p = 0{,}015$) kadrus.

S3.1 lentelė. Dėmesio taškų skaičius ir jų reikšmingumo lygis esant skirtingam regos diskomfortui. Statistiškai reikšmingi rezultatai ($p < 0{,}05$) yra paryškinti

Kadro trukmė	VUn	Un	MdUn	Co	VCo	F	p vertė
Visas iki DPM	12,14	13,32	13,52	14,64	11,76	1,977	0,097
1 s iki DPM	2,69	2,64	2,74	2,81	2,84	1,907	0,107
2 s iki DPM	4,54	4,30	4,55	4,58	4,77	2,597	**0,035**
5 s iki DPM	9,22	9,64	9,47	9,93	9,70	0,770	0,545
5 s po DPM	8,46	8,34	8,84	8,85	8,87	1,217	0,302
Pilnos trukmės	21,17	22,28	22,68	24,05	20,87	1,596	0,174

S3.3 lentelėje pateiktas regos nesugretinamumas kiekvienai regos diskomforto grupei, naudojant skirtingos trukmės kadro ilgį ir jų ANOVA rezultatai. Iš pateiktų rezultatų matyti, kad regos nesugretinamumas visoms kadrų trukmėms buvo panašus, tačiau kito nuo regos diskomforto. Statistiškai reikšmingas pokytis rastas naudojant 5 s iki DPM kadro ilgį ($p = 0{,}041$).

EEG signalai buvo matuoti vartotojui draugiška *Neurosky Mindwave* įranga, turinčia vieną sauso matavimo elektrodą, montuojamą ant kaktinės srities. Įrenginys yra belaidis,

todėl yra lengvai uždedamas ir patogus vartotojui. Taip pat, šis įrenginys yra naudojamas moksliniuose tyrimuose, tokiose srityse kaip žmogaus emocijų atpažinimas (Ursuţiu *et al.* 2018; Yoon *et al.* 2013), vystant dėmesio sutelkimo sistemas, kurios gali atpažinti kelis dėmesio sutelkimo lygmenis (Chen *et al.* 2017), ar matuojant kognityvinę apkrovą (Lin, Kao 2018). Maskeliunas *et al.* (2016) ištyrė vartotojui draugiškų EEG įrenginių galimybes valdymo užduotims, bei įvardino problemas, kurias reikia įvertinti naudojant tokius įrenginius. Šiame tyrime EEG aktyvumas buvo tiriamos galimybės naudoti EEG įtaiso signalą, kaip papildomą požymį regos diskomfortui nustatyti.

S3.2 lentelė. Vyzdžio dydis (milimetrais) ir jų reikšmingumo lygis esant skirtingam regos diskomfortui. Statistiškai reikšmingi rezultatai ($p < 0{,}05$) yra paryškinti

Kadro trukmė	VUn	Un	MdUn	Co	VCo	F	*p* vertė
Visas iki DPM	4,22	4,25	4,18	4,18	4,11	2,579	**0,036**
1 s iki DPM	4,12	4,23	4,19	4,14	4,06	5,424	**0,000**
2 s iki DPM	4,14	4,26	4,19	4,15	4,07	4,990	**0,001**
5 s iki DPM	4,15	4,22	4,17	4,18	4,12	1,653	0,158
5 s po DPM	4,17	4,32	4,27	4,20	4,11	8,170	**0,000**
Pilnos trukmės	4,21	4,27	4,18	4,18	4,11	3,098	**0,015**

S3.3 lentelė. Regos nesugretinamumas (pikseliais) ir reikšmingumo lygis esant skirtingam regos diskomfortui. Statistiškai reikšmingi rezultatai ($p < 0{,}05$) yra paryškinti

Kadro trukmė	VUn	Un	MdUn	Co	VCo	F	*p* vertė
Visas iki DPM	80,5	82,3	76,6	79,9	71,2	1,239	0,292
1 s iki DPM	81,3	84,3	78,3	79,4	73,1	1,583	0,176
2 s iki DPM	82,4	83,3	78,5	79,7	71,1	2,095	0,079
5 s iki DPM	83	85,8	75,9	80,5	70,9	2,502	**0,041**
5 s po DPM	83,6	85,8	82,7	79,5	75,6	1,679	0,152
Pilnos trukmės	82,3	83,5	78,9	80,3	74,1	0,836	0,502

Surinkti EEG signalai filtruoti naudojant 4 eilės skaitmeninį Batervorto filtrą, kurio pralaidumo juosta buvo nuo $0{,}01$ iki 40 Hz. Akių judesių ir kitiems artefaktams pašalinti naudotas wavelet ICA metodas (Castellanos, Makarov 2006). Naudojant šį metodą buvo pakeisti du pradiniai parametrai: slenkstinis daugiklis sumažintas iki $0{,}3$ ir ICA komponentams išskirti naudotas fastICA algoritmas (Hyvarinen 1999; Hyvärinen, Oja 2000). Gautų signalų spektrinė analizė atlikta naudojant daugiakūginę (angl. *multi-taper*) Furjė transformaciją (Thomson 1982). Šis metodas įgyvendintas naudojant Oostenveld *et al.* (2011) pasiūlytą algoritmą, taikant 1 s trukmės langą.

Regos diskomforto poveikis smegenų aktyvumui buvo analizuojamas naudojant $0{,}5$, 1, 3, 4, 5 6, 7, ir 10 s trukmės analizės kadrus iki DPM. Tiriamų EEG dažnių ruožai (alfa, beta, teta) kinta netolygiai, Cheng *et al.* (2007) tyrė ne tik dažnių ruožus, bet ir jų santykius (pvz., teta/alfa, beta/alfa ir t.t.). Taip pat, Zou *et al.* (2015) tirdami atsitiktinių taškų stereogramos poveikį naudojo šešis dažnių ruožo santykius, reikšminti skirtumai buvo rasti visuose tirtuose santykiuose, bei alfa dažnių ruože.

Šiame tyrime gautas EEG signalų spektras skirstytas į 5 dažnių ruožus: teta (θ) 4–8 Hz, alfa (α) 8–13 Hz, žemos beta (β_{l}) 13–17 Hz, vidutinės beta (β_{m}) 17–21 Hz ir aukš-

tos beta (β_{h}) 21–30 Hz bangos (Dunbar *et al.* 2007). Taip pat panaudoti septyni dažnių ruožų santykiai: α/β; $(\alpha+\theta)/\beta$; α/θ; θ/β; α/β_{l}; α/β_{m}; α/β_{h}. Santykiai buvo pasirinkti remiantis Cheng *et al.* (2007), Hsu, Wang (2013) ir Zou *et al.* (2015) tyrimų rezultatais.

S3.4 lentelė. Smegenų dažnių ANOVA rezultatai esant skirtingiems regos diskomforto lygiams. Statistiškai reikšmingi rezultatai ($p < 0{,}05$) yra paryškinti

kadro trukmė (iki DPM), s	θ	α	β_{l}	β_{m}	β_{h}
0,5	0,273	0,550	0,259	0,054	0,429
1	0,241	0,617	0,199	0,126	0,330
2	0,169	0,906	0,176	0,189	**0,014**
3	0,436	0,347	0,242	0,133	**0,002**
4	0,276	0,173	0,362	0,129	**0,002**
5	0,223	0,231	0,280	0,061	**0,000**
6	0,273	0,917	0,231	**0,017**	**0,000**
7	0,299	0,664	0,203	0,162	**0,008**
10	0,217	0,432	0,556	0,598	0,277

S3.4 lentelėje pateikti EEG dažnių ruožų ANOVA rezultatai, esant penkiems skirtingiems regos diskomforto lygiams naudojant skirtingo ilgio kadrus. Dažniuose θ, α ir β_l nebuvo rasta statistiškai reikšmingų skirtumų prie skirtingų regos diskomforto lygių naudojant visas tirtas kadro ilgio trukmes. Statistiškai reikšmingi skirtumai nustatyti β_m dažnių ruože naudojant 6 s iki DPM kadro trukmę ($p = 0{,}017$), ir β_h dažnių ruože naudojant 2, 3, 4, 5, 6 ir 7 s iki DPM kadro trukmę, reikšmingumo vertės (suapvalintos iki trijų skaičių po kablelio) atitinkamai buvo 0,014, 0,002, 0,002, 0,000, 0,000 ir 0,008.

S3.5 lentelėje pateikti EEG dažnių ruožų santykinių ANOVA rezultatai, esant penkiems skirtingiems regos diskomforto lygiams naudojant skirtingo ilgio kadrus.

S3.5 lentelė. Santykių tarp smegenų dažnių ANOVA rezultatai esant skirtingiems regos diskomforto lygiams. Statistiškai reikšmingi rezultatai ($p < 0{,}05$) yra paryškinti

kadro trukmė (iki DPM), s	θ/α	θ/β	$(\theta+\alpha)/\beta$	α/β	α/β_{l}	α/β_{m}	α/β_{h}
0,5	**0,031**	0,244	0,233	0,365	0,229	0,088	0,392
1	**0,020**	0,084	0,178	0,438	0,232	0,287	0,050
2	**0,026**	0,599	0,543	0,330	0,190	0,288	**0,005**
3	**0,005**	0,936	0,564	0,162	0,296	0,154	**0,000**
4	**0,002**	0,772	0,499	0,114	0,381	0,274	**0,000**
5	**0,002**	0,543	0,372	0,087	0,537	0,221	**0,000**
6	0,103	0,396	0,819	0,936	0,665	**0,028**	**0,000**
7	0,104	0,548	0,755	0,893	0,252	0,104	**0,020**
10	0,068	0,460	0,707	0,786	0,681	0,598	0,055

Tiriant dažnių santykius θ/β, $(\theta+\alpha)/\beta$, α/β and α/β_l nebuvo rasti statistiškai reikšmingi skirtumai esant skirtingiems regos diskomforto lygiams, naudojant visus kadro ilgius. Reikšmingi skirtumai nustatyti θ/α santykiui naudojant 0,5, 1, 2, 3, 4 ir 5 s iki DPM kadrus, gautos *p* reikšmės atitinkamai buvo 0,031, 0,020, 0,026, 0,005, 0,002 ir

0,002. Taip pat reikšmingi skirtumai rasti $\theta/\beta_{\mathrm{m}}$ santykiui naudojant 6 s iki DPM kadro ilgį ($p = 0{,}028$), santykiui $\theta/\beta_{\mathrm{h}}$ naudojant 2, 3, 4, 5, 6 ir 7 s iki DPM kadro ilgį. *P* reikšmės atitinkamai buvo gautos 0,005, 0,000, 0,000, 0,000, 0,000 ir 0,020.

Bendrosios išvados

1. Naudojant požymius išskirtus iš elektrokardiogramos ir elektroencefalogramos signalų galima aptikti patirtos kokybės lygį, kai yra rodomas audiovizualinis turinys:
   1.1. naudojant kaip požymį iš elektrokardiogramos išskirtą širdies ritmą galima įvertinti patirtą kokybę tarp aukšto ir žemo patirtos kokybės lygių audiovizualinio turinio stebėjimo metu, esant trim patirtos kokybės lygiams;
   1.2. naudojant kaip požymius iš elektroencefalogramos išskirtus dažnių ruožus galima įvertinti patirtą kokybę audiovizualinio turinio stebėjimo metu. Požymiams išskirti beta bangų dažnių ruožą reikia dalinti į žemus, vidutinius ir aukštus beta bangų dažnių ruožus.
2. Požymiai išskirti matuojant elektroencefalogramos signalus vartojojui orientuotu vieno elektrodo EEG jutikliu kaktinėje srityje yra tinkami įvertinti stereoskopinių vaizdų sukeltą regos diskomfortą:
   2.1. naudojant kaip požymį iš elektroencefalogramos išskirtą aukštą beta bangų dažnių ruožą arba alfa ir aukšto beta bangų dažnių ruožų santykį galima atpažinti regos diskomforto simptomus sąlygojančias būsenas, jei yra naudojamas 2–7 s trukmės analizės kadras iki gylio suvokimo momento;
   2.2. naudojant kaip požymį iš elektroencefalogramos išskirtą teta ir alfa bangų dažnių ruožų santykį galima atpažinti regos diskomforto simptomus sąlygojančias būsenas, jei yra naudojamas 0,5–1 s trukmės analizės kadras iki gylio suvokimo momento.
3. Požymiai išskirti naudojant akių sekimo įrenginius yra tinkami įvertinti stereoskopinių vaizdų sukeltą regos diskomfortą:
   3.1. naudojant kaip požymį akių sekimo metu apskaičiuotą vidutinį dėmesio taškų skaičių galima aptikti regos diskomforto simptomus stereoskopinių vaizdų stebėjimo metu, jei naudojamas 2 s trukmės signalo analizės kadras iki gylio suvokimo momento;
   3.2. naudojant kaip požymį akių sekimo metu apskaičiuotą vyzdžio dydį galima aptikti regos diskomforto simptomus stereoskopinių vaizdų stebėjimo metu, jei naudojamas 1, 2 s trukmės signalo analizės kadras iki gylio suvokimo momento.
   3.3. naudojant kaip požymį akių sekimo metu apskaičiuotą regos nesugretinamumą galima aptikti regos diskomforto simptomus stereoskopinių vaizdų stebėjimo metu, jei naudojamas 5 s trukmės signalo analizės kadras iki gylio suvokimo momento.

Annexes[1]

Annex A. Declaration of Academic Integrity

Annex B. The Co-authors' Agreement to Present Publications Material in the Dissertation

Annex C. The Copies of Scientific Publications by the Author on the Topic of the Dissertation

[1]The annexes are supplied in the enclosed compact disc.

Vytautas ABROMAVIČIUS

EXTRACTION AND INVESTIGATION OF BIOSIGNAL FEATURES
FOR VISUAL DISCOMFORT EVALUATION

Doctoral Dissertation

Technological Sciences,
Electrical and Electronic Engineering (T 001)

BIOSIGNALŲ POŽYMIŲ REGOS DISKOMFORTUI VERTINTI
IŠSKYRIMAS IR TYRIMAS

Daktaro disertacija

Technologijos mokslai,
elektros ir elektronikos inžinerija (T 001)

2019 08 14. 9,75 sp. l. Tiražas 20 egz.
Vilniaus Gedimino technikos universiteto leidykla „Technika“,
Saulėtekio al. 11, 10223 Vilnius,
http://leidykla.vgtu.lt
Spausdino BĮ UAB „Baltijos kopija“,
Kareivių g. 13B, 09109 Vilnius